Exhausted Carbon for the Removal of Hydrogen Sulfide and Ammonia

Jiang Xia

School of Civil & Environmental Engineering

A thesis submitted to the Nanyang Technological University

in partial fulfillment of the requirement for the degree of

Doctor of Philosophy

2010

ACKNOWLEDGMENTS

I would first like to express my deepest and most sincere gratitude and appreciation to my supervisor, **Professor Tay Joo Hwa** for his invaluable guidance and encouragement throughout the course of the research project.

I would like to extend my sincere gratitude and appreciation to **Dr. Yan Rong** for her patient guidance and advice for the research.

I also want to thank all staff and technicians in the Environmental Lab of Nanyang Technological University for their assistance and cooperation in many ways that made this research study possible.

I acknowledge the help and moral support provided by Mr. Wu Weiwei, Mr Kuang Shengli, Ms. Luo Yiqun, Dr. Zeng Ping, Dr. Li Yong, Dr. Zhang Lei, Dr. Duan Huiqi, Dr. Yi Shan, Dr. Wu Bing, Dr. Liu Xueyan, Dr. Zhu Baowei, Mr. Guo Chenhong, Ms. Xu Shiping, Ms. Liu Yajuan, Ms. Xu Huijuan, Dr. Shao Jingai, and all my colleagues and friends. I really appreciate the friendship of my fellow students for their constant supports and fruitful discussion in my study.

Last and most important, I thank my family members for their encouragement and unfailing moral support throughout my career.

TABLE OF CONTENTS

ABSTRACT

Hydrogen sulfide (H_2S) and ammonia (NH_3) have generally low odor thresholds, high toxicity to human health, and potential corrosive effects to downstream infrastructure and equipments. Biofiltration is a cost-effective and environmental friendly technology for the control of odorous compounds. Exhausted carbon is a hazardous waste from the H_2S adsorption process, which must be either regenerated or disposed of in a landfill. This study is to develop a highly efficient and economical biofiltration process for the co-removal of H_2S and NH_3 using exhausted carbon as packing material.

Firstly, the feasibility of re-using exhausted carbon in biofiltration for the removal of H_2S was evaluated. The results demonstrate that the biofilm can be formed on exhausted carbon using part of the pre-adsorbed sulfur compounds as the sole energy source for bacterial growth in off-line trials. Around 18-47% of the pre-adsorbed sulfur on carbon was regenerated. On-line biofilter immobilization showed better biofilm development on exhausted carbon than in off-line incubation. During the biofiltration, the pre-adsorbed sulfur compounds on exhausted carbon were also biodegraded dramatically. The biofilters packed with exhausted carbon demonstrated a fast start-up (about 80 hours) and achieved high removal efficiency (>95%) at a short empty bed retention time (EBRT) of 4 s. The removal efficiency of H_2S was almost identical in the biofilters packed with exhausted carbon and fresh carbon. Therefore, it is highly feasible and effective to transfer exhausted carbon into biological activated carbon for the removal of H_2S.

Furthermore, a mathematical model was developed to explore and explain the different

mechanisms of H_2S removal in biofilters employing exhausted carbon (Column EC) and fresh carbon (Column FC). The experimental data of removal efficiency in the two columns can be predicted by the developed model very well. The ratios of H_2S removal by the adsorption and biodegradation were also simulated, respectively. During the start-up stage, the removal of H_2S in Column EC was attributed to the adsorption mechanism much less than in Column FC. The removal of H_2S by the adsorption was affected greatly by the biodegradation. The ratios of H_2S removal by the biodegradation in Column EC were higher than those in Column FC. The steady-state biodegradation was obtained in a shorter time in Column EC than in Column FC. Under the steady-state conditions, the removal of H_2S was mainly attributed to the biodegradation mechanism. The adsorption of H_2S into carbon can be ignored.

Afterwards, the effect of substrates acclimation strategy on simultaneous biodegradation of NH_3 and H_2S were evaluated in three parallel biofilters. Removal performances of H_2S and NH_3 were different in the three biofilters with various substrates acclimation strategies. A shorter acclimation time for the biodegradation of NH_3 was achieved in the biofilter feeding NH_3 followed by H_2S. This strategy also exhibited higher removal efficiency of NH_3 (>95%) under high loadings of H_2S and NH_3. Moreover, the removal of NH_3 gas under this strategy was significantly attributed to the biodegradation (over 50%), rather than the adsorption and chemical reaction under other two strategies. A microbial population capable of degrading NH_3 that was acclimatized firstly in this biofilter benefited the fast acclimation and high removal of NH_3 in the co-removal system.

A horizontal biotrickling filter (HBTF) packed with exhausted carbon was investigated for the co-removal of H_2S and NH_3 for a long-term operation. The results demonstrate that simultaneous biodegradation of H_2S and NH_3 was highly efficient and effective by the HBTF over 316 days. Complete removal and biodegradation of H_2S and NH_3 was

obtained at the beginning of 30 days operation. Over 95 % and 90 % of NH_3 and H_2S were removed in most cases, respectively. Maximum elimination capacities were 131 and 119 g m^{-3} h^{-1} for NH_3 and H_2S respectively. The metabolic products of NH_3 and H_2S were analyzed. The results explore that the physical/chemical adsorption and biodegradation played different roles in the removal of H_2S and NH_3 under the steady and unsteady-state conditions. In most cases, NH_3 was biodegraded into NO_2/NO_3^- with high ratio ($\geq$85 %) and H_2S was biodegraded into sulfate as main product ($\geq$95 %).

The long-term high performance of the HBTF was significantly attributed to low accumulation of biomass and degradation products, stable carbon characteristics and microbial communities. The low biomass accumulation on carbon (0.4 and 1.6 mg protein g^{-1} carbon) avoided the problem of bed clogging. The low accumulation of biodegraded products on carbon benefited the stable operation of the HBTF, due to preventing the accumulation of metabolic products in a toxic concentration. Neutral pH values of carbon overcame the system acidification and stable micropore structure of carbon let the adsorption still happening during shock loadings. Furthermore, the microbial communities of biofilm in the HBTF were also studied by using denaturing gradient gel electrophoresis (DGGE). The high population diversity in the HBTF was observed. The population communities have both some degree of stability and the adequate dynamics capable of adapting to accommodate varying reactor conditions. These advantages of the HBTF system significantly contributed to the high performance in the HBTF over a long-term operation.

PUBLICATIONS

Jiang, X., Tay, J.H., 2010. Microbial community structures in a horizontal biotrickling filter degrading H_2S and NH_3. Bioresource Technology, 101, 1635-1641.

Jiang, X., Yan, R., Tay, J.H., 2009. Impact of substrate acclimation strategy on simultaneous biodegradation of hydrogen sulfide and ammonia. Bioresource Technology, 100, 5707-5713.

Jiang, X., Yan, R., Tay, J.H., 2009. Simultaneous autotrophic biodegradation of H_2S and NH_3 in a biotrickling filter. Chemosphere 75, 1350-1355.

Jiang, X., Yan, R., Tay, J.H., 2008. Reusing H_2S-exhausted carbon as packing material for odor biofiltration. Chemosphere 73, 698-704.

Jiang, X., Yan, R., Tay, J.H., 2009. Transient-state biodegradation behavior of a horizontal biotrickling filter in co-treating gaseous H_2S and NH_3. Applied Microbiology Biotechnology 81, 969-975.

Jiang, X., Yan, R., Tay, J.H., 2009. Developing sulfide-oxidizing biofilm on H_2S-exhausted carbon for sustainable bio-regeneration and biofiltration. Journal of Hazardous Materials 164, 726-732.

Jiang, X., Tay, J.H., 2009. Operational characteristics of efficient co-removal of H_2S and NH_3 in a horizontal biotrickling filter using exhausted carbon. Journal of Hazardous Materials, In press, DOI: 10.1016/j.jhazmat.2009.11.079.

LIST OF TABLES

LIST OF FIGURES

LIST OF ACRONYMS

AC	Activated carbon
AOB	Ammonia-oxidizing bacteria
APHA	American Public Health Association
ASTM	American Standard Test Method
b	Loss rate of the organisms due to endogenous decay
BAC	Biological activated carbon
BET	Braunner-Emmett-Teller
BF	Biofilter
BTEX	Benzene, toluene, ethylbenzene, o-xylene
BTF	Biotrickling Filter
C_f	Concentration of substrate in biofilm, $g \cdot m^{-3}$
CFU	Colony forming unit
C_g	Substrate concentration in air phase, $g \cdot m^{-3}$
CHNS	Carbon, hydrogen, nitrogen, sulfur
Con.	Concentration
C_s	Concentration of substrate in carbon, $g \cdot m^{-3}$
D_f	Diffusivity of substrate in the biofilm, $m^2 \cdot s^{-1}$
D_g	Dispersion coefficient in air phase, $m^2 \cdot s^{-1}$
DGGE	Denaturing gradient gel electrophoresis
DO	Dissolved oxygen
d_p	Particle's diameter, m

D_s	Internal pore diffusivity of substrate within a carbon pellet, $m^2 \cdot s^{-1}$
DTG	Derivative Thermogravimetry
EC	Exhausted carbon
EBRT	Empty bed retention time (=bed volume/air flow rate)
EDX	Energy-dispersive X-ray spectrometry
FC	Fresh carbon
GAC	Granular activated carbon
h	Hour
H	Henry's Constant
H_2S	Hydrogen sulfide
HBTF	horizontal biotrickling filter
HSDM	Homogeneous surface diffusion model
k_{ad}	The first order reaction rate constant that describes absorption in activated carbon particles, d^{-1}.
K_s	Half-saturate constant, $g \cdot m^{-3}$
L	Filter bed length, m
LDF	Linear driving force
MATLAB	Matrix Laboratory (Math software developed by Mathworks)
MEK	Methyl ethyl ketone
MIBK	Methyl isobutyl ketone
NH_3	Ammonia
MPN	most probable number
N	Nitrogen
NOB	Nitrite-oxidizing bacteria
NTU	Nanyang Technological University
OUR	Oxygen uptake rate
PCR	Polymerase chain reaction
PDEs	Partial differential equations

ppb	Parts per billion
ppm	Parts per million
ppmv	Parts per million by volume
psi	Pounds per square inch
Q	Airflow rate
R	Equivalent radius of carbon pellet, m
r	Radius distance in carbon pellets, m
RE	Removal efficiency
rpm	Revolutions per minute
S	Sulfur
S_{BET}	BET surface area
SDS	Sodium dodecyl sulfate
S^{el}	elemental sulfur
SEM	Scanning electron microscope
S_{ext}	External surface area
S_{mic}	Micropore surface area
SOB	Sulfide-oxidizing bacteria
SOUR	Substrate-induced oxygen uptake rate
t	Time
TCE	Trichloroethylene
TGA	Thermogravimetric analysis
TS	Thiosulfate
UPGMA	Un-weighted pair group method using arithmetic averages
UPW	Ultra pure water
V	Axial interstitial air velocity, $m \cdot s^{-1}$
V_f	Filter bed volume, m^3
V_m	Maximum apparent removal rate, g day^{-1} kg^{-1} dry AC
V_{mic}	Micropore volume

VOCs	Volatile organic compounds
V_p	Volume of a carbon particle, m^3
VSS	Volatile suspended solids
WWTPs	Wastewater treatment plants
x	Distance in the biofilm, μm
X_b	Biomass concentration in the biofilm on carbon, g g^{-1} AC
X_f	Biomass density, $g \cdot m^{-3}$
XRF	X-ray Fluorescence
Y	Microbial yield coefficient, g g^{-1}
z	Distance of travel in filter, m
ε	Bed porosity of the filter column
μ_m	Maximum degradation rate, s^{-1}
ρ_p	Carbon particle density, g m^{-3}
δ	Biofilm thickness

Chapter 1
Introduction

1.1 Background

Odor emissions from Wastewater Treatment Plants (WWTPs) raise environmental concerns. Hydrogen sulfide (H_2S) and ammonia (NH_3), the two most common odorous pollutants found in the off-gases of WWTPs, are highly toxic, corrosive and irritating with very low odor threshold concentrations (Devinny et al., 1999). In current practice, NH_3 and H_2S are widely treated using an integrated system of chemical acid scrubbers (for NH_3) followed by activated carbon tanks (for H_2S). However, chemical scrubbing is generally expensive in terms of the recurrent use of chemicals and wastewater is produced. Meanwhile, adsorption on activated carbon is also costly and exhausted carbon requires either regeneration or disposal as hazardous waste (Devinny et al., 1999).

Compared with the physical and chemical options, biological abatement technologies, especially biofiltration, have been proven to be more cost-effective and environmental friendly for the control of air pollution (Shareefdeen and Singh, 2005). In particular, biofiltration can treat several contaminants simultaneously, and is an economical alternative to treat a large volume of air with low concentrations of contaminants (Devinny et al., 1999; Shareefdeen and Singh, 2005). Moreover, several advantages make biofiltration technology attractive, including low capital and operating costs, low energy requirement, and the absence of residual products requiring further treatment or disposal (Ergas et al., 1995).

Activated carbon has been used as packing material in biofiltration for odor control with high efficiency (Chung et al., 2004; Yan et al., 2004; Duan et al., 2005a). Compared with traditional packing materials, e.g. compost solids, the technology offers several advantages, such as: (1) shorter gas residence time and thus smaller bioreactor required; (2) higher removal efficiency due to a combination of adsorption and biodegradation; (3) stronger resistance to fluctuation in loadings and pH; (4) favored biofilm formation; and (5) longer service lifetime. The scale-up of activated carbon biofilters is highly promising in industrial applications to be an alternative of physiochemical treatment technologies. The technology has been used successfully for full-scale treatment of petroleum hydrocarbons from a refinery (Graham, 1996).

However, activated carbon is relatively expensive compared with other packing materials (Webster et al. 1996). For example, activated carbon costs about \$900-1000 per m^3, while compost solids, the most widely used packing material previously, cost approximately \$25 per m^3 (Webster et al., 1997). The high cost renders the technology economically unattractive and prevents it from broad application (Medina et al., 1995; Webster et al., 1997).

One of the alternatives to activated carbon as packing material in biofiltration could be exhausted carbon. Exhausted carbon comes from the H_2S adsorption process and has become a common environmental problem in WWTPs (Hodge and Devinny, 1995; Devinny et al., 1999). For instance, the New York City Department of Environmental Protection operated 109 activated carbon tanks in WWTPs, each of which contained 11 tons of carbon. When the capacity of activated carbon for removing H_2S was exhausted due to the deposition of sulfur compounds, the exhausted carbon had to be replaced by fresh carbon (Bagreev et al., 2002). The replaced exhausted carbon requires thermal regeneration or disposal in landfills as hazardous wastes (Hodge and Devinny, 1995). Disposal is often done, because thermal regeneration breaks down the carbon resulting in more "fines" and its energy cost has also been increasing. Therefore, economic requirements have driven the re-use of exhausted carbon. It has been reported that exhausted carbon, loaded with pollutants such as phenol and surfactants, can be bio-regenerated by bacterial activity (Walker and Weatherley, 1998;

Klimenko et al., 2004; Aktas and Cecen, 2006). These phenomena suggest that the pre-adsorbed sulfur compounds on exhausted carbon could possibly be utilized by bacteria as an energy source.

Based on the assumption, if exhausted carbon is re-used in biofiltration, several advantages can be expected: (1) Low capital cost is required to use exhausted carbon (i.e., hazardous waste) as packing material; (2) Exhausted carbon could promote initial biofilm formation by providing pre-adsorbed sulfur compounds; (3) Part of adsorption capacity of exhausted carbon could be recovered for additional buffer in biofiltration system; (4) The start-up time of biofiltration could hopefully be shortened due to additional sulfur source; and (5) The service life of exhausted carbon will be extended.

In an industrial situation, except for H_2S, most emissions from WWTPs consist of other compounds, such as NH_3. Previous research is mostly simplified by examining the fate of a single gas, such as H_2S or NH_3 (Gracian et al., 2002; Duan et al., 2006; Kim et al., 2007). This allows an easier and more accurate interpretation of laboratory results observed. Only recent years, co-treatment of H_2S and NH_3 by biofiltration was reported (Malhautier et al., 2003; Chung et al., 2005; Galera et al., 2008). When biofilters were supplied with a mixture of H_2S and NH_3, substrate inhibition and microbial interactions were observed. NH_3 biodegradation (i.e. nitrification) was more difficult than H_2S biodegradation in the co-removal systems. The poor nitrification caused relatively low elimination capacity of NH_3 gas in co-removal biofiltration. Moreover, the removal of NH_3 gas was mostly attributed to absorption, adsorption or chemical reaction in terms of NH_3/NH_4^+ in liquid phase (Kim et al., 2002; Lee et al., 2005; Shanchayan et al., 2006; Galera et al., 2008). Since NH_3 gas was only transferred into liquid phase, liquid effluent from the biofiltration system requires a further treatment. Thus, a more efficient and effective process need to be developed to promote nitrification for the improvement of NH_3 gas removal and for the elimination of NH_3/NH_4^+ effluent from the co-removal system.

Biofiltration system can be improved by optimizing bioreactor types and substrates

acclimation strategy, besides packing material (Cho et al., 1992; Kar et al., 1996; Chung et al., 2007). Biofilters have been widely used in the removal of NH_3 or/and H_2S. The low nitrification was caused by either the accumulation of S and N compounds on the packing (Kim et al., 2002), or acidification of the system (Chung et al., 2001). In biotrickling filters, the recirculation liquid can remove metabolic products on the packing, and the packing acidification can be avoided due to better control of pH (Fortin and Deshusses, 1999). Moreover, biotrickling filter is an attractive technology for the removal of NH_3 because of its high water solubility. In addition, it was reported that substrates acclimation strategy was important for the removal of mixed substrates successfully (Kar et al., 1996). Through applying an optimal acclimation strategy, the removal of volatile organic compounds (VOCs) was enhanced greatly (Rozich and Colvin, 1986; Kar et al., 1996; Park, 2004). However, few studies have been found on applying a biotrickling filter and on optimizing substrates acclimation strategy for the co-removal of H_2S and NH_3.

1.2 Objectives and work scope

The overall objective of this study is to develop a highly efficient and economical biofiltration process for the co-removal of H_2S and NH_3 using H_2S-exhausted carbon as packing material. For this purpose, the following tasks are set for the study:

(I) Evaluating the feasibility of transferring exhausted carbon into biological activated carbon for the removal of H_2S in biofiltration

(II) Exploring and explaining the different mechanisms of H_2S abatement in biofilters using fresh carbon and exhausted carbon.

(III) Investigating the effect of substrates acclimation strategy on simultaneous biodegradation of H_2S and NH_3, especially on nitrification.

(IV) Evaluating a horizontal biotrickling filter (HBTF) packed with exhausted carbon for the co-removal of H_2S and NH_3 over a long-term operation.

1.3 Organization of the thesis

Chapter 2 is a detailed literature review and discussion on biofiltration as well as

biological activated carbon application in biofiltration. Chapter 3 describes the materials and methodology used in this study. Chapter 4 evaluates the feasibility of re-using exhausted carbon in biofiltration for the removal of H_2S. Chapter 5 focuses on the removal mechanisms of H_2S employing exhausted carbon in biofiltration by mathematical model simulation together with experimental data. Chapter 6 investigates the effect of substrates acclimation strategy on simultaneous biodegradation of H_2S and NH_3. Chapter 7 evaluates the HBTF packed with exhausted carbon for the co-removal of H_2S and NH_3 over a long-term operation. Chapter 8 summarizes some important conclusions from the experimental results and outlines some recommendations for future work.

Chapter 2
Literature Review

2.1 H_2S and NH_3: two major odorous compounds

Odor-causing compounds, such as hydrogen sulfide (H_2S) and ammonia (NH_3), are one of major categories of anthropogenic inorganic nitrogen (N) and sulfur (S) air pollutants (Shareefdeen and Singh, 2005). H_2S and NH_3 often co-exist and are released in large quantities from agricultural activities and industrial processes such as livestock farming, food and rubber processing, leather manufacturing, wastewater treatment, landfills for waste disposal, and hog manure (Devinny et al., 1999; Malhautier et al., 2003; Jones et al., 2004; Shanchayan et al., 2006). Particularly, H_2S and NH_3 are the major contributors of sewage odor with very low odor thresholds (1.1 ppbv for H_2S and 37 ppbv for NH_3) and high toxicity (Kim et al., 2002; Chung et al., 2007).

2.1.1 H_2S

Table 2.1 presents the sources and the typical concentrations of H_2S measured in wastewater treatment plants (WWTPs). Depending on the process unit involved, H_2S concentrations can range from 1 to several hundred ppmv.

H_2S has dominated the literature in studies on the control of sewer odors associated with municipal and industrial wastewater treatment. This is likely due to three

characteristics of H_2S: (1) an extremely low odor threshold, with a threshold of only 1.1 ppbv; (2) a very high and acute toxicity; and (3) easily absorbed into moisture on sewer pipe walls, with subsequent biological conversion by sulfide-oxidizing bacteria (SOB) to sulfuric acid, which leads to corrosion of the sewer pipe. At low concentrations, H_2S gas has a rotten egg smell, and will cause throat and eye irritations. It quickly deadens the sense of smell, and is lethal at high concentrations. H_2S enters the body through the lungs, and causes the respiratory system of the body to shut down, which eventually causes the heart to stop. The maximum permissible 8-hour H_2S concentration is about 20 ppmv. A 5-minute exposure to 1000 ppmv concentration in air can be fatal to humans.

Table 2.1 H_2S source characterization in WWTPs

Source	**Concentration (ppmv)**	**Reference**
Pump station	40-140	(Vaith et al., 1996)
Lift station	5-150	(Burrowes et al., 2001)
Headworks	6-94	(Jubinville et al., 1997)
Grit channels	6-20	(Jubinville et al., 1997)
Headworks/Primary clarifiers	250-300	(Vaith et al., 1996)
	50-290	(Burrowes et al., 2001)
Aerated grit tanks	0.01-3.9	(Witherspoon et al., 1999)
Primary clarifier launder	4-35	(Jubinville et al., 1997)
Primary sedimentation tanks	0.1-12	(Witherspoon et al., 1999)
Primary clarifiers	5.6	(Bowker, 1999)
Primary clarifier feed wells/launders	77	(Bowker, 1999)
Aeration tanks	10 (peak)	(Koe and Yang, 1999)
Digester vents	1-20	(Witherspoon et al., 1999)
Biosolids holding tank	100	(Bowker, 1999)
Biosolids gravity thickener tank	50-200	(Burrowes et al., 2001)
Biosolids dewatering and storage	3	(Burrowes et al., 2001)
Biosolids holding tank	111	(Jubinville et al., 1997)

2.1.2 NH_3

NH_3 is a colorless, toxic, reactive, and corrosive gas with a very sharp odor (Busca and Pistarino, 2003). A considerable amount of NH_3 is emitted from different industrial processes, such as wastewater treatment, composting, livestock production, farming, petrochemical refining, food processing, and paper and pulp manufacturing, etc. (Chung et al., 1997; Busca and Pistarino, 2003; Hong and Park, 2005; Gabriel et al., 2007). Overall, of the total anthropogenic N compound emissions, NH_3 accounts for about 55%, equivalent to approximately 43 million tones of N (Krupa, 2003). NH_3 emissions in a composting process of organic fraction of municipal solid wastes varies between 18 and 150 g NH_3/mg waste (Clemens and Cuhls, 2003). NH_3 concentrations up to 460 ppmv have been reported in exhaust gases from sludge composting (Haug, 1993). High temperature and alkaline pH levels encountered during aerobic composting processes are conducive to the release of NH_3.

It has been reported that exposure to NH_3 above 1 ppmv could cause nausea, headaches, bronchial tracts irritation and burning sensation in the eyes and skin (Taghipour et al., 2008). 400 ppmv of NH_3 can cause immediate irritation of the throat, above 1500 ppmv can produce cough, and above 2500 ppmv are life threatening. The US Occupational Safety and Health Administration (OSHA) have set a limit of 50 ppmv over an 8-h work day, 40-h work week for ammonia vapor in ambient air (Busca and Pistarino, 2003). As an atmospheric pollutant, NH_3 gas can undergo various photochemical, thermal, aqueous phase and heterogeneous reactions to form NH_3 aerosols or particulate matter. It ultimately gets deposited onto the land or in water bodies, and has the potential to cause secondary problems such as eutrophication of water bodies or acidification of land masses. NH_3 gas is highly soluble in water and readily forms ammonium ions in solution. The ammonium ion is the predominant form in most environmentally problematic solutions.

Therefore, the control of H_2S and NH_3 gas is essential to mitigate the environmental impact and to protect public health.

2.2 Biofiltration for odor abatement

The traditional technologies for odor control can be segregated into either physical treatment (e.g. activated carbon sorption, incineration) or chemical methods (e.g. chemical scrubber, thermal and catalytic oxidation). In the adsorption process, adsorption capacity is limited and exhausted adsorbents need to be land-filled or incinerated. Incineration is an expensive method due to high energy requirements and it is not economical if concentration levels are low and large airflow volumes need treatment. This process also produces the highest amount of greenhouse gases (i.e., CO_2, NO_x gases). In scrubbing process, chemical costs are often high and liquid waste is produced, which needs further treatment.

Compared with physical and chemical methods, biological abatement technologies, especially biofiltration, offer more economical and environmentally benign method for the control of air pollution (Shareefdeen and Singh, 2005). It doesn't require a large amount of chemical addition (nutrition can be the secondary effluent from a WWTP) and can be operated at room temperature. Furthermore, biological digestion transforms certain pollutants into less toxic and odorless compounds. Biological treatments are energy-efficient, and particularly well suited to treat low-concentration emissions when the pollutants are readily biodegraded (Devinny et al., 1999).

Biofiltration is also believed to be the most economical option for treating odor-causing compounds (Leson and Winer, 1991). It was estimated that the operational and maintenance costs of a lava rock biotrickling filter for odor control would be US$120 per million m^3 of air treated, which was only 20% of the cost of a sodium hydroxide chemical scrubber ($600 per million m^3 of air treated) (Morton and Caballero, 1996). The estimated capital costs for a carbon adsorption bed, an incineration system and a biofilter were US$625,000, US$612,000 and US$430,000, respectively, and the annual operational and maintenance costs were US$1,950,000, US$380,000 and US$94,000, respectively (Laustsen et al., 1999). The capital costs can be even less when full-scale biofiltration systems are retrofitted from the existing chemical scrubber (Gabriel and Deshusses, 2003).

The following sections will provide a general view of the usage of the biofiltration technology for odor removal, including biofiltration configurations, parameters that affect biofiltration operation, and degradation mechanisms of odorous pollutants.

2.2.1 Biofiltration configurations

The two most promising and widely utilized bioreactors for odor control are biofilters and biotrickling filters (Schroeder, 2002; Cox and Deshusses, 2002b). In a biofilter (Figure 2.1a), the contaminated air passes through a moist packed bed either in an up-flow or a down-flow mode, generally packed with natural material (e.g. compost, soil). A humidification chamber is necessary in order to saturate air with water for an optimal biodegradation activity. Microbial communities grow as biofilm on the packing surface. Biofilters can be operated in two or more individual beds, in parallel, or in series. Biofilters operated in parallel offer the flexibility to isolate individual beds for maintenance without completely shutting the total system down. Beds in series allow for the treatment of individual contaminants through different beds. For instance, two-stage biofilters had been used to treat waste air stream containing H_2S and NH_3 (Chung et al., 2007).

A biotrickling filter (Figure 2.1b) works in a similar manner as a biofilter. The packing material is usually made of some synthetic or inert materials. Odorous air is introduced either down-flow and up-flow or cross-flow through the packed bed (Figure 2.2). A distinctive feature of biotrickling filters is the recirculation of a liquid phase over the packing. Liquid is pumped from a reservoir and added to the top of the vessel, and flows downward over the packing. The recirculation liquid supplies water and nutrients, such as nitrogen, phosphorus and potassium, as well as a buffer solution, etc., to the biofilm. Moreover, the liquid can remove metabolic products that would otherwise accumulate in the biofilm in possibly toxic concentrations. The bed acidification can be avoided due to better pH control (Fortin and Deshusses, 1999).

Continuous monitoring and adjustment of chemical parameters in the recirculation liquid allow for better control of microbial activity in the biofilm. This is an important

advantage of biotrickling filters over biofilters. In general, most of the pollutant is biodegraded in the biofilm, but part may also be removed by microbes suspended in the liquid (Cox et al., 2000). Biodegradation products will leave the system via the liquid purge, along with small amounts of biomass and dissolved pollutant.

Currently, odor emissions are usually controlled by chemical scrubbing in WWTPs. There would be significant economical and safety benefits if chemical scrubbers could be converted to biotrickling filters. It is cheaper to operate biotrickling filters than scrubbers. It is not necessary to use toxic and dangerous chemicals in biotrickling filters. In the past several years, some full-scale chemical scrubbers have been conversed into biotrickling filters successfully (Koe et al., 2002; Gabriel and Deshusses, 2003).

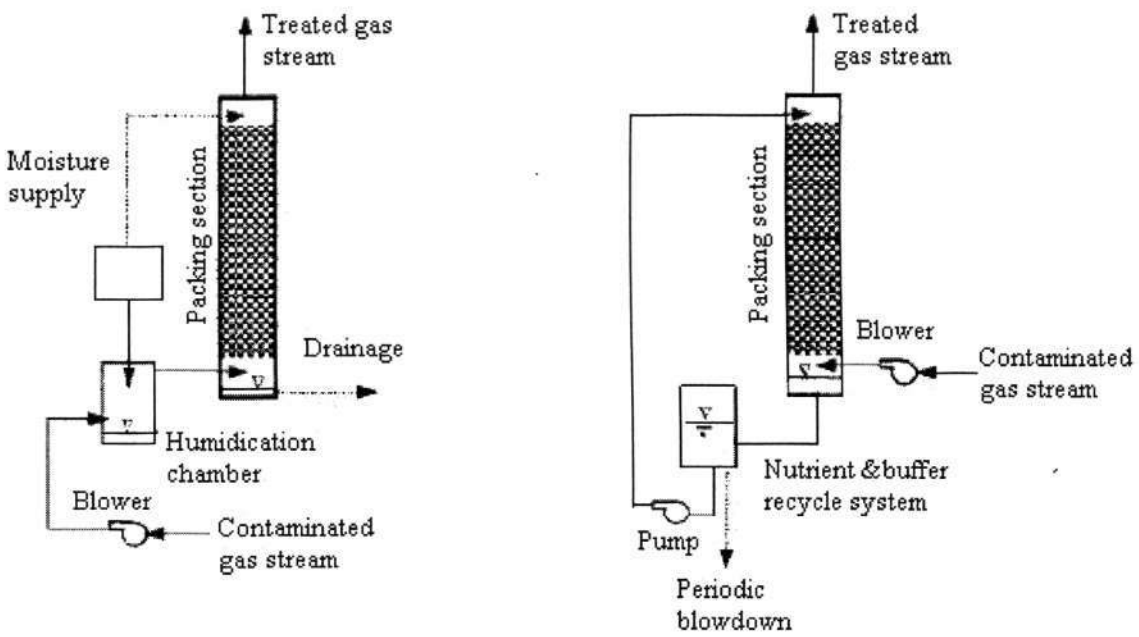

(a) Biofilter (b) Biotrickling filter

Figure 2.1 Typical biofilter and biotrickling filter systems (Schroeder, 2002)

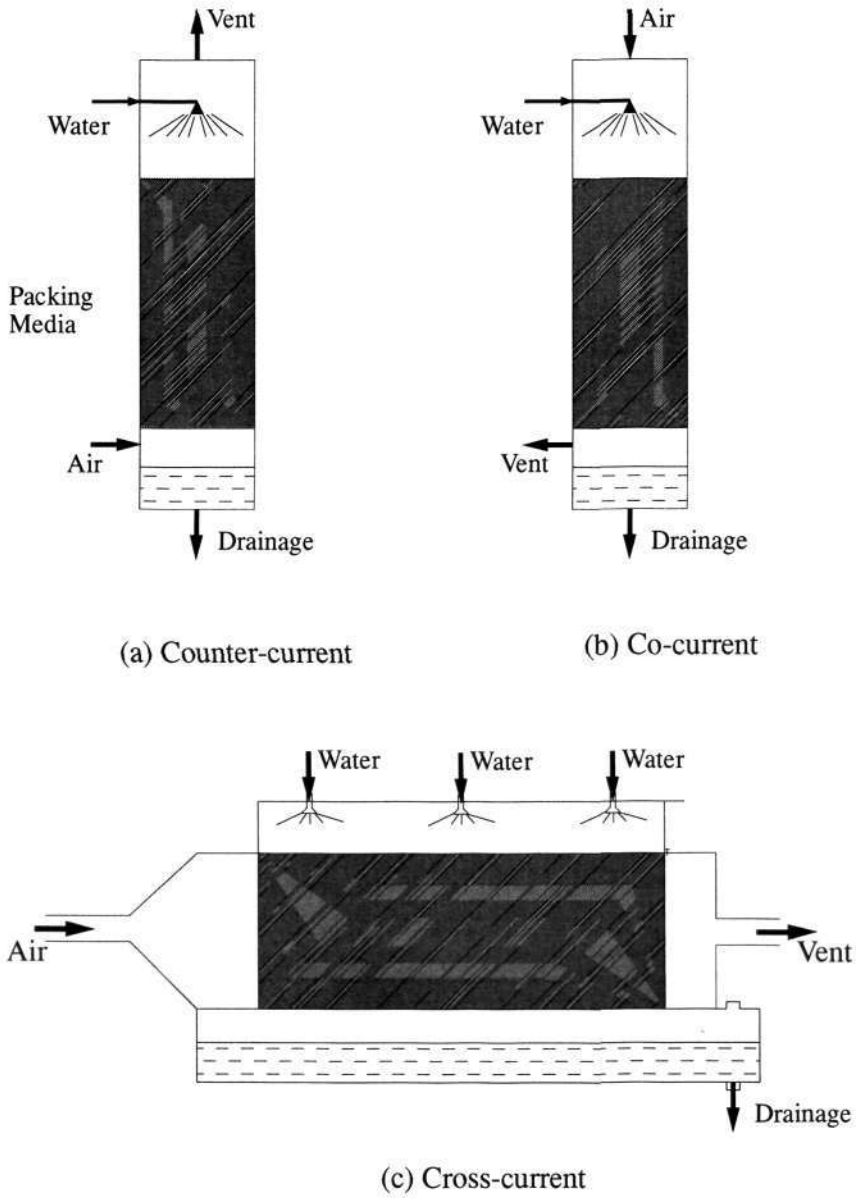

Figure 2.2 Existing configurations of a biotrickling filter

Table 2.2 shows the advantages and disadvantages of biofilters and biotrickling filters. It can be seen that biotrickling filters can overcome some obstacles in biofilters. One drawback of biotrickling filters is transferring odorous pollutants from the gas phase to the liquid/biofilm phase because of the additional aqueous phase formed over the biofilm with continuous water trickling. However, H_2S and NH_3 can be dissolved in

water film easily and then biodegraded. Hence, it will be suitable to treat the two pollutants by biotrickling filters.

Table 2.2 Advantages and disadvantages of biofilters versus biotrickling filters (Shareefdeen and Singh, 2005)

	Advantages	**Disadvantages**
Biofilters	• Less complex to build and to operate; • Simple and flexible design with low capital costs	• Poor process control; • Poor control of water content; • Not applicable to treat pollutants that are degraded to acid end products; • Medium change-out required frequently; • A relatively large footprint required
Biotrickling filters	• Good process control; • Optimal water content obtained; • Applicable for pollutants that are degraded to acid end products; • High degradation capacities; • Relatively small footprint; • No pre-humidifier required; • No media change-out; • Low pressure drop; • Low operational cost	• More complex to build and to operate; • Biomass accumulation in the bed; • Transferring limitation from gas phase to liquid/biofilm phase

2.2.2 Design and operation considerations

2.2.2.1 Filter bed material

The main function of filter materials is to provide the contact between the gas-phase contaminants and active microbial cultures as a biofilm on the packing surface (Shareefdeen and Singh, 2005). The other functions of the packing are to distribute the gas flow evenly within the bed's cross-sectional area with low pressure drop, distribute any liquid nutrients sprayed on the bed's surface, and prevent the accumulation of biomass to clogging. Thus, selecting a proper packing material is an important step towards the development of a successful biofiltration operation (Cho et al., 2000). Natural organic packing materials, such as soil (Swanson and Loehr, 1997), compost (Yang and Allen, 1994), peat (Yoon and Park, 2002), wood bark (Smet et al., 1996), and synthetic media, such as ceramic saddles (Hirai et al., 2001), polyethylene pall rings (Koe and Yang, 2000), activated carbon (Duan et al., 2006), have been used in biofiltration.

Natural packing materials contain bacteria dispersed within the structure of the medium itself, rather than as a distinct biofilm on the surface and within the pores. Synthetic packing materials consist of structures in which active bacteria have to be inoculated and are not inherently present in the medium's structure. Synthetic media can be broadly classified as one of two types: (1) adsorbing, which exhibit significant physical adsorption of the contaminants; and (2) non-adsorbing, where there is negligible physical adsorption of the contaminants by the media. The adsorption on the packing materials can increase biofiltration rates, mainly due to a combination of adsorption-desorption and biodegradation within the biofilm. It results in increased amounts of active biomass within the biofilter (Shareefdeen and Singh, 2005). It should be noted that this increase in biofiltration rates is only observed when the adsorbed contaminant can desorb effectively from the packing material.

Table 2.3 summarizes the advantages and disadvantages of several natural and synthetic packing materials that have been used in biofiltration. It can be seen that there is some inefficiency relative to the natural media, which at present render the

technology economically non-viable. When biotrickling filters are used, synthetic support media have several important advantages over the natural media. It includes high interfacial area, capability to support growing biofilm, stable composition over time, much more homogenous, minimizing the problems of pressure drop and channeling. However, the absence of nutrients and microorganisms are their drawbacks. To some extent, the external addition of nutrients allows a better control and regulation on the amount of nutrients available to the microorganisms.

Table 2.3 Analysis of packing materials for biofiltration (Devinny et al., 1999; Shareefdeen and Singh, 2005)

	Material	**Advantages**	**Disadvantages**
Natural organic media	Compost	Large diversity of microorganisms; good water retention; neutral pH; inexpensive; nutrient rich	High pressure drop; subject to bed compaction, clogging; short circuiting aging; heavy metals; requiring medium replacement
	Soil	Inexpensive; large microbial population	Low permeability; low elimination capacities; high pressure drop; large space requirement; short-circuiting and clogging; difficult moisture control
	Wood chips	Inexpensive	No nutrient; low pH-buffering capacity; low specific surface areas; requiring medium replacement
	Peat	Low pressure drop	Inoculation requirement; difficult moisture control
Inorganic or synthetic media	Gravel, lava rock	Low cost; rough surface	Low surface area; low void fraction; high bulk density; gas channeling; not chemical inert
	Polymeric foam	Good retention of water; low bulk density; high porosity	Easily clogged; difficult to slough-off biomass growth; compacts due to biomass weight
	Plastic packing	Good liquid distribution; low gas pressure drop; low bulk density	Surface unsuitable for biofilm attachment and growth; insufficient void fraction; high cost
	Ceramic	High surface area; high void fraction; low bulk density	High cost; not manufactured in large sizes; have to be cut to fit vessel; high bulk density
	Activated carbon	Excellent structural properties; uniform particle size; good resistance to crushing; substantial water-holding capacity; good adsorption capacity; good surface for microbial attachment; long lifetime	High cost

2.2.2.2 Microorganisms

Several groups of microorganisms, primarily bacterial species, are responsible for degradation of air pollutants in bioreactors. A number of bacteria capable of oxidizing H_2S were exploited, including phototrophic (e.g., *Chlorobium limicola f. thiosulfatophilum*), heterotrophic (e.g., *Xanthomonas, Pseudomons)*, and autotrophic (e.g., *Thiomicrospira, Thiobacillus and Thiosphrera*) bacteria. Chemoautotrophic bacteria, e.g., *Thiobacilli*, are particularly advantageous because of their simple nutritional requirement, high removal rate, using only CO_2 as carbon source, and low microbial cell yield (Sublette and Sylvester, 1987; Jensen and Webb, 1995; Hautakangas and Mihelcic, 1999). They are naturally present in the sanitary sewer system and treatment plant, and converts H_2S to sulfate in a low growth and energy intensive manner. The genus *Thiobacillus* includes both acidophobic bacteria that prefer a pH near 7 and acidophilic bacteria that grow at low pH values. It allows an efficient H_2S oxidation over a wide pH range. However, most known heterotrophs prefer neutral pH (Chung et al., 2001).

Bacteria able to grow at the expense of reduced inorganic nitrogen compounds are called nitrifying bacteria. No bacteria are known to carry out the complete oxidation of NH_3 to nitrate. Thus, the oxidation process results from the sequential action of two separate bacteria groups, ammonia-oxidizing bacteria (AOB) and nitrite-oxidizing bacteria (NOB). An efficient nitrification process requires balanced activity of the two bacterial groups. Most of the nitrifying bacteria are obligate chemoautotrophy (Madigan et al., 2002), utilizing CO_2 or HCO_3^- ion as the sole carbon source for cell growth (Shuler and Kargi, 1992). Autotrophic nitrifiers are notoriously slow growers, and are also sensitive to a variety of growth conditions, in particular pH, temperature, and salt concentrations. This slow growth does not allow nitrifiers to be maintained in activated sludge of wastewater treatment facilities unless special attention is paid to sludge age and retention. Thus, nitrification typically involves fixed growth systems.

Degradation of NH_3 can also take place by heterotrophic nitrifiers (e.g., *Alcaligenes*, *Pseudomonas*, and *Arthrobacter sp.*), which perform better under acidic environments (Chung et al., 1997). However, the process of heterotrophic nitrification does not

generate energy and may not oxidize NH_3 completely: the final product is often nitrite instead of nitrate (Chung et al., 1997). The nitrification rate of heterotrophs is significantly lower than that of autotrophs, resulting in higher population size during NH_3 degradation. In addition, the heterotrophs require an external organic carbon source, which results in clogging problems due to quick biomass growth. The biomass concentrations of heterotrophic nitrifiers were 10^3-10^4 times larger than those of autotrophs at the similar removal capacity (Prosser, 1989; Laanbroek et al., 1994).

Hence, the strict autotrophic bacteria are preferred in the removal of H_2S and NH_3 to simplify nutritional requirements, obtain high performance and avoid clogging problems.

2.2.2.3 Inoculation and acclimation

Biotrickling filters need to be inoculated with microorganisms. Selection of the inoculums is potentially a major factor determining the removal efficiency in bioreactors (Sercu et al., 2005). The following sources are commonly used (Kennes and Veiga, 2001): (1) activated sludge from WWTPs; (2) soil or water samples from sites or plants contaminated with the pollutant of interest; (3) consortia that are enriched in the laboratory on the pollutant of interest; (4) pure cultures, degrading the pollutant of interest; (5) samples of biotrickling filters treating the same or a comparable waste gas stream. Mixed consortia are preferred for biological treatment systems placed in the field since maintaining a pure culture is not feasible, and in many cases, not desirable. Moreover, the start-up phase could be significantly reduced by inoculation with an adapted consortium, compared with activated sludge. Selection of the inoculum source becomes increasingly important when the pollutant is more difficult to degrade (Figure 2.3).

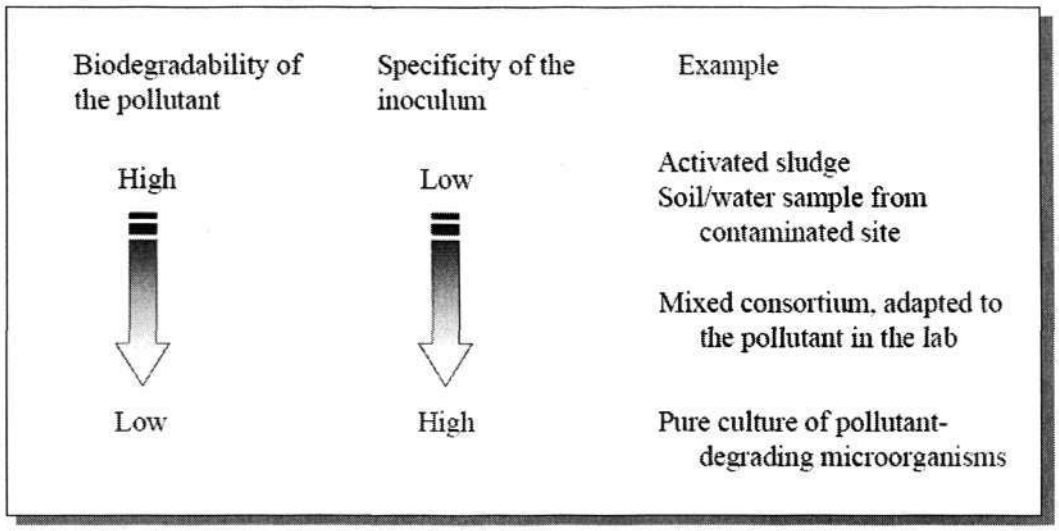

Figure 2.3 A inoculation guide for biotrickling filters (Kennes and Veiga, 2001)

Acclimation is a period required for the development of optimum population of substrate-consuming microorganisms before they start vigorous biodegradation (Jones et al., 2004). Selective acclimation (enrichment) of suitable microbial populations in biotrickling filters is a key condition for successful treatment (Cox and Deshusses, 2002a). Acclimation period is dependent on substrate, concentration, packing materials, operation and environmental conditions (Swanson and Loehr, 1997). An acclimation period or lag period during the start up of biofiltration operations is always reported (Gracian et al., 2002; Choi et al., 2003; Chen et al., 2005). Choi et al. (2003) reported that a ten-day acclimation period was required before steady state conditions were observed in their systems for treating NH_3 gas. Gracian et al. (2002) observed that the acclimation period was 3-4 weeks for the appearance of nitrite and nitrate for the removal of NH_3 in a biofilter. Acclimation periods have also been reported in biofiltration systems after periods of shut down, when concentrations have been increased, or due to shock loads (Chen et al., 2004; Ho et al., 2008). Restart acclimation times are generally shorter than those during the initial start-up.

Explanations of the acclimation period include: 1) microbial enzymes may be induced only after exposure to the chemical or 2) initially small populations of microorganisms capable of degrading the pollutant may be present, thus time is

required to allow them to grow up and cover sufficient surface to the point where significant degradation can occur. It indicates that for some slow-growing organisms, such as nitrifying bacteria, a lengthy acclimation period may be required and pre-acclimation prior to bringing a system on-line may be necessary.

The suitable acclimation method was very important for the removal of mixed substrates (Kar et al., 1996). Substrate and microbial interactions were observed for the removal of H_2S and NH_3 during the start-up period. Nitrification happened after 3-7 weeks of operation, while H_2S biodegradation was carried out at the beginning of biofiltration (Malhautier et al., 2003; Chung et al., 2005; Galera et al., 2008). Generally, substrate interactions and degradation patterns in biofilters will depend on the microbial community that is established in the column which, in turn may be a function of the acclimation history. The substrate interactions can be different even in the same microbial culture, depending on how the microbial culture was initially acclimated (Kar et al., 1996; Swaminathan et al., 1999). Once an adequate culture is established, the level of substrate interactions was somewhat reduced (Rozich and Colvin, 1986).

2.2.2.4 Contaminant composition and dynamic mass loading

The contaminant composition affected both mass transfer rate and biodegradation rate. Many lab-scale studies have been undertaken with a single pollutant that allows an easier and more accurate interpretation of results and phenomena observed. However, at the industrial scale more than one pollutant will appear in many cases. For example, waste gases emitted from composting facilities in WWTPs contain NH_3 mixed with other odorous compounds such as H_2S. To degrade these compounds, a specialized mixture of microorganisms is required. But not all these microorganisms will present optimal activity under the same process conditions. It can be expected that the biofiltration process be influenced by microbial interactions like symbiosis, competition or inhibition. Substrate and microbial interactions were observed when the biofilters were supplied with a mixture of H_2S and NH_3 (Malhautier et al., 2003; Chung et al., 2005; Galera et al., 2008).

The mass loading rate is defined as the amount of odor-generating compounds that was introduced to the system per unit time per unit volume of the packing material. One underlying assumption is that the performance depends only on the pollutant load. Hence, low concentration-high flow rates conditions lead to similar elimination capacities as high concentrations-low flow rates. The maximum elimination capacity of a bioreactor is the maximum odor loading rate that the bioreactor can bear without inhibiting its microbial activity. There are essentially three operating regimes: (1) Low loading, also called first-order regime, the elimination capacities and loadings are identical and the pollutant is completely removed; (2) Intermediate range, breakthrough of the pollutant occurs; and (3) High loading, also called zero order regime, the bioreactor is operated at its maximum elimination capacity. Increases in loading do not result in further increases in elimination capacities, and the removal efficiency decreases.

At extremely high loadings, biofiltration technology is not the best choice for pollutant removal because of potentially inhibitory effects on biomass activity. Under most conditions, the high loadings will result in poor performance (Hartikainen et al., 1996; Cho et al., 2000; Kim et al., 2000a; Kim et al., 2000b), which may partly be buffered and avoided by using carrier materials with high adsorptive capacity, i.e., activated carbon (Weber and Hartmans, 1995). Microorganisms work best when loadings are constant. Periods without contaminant will gradually cause the ecosystem to lose its ability to degrade the compound. Some studies have reported on removal performance of the transient loading (shock loadings or starvation) of odor or VOC pollutants (Wani et al., 1998; Marek et al., 2000; Duan et al., 2005a). However, the relationship between transient loadings and bioreactor response remains poorly understood (Wright et al., 2005). Moreover, minor attention has been given to understand the characterization and activity of the process culture during shock loadings and starvation of bioreactor (Cox and Deshusses 2002).

2.2.2.5 Liquid trickling

A liquid phase flowing through a biofilter/biotrickling filter bed may serve a number of purposes. It may maintain adequate moisture content, dilute toxic metabolic

products, provide additional nutrients for bacteria growth and provide buffering for pH stability (McNevin and Barford, 2000). The amount of water is perhaps one of the most important parameters in a biofilter. Neglect of the water content or difficulties in controlling it is the most common cause of poor biofilters operation. Microorganisms cannot be active without water whilst the presence of water affects the transfer of contaminant from the air to biofilm. For the low moisture content (27.6%), biofilters had little removal of H_2S and NH_3 (Nicolai and Janni, 2001). 40 ~60 wt% water content was found to result in the best biofilters performance (Yang and Allen, 1994).

The recirculation of a liquid phase over the packing is a distinctive feature of biotrickling filters. The effect of liquid trickling rate on the elimination of H_2S was found to be nil at low gas velocity, and significant at high gas velocity (Kim and Deshusses, 2005). Treatment of pollutants that release acid end-products, such as H_2S and NH_3, is a case that requires special attention. When a trickling rate is too low, the liquid may not be able to remove the produced acids fast enough so that the pH could be reduced to the extent of inhibiting microbial activity (Oh and Bartha, 1994). However, when the liquid flow rate is higher, the lower amount of H_2S was degraded (Jin et al., 2005a). It was possibly because the increased thickness of the liquid phase limited the mass transfer between the gas phase and the liquid/biofilm phase (Zhu et al., 1998b).

2.2.2.6 pH

Most biofilters are designed for operation near a neutral pH, which is generally accepted as a benign condition (Kim and Deshusses, 2005). Microorganisms often do not tolerate pH fluctuations of more than about 2 or 3 pH units for maintaining appreciable growth and biodegradation rates. Variations of pH can result in a loss of diversity in the microbial population and even destroy the resident population with subsequently marked reduction in removal rates of some odorous compounds. The pH ranges for the growth of autotrophic nitrifying bacteria, *Nitrosomonas sp.* and *Nitrobacter sp.*, are 5.8-8.5 and 6.5-8.5, respectively (Villaverde et al., 1997). Hartikainen et al. (1996) demonstrated that nitrification did not occurre at pH 4. pH control is important significantly for maintaining high removal of ammonia (Yani et

al., 1998).

A biofilter is often acidified in gas streams containing H_2S (Cho et al., 1992; Yang and Allen, 1994; Shinabe et al., 1995), which result in substantial reduction in treatment efficiency. Optimal activity for both autotrophs and heterotrophs for H_2S biodegradation was at pH 6.0-7.0 (Chung et al., 1996a; Jin et al., 2005b), but a notable exception is *acidophilic thiobacilli* which thrive at low pH (Jin et al., 2005a). However, at low pH, fungi may overgrow the bacteria, which may affect bioreactor performance negatively (Cox et al., 1993). Moreover, low pH will not benefit the adsorption of H_2S on the surface of packing material or biofilm.

Special provisions must be made to treat chemicals whose biodegradation results in acid end products, because biofilters are not designed with continuously trickling liquid streams to washout acids. The solid media and microbial population must be replaced when a biofilter becomes too acidic, which make all microbial activity lost (Cho et al., 1992; Yang and Allen, 1994). Therefore, if biofiltration leads to the accumulation of acids like nitric acid and sulfuric acid in the biofilm, periodical backwashing or adding buffering materials may have to be considered to control the pH in biofilters (Ergas et al., 1995; Kapahi and Gross, 1995).

2.2.2.7 Pressure drop

The bed pressure drop is an important parameter in biofiltration because it is taken into account in the operating costs. In general, there is an approximately linear increase in pressure drop with increasing gas flow rate (Ergas et al., 1995), which begins to become exponential at higher flow rates (Morgan et al., 2001). At a given gas flow rate, the pressure drop increase exponentially with increased biomass (Morgan et al., 2001) and with decreasing particle size, especially for particles less than 1 mm (Brennan et al., 1996). The over watering and compaction of the filter bed over extended periods of usage will also give rise to prohibitive pressure drops (Pinnette et al., 1994). Pressure drop should not be too high so that energy costs can be maintained at low level during the running of a filter.

The methods that alleviate pressure drop includes increasing packing particle size, increasing bed porosity, or reconfiguring the biofiltration system (e.g. convert gas-liquid flow directions from counter-current to co-current or cross-current, divide bed height into several individual biofiltration systems in series). Synthetic packing materials generally lead to lower pressure drops than natural organic ones. Moreover, a non-uniform flow distribution and channeling are also more typical of organic carriers than of structured synthetic ones. Hence, the addition of bulking agents (e.g., perlite, bark, etc.) to natural organic packing allows slowing down the increase of pressure drop and optimizing flow characteristics in conventional biofilters.

2.2.3 Removal of H_2S or/and NH_3 by biofiltration

Tables 2.4, 2.5 and 2.6 summarize some representative studies on the treatment of H_2S, NH_3 and the mixture using biofiltration, respectively. Bioreactor types, packing materials, microbial culture, inlet concentration, empty bed residence time (EBRT) and pollutant removal performance were listed for easy references. In order to gain a perspective viewpoint on the current state-of-the-art of biofiltration, a direct comparison was made after standardizing the different units used in these studies. The following general observations can be found:

(I) For bioreactor types, biofilters (BF) were used more than biotrickling filters (BTF) in the biofiltration processes, especially for the removal of NH_3 and the mixture.

(II) For packing materials, organic and inorganic materials have attracted almost the same extent of attention, but more organic materials have been used for the removal of NH_3.

(III) For microbial culture, activated sludge was used widely. *Thiobacillus sp.* was applied in H_2S biodegradation while enriched nitrifiers were used for NH_3 degradation.

(IV) For inlet concentration, a wide range was applied and averaged at about 100 ppmv for H_2S only, and averaged at about 150 ppmv for NH_3. However, inlet concentrations were lower for mixed odors, possibly due to certain complex interactions between the two odor gases.

(V) For EBRT, a wide range has been applied, 2-200 s, while a longer EBRT (20-180 s) was needed for the biodegradation of mixed gases than that of a single gas.

(VI) For removal performance, large fluctuations in the removal efficiency and removal capacity were reported. The removal efficiency of NH_3 was relatively low in the co-removal biofiltration. The effectiveness of biofilters toward treating high concentrations of NH_3 is debatable.

(VII) Co-treatment of H_2S and NH_3 by biofiltration starts to be considered only recently.

As shown in Table 2.6, simultaneous elimination of H_2S and NH_3 occurred in biofiltration. The removal of NH_3 was generally inhibited at high loadings of H_2S and NH_3 (Kim et al., 2002; Malhautier et al., 2003), while the removal of H_2S was not as difficult as that of NH_3 in a co-removal system. The low removal capacity of NH_3 was caused by either the accumulation of elemental sulfur and $(NH_4)_2SO_4$ on the packing (Kim et al., 2002; Malhautier et al., 2003), or acidification of the system (Chung et al., 2001). The products accumulation and bed acidification could be attributed to the use of biofilters.

Biotrickling filters could allow a better control of operational conditions (Fortin and Deshusses, 1999a), e.g., proper pH and less toxic accumulation of biodegradation products (Armeen, 2006). In other words, bed acidification can be avoided due to the fact that biodegradation products are washed out of the filter continuously. Moreover, biotrickling filter is an attractive technology for the removal of NH_3 because of its high water solubility. However, very few studies have been found on using a biotrickling filter for the co-removal of the two odors (Chung et al., 2005). The fundamentals insight into the interaction between the two odors and removal mechanisms in biofiltration is not understood clearly.

Table 2.4 A summary of previous work on the removal of H_2S in biofiltration

Bioreactor	Packing material	Microbial culture	Inlet conc. (ppmv)	EBRT[a] (s)	EC[b] (g m^{-3}·h^{-1})	RE[c] (%)	Reference
BTF	Polypropylene	*T. Thioparus TK-m*	35	8	25	95	(Tanji et al., 1989)
BF	Peat	Night soil	40-300	18-120	25		(Hirai et al., 1990)
BF	Peat	A. *Thiobacillus* HA43	100-200		50		(Cho et al., 1991)
BF	Compost	No	5–2650	23–200	130	99	(Yang and Allen, 1994)
BTF	Ceramic	Activated sludge	100-200	10-16	0.9g kg^{-1}.d^{-1}		(Shinabe et al., 1995)
BF	Ca-alginate	A. *Thiobacillus thiqmus CH11*	5-100	28-140	23	70	(Chung et al., 1996b)
BTF	Plastic fibers	Activated sludge	27-4416	38	63	97.8	(Li et al., 1998)
BF	Immobilized beads	*T. novellus CH3*	10-60	72-144		99.5	(Chung et al., 1998)
BTF	Pall ring	A. *T. thiooxidans*	0.5-25	10-15	82	90	(Zhou, 2000)
BF	Porous lava	A. *T. thiooxidans AZ11*	200-900	9-18	455	99.9	(Cho et al., 2000)
BTF	Pall rings	A. *Thiobacillus thiooxidans*	20-100	5-30		70-90	(Wu et al., 2001)
BF	Pig manure + sawdust	No	50-220	14-27	41	> 90	(Elias et al., 2002)
BTF	Plastic Pall rings	A. mixed culture	0-190	11-84	23	100	(Jin et al., 2005a)
BTF	AC	A. *Thiobacillus sp.*	20	4	113	98	(Duan et al., 2005a)
BF	Biomedia	Mixed culture	10-130	32-51	8	52	(Kim et al., 2008)
BF	UP20	Activated sludge	100	57	9	93	(Dumont et al., 2008)
BTF	Iron foam	Activated sludge	20-280	20-60	41	95	(Goncalves and Govind, 2008)
BF	AC	Mixed culture	200-4000	103-240	125	84	(Rattanapan et al., 2009)

Remark: [a] EBRT: empty bed residence time; [b] EC: elimination capacity; [c] RE: removal efficiency. BF = biofilter; BTF = biotrickling filter.

Table 2.5 A summary of previous work on the removal of NH_3 in biofiltration

Bioreactor	Packing material	Microbial culture	Inlet conc. (ppmv)	EBRT[a] (s)	EC[b] (g m^{-3}·h^{-1})	RE[c] (%)	Reference
BF	Ca-alginate	*Arthrobacter oxydans CH8*	10-60	35-70	1.2 g N/kg media.d	97	(Chung et al., 1997)
BF	Peat	Night soil sludge	28-220	10-55	33	93	(Yani et al., 1998)
BF	Rock wool	Night soil sludge	42-290	12-53	60.7		(Kim et al., 2000a)
BF	Compost/GAC	Activated sludge	20-500	32-80	13.5	95	(Liang et al., 2000)
BF	Compost	Nitrifying culture	110-137	40-131	5.8–9.4	94	(Smet et al., 2000)
BF	Perlite	Nitrifying culture	20-50	138		99.9	(Joshi, 2000)
BF	Compost	Mixed culture	>100	21	12.5	87	(Demeestere et al., 2002)
BF	Granulated sludge	Activated sludge	46-138	18-36	5.8	90	(Gracian et al., 2002)
BF	Compost + bark + peat	Activated sludge	40-250	77	16.7	100	(Choi et al., 2003)
TF	Porous ceramics	Nitrifying culture	10-85	4.5	51	98	(Kanagawa et al., 2004)
BF	Sludge	No	26-264	18-60	10.1	95-99	(Chen et al., 2005)
BF	Compost	No	40-700	86	85.2	88	(Pagans et al., 2005)
BF	Coconut fibre	Acclimated biomass	45-300	19-36	33.3	100	(Gabriel et al., 2007)
BF	Immobilized cell	Mixed culture	10-150	32-85	5.5	73	(Kim et al., 2007)
BF	Compost + sludge + plastics	Activated sludge	51-236	30-60	9.8	99.9	(Taghipour et al., 2008)

Remark: [a] EBRT: empty gas residence time; [b] EC: elimination capacity; [c] RE: removal efficiency. BF = biofilter; BTF = biotrickling filter.

Table 2.6 A summary of previous work on the co-removal of H_2S and NH_3 in biofiltration

Bioreactor	Packing	Pollutant	Microbial culture	Inlet conc. (ppmv)	EBRT[a] (s)	EC[b] (g m^{-3} h^{-1})	RE[c] (%)	Reference
BF	Ca-alginate immobilized cells	H_2S	*T. thioparus* CH11	60-120	72	4.0		(Chung et al., 2000)
		NH_3	*Nitrosomonas europaea*	60-120		6.8	95	
BF	compost + wood chips	H_2S	Mixed culture	2	20	0.1	92.8	(Sun et al., 2000)
		NH_3	Mixed culture	20		0.5	90.3	
BF	Wood chips	H_2S	*T. thioparus*	35-440	20-60	79.3	99	(Kim et al., 2002)
		NH_3	Nitrifying culture	23-200		12.6	92	
BF	Granulated sludge	H_2S	Activated sludge	46-184	50	28	100	(Malhautier et al., 2003)
		NH_3	Nitrifying culture	46-184		14.2	80	
BF	wood chip	H_2S	No	20-100	40	13.7	85	(Jones et al., 2004)
		NH_3	No	80		5.5	90	
BTF	GAC	H_2S	*Pseudomonas putida* CH11	27-220	23-180	6.6	100	(Chung et al., 2005)
		NH_3	*Arthrobacter oxydans* CH8	80-120		7.3	87	
BF	Coarse root wood	H_2S	Activated sludge	2-10	180	0.1	99	(Shanchayan et al., 2006)
		NH_3	Activated sludge	40-70		0.3	86	
BF	GAC	H_2S	*T. thioparus* CH11	30-300	23-180	48.5	73	(Chung et al., 2007)
		NH_3	*Nitrosomonas europaea*	30-120		5.4	97.5	
BF	Rock wool-compost	H_2S	*AMM*	50-220	25	38.5	68.1	(Galera et al., 2008)
		NH_3	*Pseudomonas sp.* SUL4	50-250		23.7	78.6	

Remark: [a] EBRT: empty gas residence time; [b] EC: elimination capacity; [c] RE: removal efficiency. BF = biofilter; BTF = biotrickling filter.

2.2.4 Mechanisms of H_2S or/and NH_3 biofiltration

2.2.4.1 Mechanisms of biofiltration

The underlying mechanisms in a biofilter/biotrickling filter are complex. They involve physical, chemical and biological interactions that result in the transformation of the pollutants to other substances with less health and environmental impact (Shareefdeen and Singh, 2005). As shown in Figure 2.4, it is comprised of a series of steps beginning with the transfer of contaminants from the air to the water phase, adsorption to the medium or absorption into a water film, and finally biodegradation of contaminants within a biofilm. Understanding and enhancing the steps that are rate-limiting provide opportunities to predict and improve the performance of biofiltration.

Gas-liquid transfer

The filter contains a porous medium whose surface is covered with water and microorganisms. Treatment begins with the transfer of the gas pollutant from air stream to the water phase by diffusion and by advection in the air. Contaminants may also be adsorbed on the surface of biofilm, or adsorbed within the packing material (Devinny et al., 1999). For highly soluble contaminants such as NH_3, the dissolved form may be dominant. For more hydrophobic contaminants, such as H_2S, the major reservoir may be adsorbed on the surface of the packing material. The liquid phase may be static in a biofilter or flowing over the biofilm in a biotrickling filter. The transfer mechanism is dependent on the gradient, the transfer surface, and an overall mass transfer coefficient.

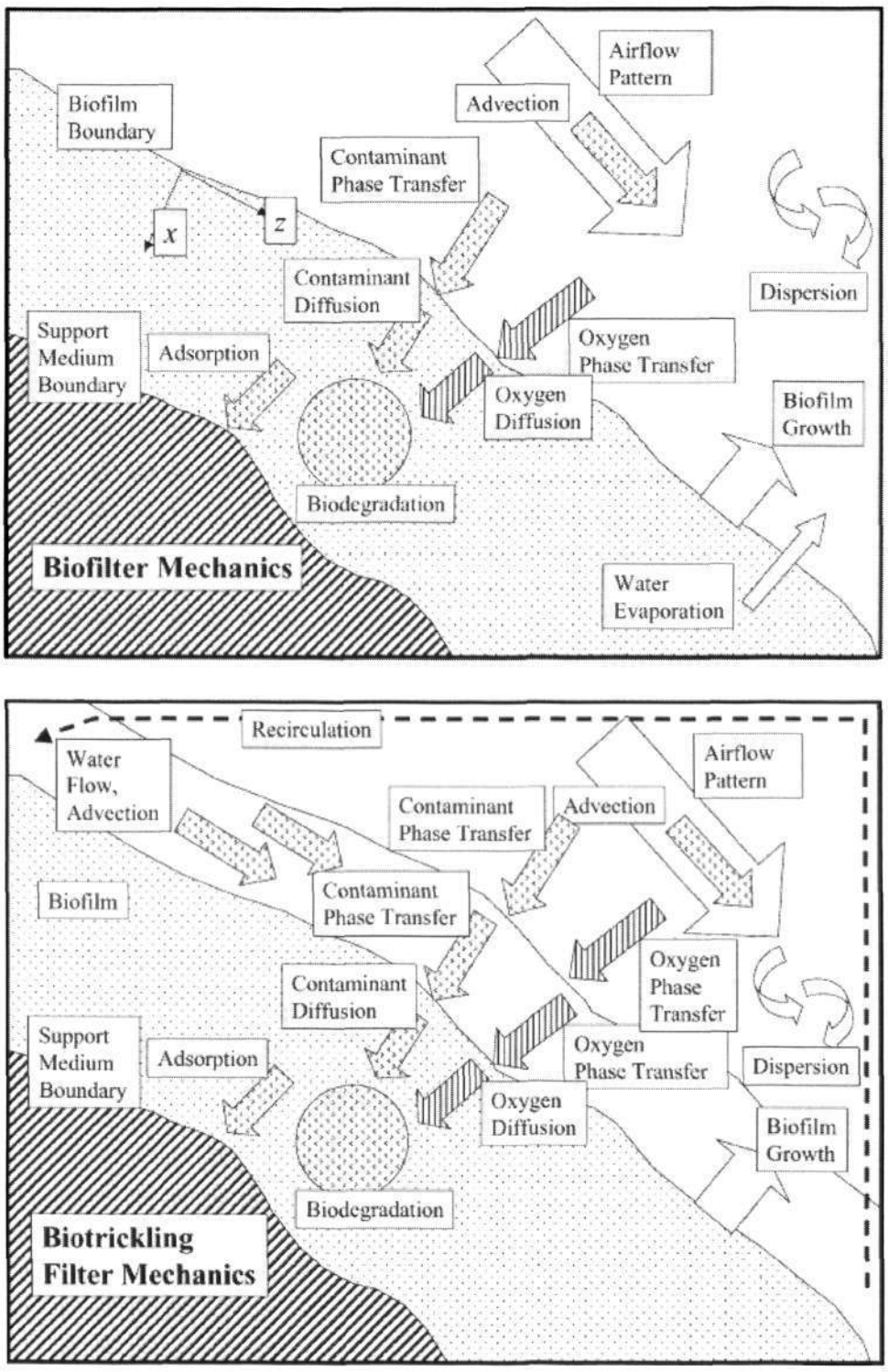

Figure 2.4 Pollutant removal mechanisms in a biofilter and biotrickling filter (Devinny and Ramesh, 2005)

The liquid/biofilm phase: physical and chemical processes

Once the pollutants and oxygen are solubilized in the moist solid phase, they interact with the water and the microorganisms. Among the physical interactions, there are equilibrium-driven processes such as adsorption and absorption. Certain pollutants undergo chemical reactions in the liquid phase. The most common reactions take place when charged molecules establish ionic equilibrium depending on the pH of the aqueous phase. This ionic interaction is relevant as it may displace gas-liquid equilibrium. For example, H_2S may be ten times more soluble at pH 8 than at pH 4. Absorption of volatile inorganic acids such as H_2S tends to acidify the medium, while base such as ammonia tends to alkalify. For certain compounds such as H_2S, chemical oxidation occurs simultaneously with the biological reaction, even though the rates are much lower than those by microbes in biological processes.

Biodegradation

The biofilm is the key element of the biofilter/biotrickling filters, involved in destroying contaminants. This is the mass of organisms growing on the surface of the solid medium, where the metabolic activities are carried out to transform the contaminant into biomass, metabolic by-products, or carbon dioxide and water (Devinny et al., 1999). If the contaminant contains nitrogen or sulfur, metabolic products will appear as nitrate/nitrite and sulfate respectively. Microorganisms use pollutants to draw chemical energy for the growth and maintenance of biological activity. In biological air treatment systems, the interest is to sustain a high removal so that the pollutant degradation is more important than the growth. Microbes degrade the pollutants when there is growth, but degradation also occurs even when the net growth rate is zero.

2.2.4.2 H_2S biodegradation pathway

H_2S has low water solubility and relatively high vapor pressures. It is a negative factor for the mass transfer from air to aqueous system efficiently, and then low removal efficiencies would be expected for H_2S in a biofilter. However, many biofilter systems have successfully treated H_2S with very high removal efficiency. It is attributed to its

good biodegradation.

H_2S may be utilized by microorganisms in three different ways: assimilation, mineralization and sulfur oxidation (Atlas and Bartha, 1981; Grant and Long, 1981). The oxidation of H_2S to gain energy is the most important and efficient way for microorganisms to utilize H_2S. *Thiobacillus* sp. is widely used in studies of the conversion of H_2S and other sulfur compounds by biological processes (Chung et al., 1996b; Cho et al., 2000; Wu et al., 2001). Some of the microbial sulfide degradation reactions are stated as below (Brock and Madigan, 1991):

Aerobic zone

$$H_2S + 2O_2 \rightarrow SO_4^{2-} + H_2O \quad \text{(SOB)} \qquad \text{Eq. 2-1}$$

$$S + 2O_2 \rightarrow SO_4^{2-} \quad \text{(SOB)} \qquad \text{Eq. 2-2}$$

Microaerophilic zone

$$H_2S + 0.5O_2 \rightarrow S + H_2O \quad \text{(SOB)} \qquad \text{Eq. 2-3}$$

Anaerobic zone

$$H_2S + CO_2 + \text{light} \rightarrow S + CH_2O \quad \text{(Anoxygenic prototroph)} \qquad \text{Eq. 2-4}$$

$$SO_4^{2-} + 4[2H] \rightarrow H_2S + 2H_2O + 2OH^- \quad \text{(Sulfate-reducers)} \qquad \text{Eq. 2-5}$$

Suzuki (1999) reported that the enzymatic H_2S oxidation proceeds mainly via the reaction pathway shown in Figure 2.5. Reaction 1 is the fastest of the reactions. When the supply of H_2S has been depleted, additional energy can be obtained from the oxidation of sulfur to sulfate. When reaction 2 is not fast enough, sulfur accumulates in the system. When reaction 3 is slower than reaction 2, sulfite accumulates and the reaction of sulfur with sulfite yields thiosulfate as the oxidation product (reaction 4) and other intermediate product (reaction 5). The final product of oxidation in most cases is sulfate (SO_4^{2-}).

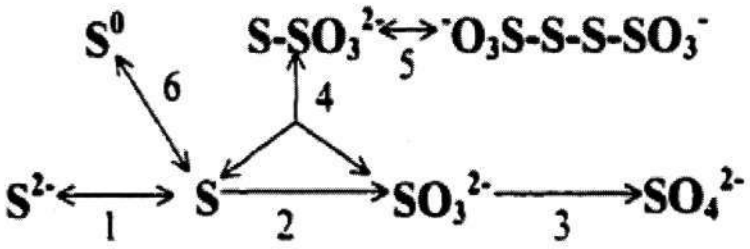

Figure 2.5 Enzymatic oxidation pathways of inorganic sulfur compounds (Suzuki, 1999)

A complete oxidation to sulfate is favorable from an environmental point of view (Jin et al., 2005b). However, different sulfur metabolic products were reported in H_2S biofiltration process under different operation conditions. The end products for H_2S biodegradation were identified to be SO_4^{2-} (38%), SO_3^{2-} (6%), S^{2-} (3%) and S^0 (53%) in an immobilized cell biofilter (Kim et al., 2008). The main product was elemental sulfur (82%), followed by sulfate and thiosulfate (<8%) in a biofilter (Elias et al., 2002). Chung et al. (1996b) observed that the major product became sulfate (75%) under 5 ppmv inputs of H_2S, while the major product was elemental sulfur (72%) under 60 ppmv of H_2S.

2.2.4.3 NH_3 biodegradation pathway

NH_3 has high water solubility and low Henry's law coefficient, which benefits the mass transfer from air to aqueous system. Gaseous NH_3 can be removed in biofiltration through adsorption to the media, absorption into the water phase (McNevin et al., 1999), chemical neutralization with acidic components in the media (Cho et al., 1992; Lee et al., 2005), biologically oxidation (i.e. nitrification) (Chung et al., 1997; Liang et al., 2000; Smet et al., 2000; Chen et al., 2005) or assimilation (Chung et al., 2004b). In views of environmental friendly aspect, nitrification should be the main mechanism for the removal of NH_3. Nitrification is a sequential transformation of NH_3 to nitrite (NO_2^-) and then nitrate (NO_3^-) in a two-step process.

However, nitrification did not mainly contribute to the removal of NH_3 in most cases. Some researchers (Smet et al., 2000; Kanagawa et al., 2004) found that about 50% of the NH_3 removal was attributed to nitrification. Only 8-46% of NO_2/NO_3-N were observed in a granulated sludge biofilter (Gracian et al., 2002). The products of nitrification included about 30% of NO_2-N and 44% of NO_3-N in another study (Kim et al., 2007). In addition, the failure of bioreactors was observed after some time due to the accumulation of metabolites (Hartikainen et al., 1996; Smet et al., 2000; Sorial et al., 2001). It may result from the fact that nitrification is sensitive to media conditions such as pH, ionic strength, available nutrients and presence of inhibitors. Both free ammonia and free nitrous acid are known to be inhibitors of nitrification (Weckhuysen et al., 1994; Baquerizo et al., 2005).

Heterotrophic nitrification has generally been viewed as less significant than autotrophic nitrification, due to the significantly higher activity rates of the autotrophs (Rittmann and McCarty, 2001). The process of heterotrophic nitrification is not coupled to energy generation and may not go to completion, that is, the final product of heterotrophic nitrification is often nitrite (Chung et al., 1997). Nitrite accumulation might pose additional problems, because it may hamper biological treatment of spent nutrient solution in a large-scale application of the process (Chung et al., 2007). In addition, the use of common heterotrophic bacteria to biodegrade NH_3 is inefficient because the demand for a nitrogen source in these bacteria is one-tenth of the demand for a carbon source. This indicates that a continuous supply of organic carbon source is essential.

The intake and release of nitrogen in biofiltration process involved many complex transformations. Figure 2.6 shows the nitrogen cycle for possible nitrogen transformation in a biofiltration system.

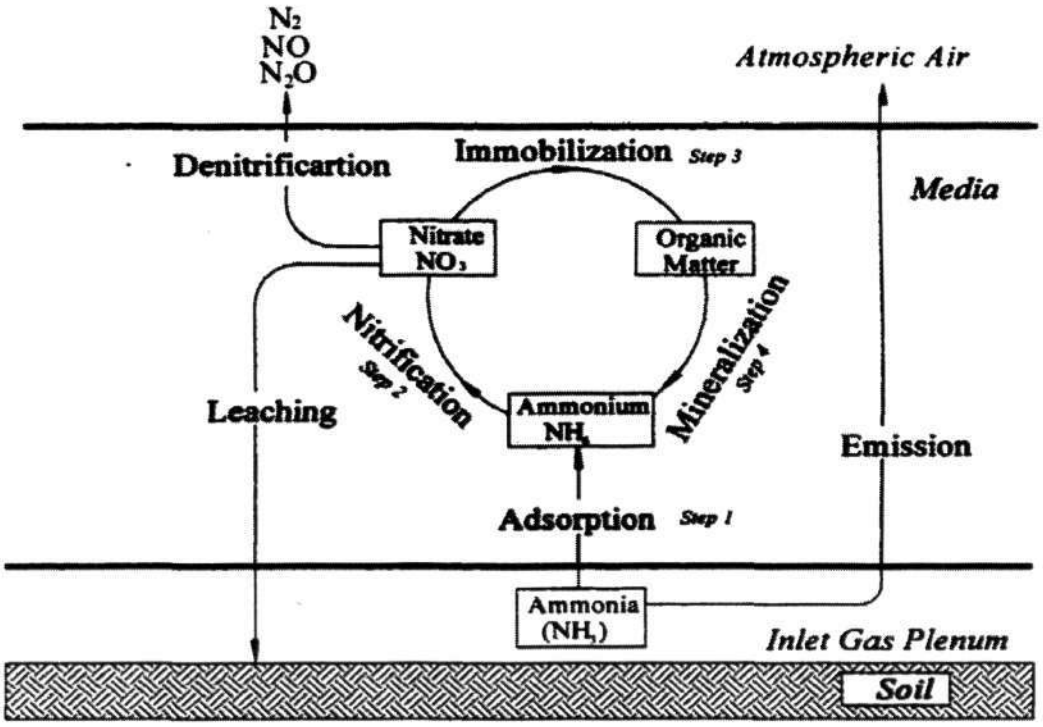

Figure 2.6 Illustration of the nitrogen cycle occurring in a biofilter (Nicolai, 2002)

Step 1: NH_3 is absorbed into water or adsorbed in the biofilm surrounding the media and converted to ammonium. The maximum concentration in liquid phase will be defined by the Henry's law coefficient of NH_3. However, liquid phase concentration may be less than equilibrium values due to the effects of gas-liquid mass transfer limitations, protonation of the ammonia, and potential bio-transformations in the liquid phase (Shanchayan et al., 2006).

$$NH_{3(g)} \rightarrow NH_{3(aq)} \qquad \text{Eq. 2-6}$$

$$NH_{3(aq)} + H_2O \leftrightarrow NH_4^+ + OH^- \qquad \text{Eq. 2-7}$$

Step 2: Biological nitrification is mainly carried out by AOB (e.g., *Nitrosomonas sp.*) that oxidize NH_3 to NO_2^- with CO_2 or HCO_3^- for growth, and subsequently by NOB (e.g., *Nitrobacter sp.*) that oxidize the produced NO_2^- to NO_3^- (Devinny et al., 1999).

$$NH_4^+ + 0.5O_2 \rightarrow NO_2^- + 2H^+ + H_2O + \text{energy} \quad \text{(AOB)} \qquad \text{Eq. 2-8}$$

$$NO_2^- + 0.5O_2 \rightarrow NO_3^- + \text{energy} \quad \text{(NOB)} \qquad \text{Eq. 2-9}$$

Step 3: Nitrate may be utilized in three ways: 1) by denitrification reduced to N_2 in the areas of low oxygen or anoxic zones usually formed in the inner regions of biofilm; 2) by leaching; and 3) by assimilation to organic matter (Chung et al., 2004b).

Step 4: Mineralization of organic N refers to the decomposition of organic compounds to release NH_4^+(Coyne, 1999).

2.2.4.4 Mixture of H_2S and NH_3

Some studies have been conducted on simultaneous removal of NH_3 and H_2S in biofiltration (Kim et al., 2002; Chung et al., 2005; Galera et al., 2008). The results showed that the co-removal of NH_3 and H_2S occurred in the biofilters. The interactions of the two pollutants biodegradation were observed.

If biodegradation of NH_3 and H_2S happened in parallel and simultaneously, the degradation end products should be nitrate and sulfate respectively. However, it was found that both nitrite and nitrate have a very small amount in the co-removal biofiltration system. NH_3 was mostly removed by chemical reaction with sulfate (the final product of H_2S bio-oxidation) to form $(NH_4)_2SO_4$ instead of NO_3^- (Kim et al., 2002; Lee et al., 2005; Galera et al., 2008). Almost 88% of the total N in a biofilter was NH_4-N, while remaining 12% was nitrification products (NO_2/NO_3-N) (Shanchayan et al., 2006). These reactions taking place in the co-removal biofiltration can be shown as follows:

$$H_2S + 2O_2 \rightarrow SO_4^{2-} + 2H^+ \quad \text{(SOB)} \qquad \text{Eq. 2-10}$$

$$NH_{3(aq)} + H_2O \leftrightarrow NH_4^+ + OH^- \qquad \text{Eq. 2-11}$$

$$2NH_4^+ + SO_4^{2-} \rightarrow (NH_4)_2SO_4 \quad \text{(chemical neutralization)} \qquad \text{Eq. 2-12}$$

It is not an environmental-friendly approach since NH_3 gas was only transferred from gas phase to liquid phase. Liquid effluent from the biofiltration system contains a large quantity of NH_4^+, which requires a further treatment. In addition, under high loadings of H_2S, the efficiency of nitrification decreased (Chung et al., 2000; Kim et al., 2002; Malhautier et al., 2003). This was mostly attributed to the incomplete biodegradation products of H_2S (e.g. sulfide, sulfur), which have negative effect on the

growth of nitrifying bacteria. On the other hand, when high inlet NH_3 concentration was introduced, the conversion ratio of SO_4^{2-} decreased remarkably (Chung et al., 2001). Hence, how to overcome these limitations and problems becomes the key point to co-remove NH_3 and H_2S through biofiltration technology efficiently.

2.2.5 Mathematical modeling of biofilters/biotrickling filters

Biological treatment of contaminated air in biofilters/biotrickling filters involves a complex combination of physical, chemical and biological processes (Figure 2.4). This makes it very difficult to understand and integrate the subtle details of the phenomena occurring during treatment. Mathematical models help to build a fundamental understanding of the process, and to accomplish engineering tasks such as reactor design and scale-up, or process optimization (Shareefdeen and Singh, 2005).

Ottengraf's model (Ottengraf et al., 1986) remains the most commonly referenced biofiltration model, and most current models were developed from it. The model assumes plug flow in the gas phase, and flat geometry for the biofilm. The model neglects gas film mass transfer resistance, and assumes the pollutant to be in equilibrium at the air/biofilm boundary and related by Henry's law. Pollutant transport in the biofilm is by diffusion and can be described by an effective diffusion coefficient. For the micro-kinetics of biodegradation occurring in the biofilm, the model starts with the Michaelis-Menten-type expression (growth is neglected), and considers two limiting cases of first- and zero-order kinetics. This model laid the fundamental framework for biofiltration modeling, even though it was limited to steady-state conditions.

In practice, transient operations are more common than steady-state ones, due to fluctuating concentrations and process conditions. Under unsteady state, when an adsorbent medium is used, the adsorption of pollutants on the adsorbent medium in biofiltration can not be ignored. It has been reported that adsorptive activated carbon improved the performance in biofilters (Abumaizar et al., 1997; Zhu et al., 1998a; Duan et al., 2005a). While the adsorption capacity of the activated carbon was

substantially reduced by water and microbial growth, it remained high (Hodge and Devinny, 1995). Thus, modeling adsorption is necessary for biofilters using activated carbon as packing materials to accurately describe the treatment of waste streams during the early stages and transient loadings (Devinny and Ramesh, 2005).

Some transient models considering adsorption in biofiltration have been developed. Shareefdeen and Baltzis (1994) considered the adsorption phenomenon that plays a major role during the startup and fluctuations in process conditions. Hodge and Devinny (1995) separated the effects of contaminant adsorption and biodegradation processes. During the initial start-up, the adsorption capacity of the filter material is responsible for the majority of the contaminant removal, and biological processes dominate the removal after the filter material is saturated with contaminant. Deshusses et al. (1995a) described the details of diffusion processes within the biofilm. In the biofilm, the pollutants simultaneously diffuse and are consumed by the microorganisms. Adsorption of the pollutants is possible, but only after their diffusion through the entire thickness of the biofilm. Den and Pirbazari (2002) also addressed biofilm diffusion, biodegradation and adsorption in a biotrickling filter. Furthermore, they incorporated additional features, including film transport through the external liquid layer and intra-particle diffusion inside the adsorbent phase. In addition, in water treatment systems, the models which incorporated both adsorption and biodegradation process have also been addressed (Chang and Rittmann, 1987; Speitel and Zhu, 1990).

Some representative models considering adsorption are listed in Table 2.7, including both wastewater/water and waste gas treatment systems. In most of these models, the biofilm layer was assumed to fully cover the surface area of the packing and there are no biodegradation happening inside the adsorbent. Shareefdeen and Baltzis (1994) introduced the concepts of partial coverage of the support media with biofilm as well as direct adsorption of toluene on the solid media through the uncovered portion. In wastewater/water treatment system, patchy biofilm coverage was also applied in modeling development (Herzberg et al., 2003). However, as a normal biofilter operation for waste gas streams, the bare solid surface of a biofilter medium is still

covered with liquid layer even though there are patches of biofilm on the solid surface. Thus, it is not realistic that the bare solid/air interface exists in the normal performance of a biofilter. Even if it exists, it is very difficult to determine the percentage of carbon surface area covered by biofilm in a biofilter.

In addition, it is important to note a key assumption: biodegradation of pollutants occurs in adsorbents (Abumaizar et al., 1997; Amanullah et al., 1999). It relates to the accumulation of microorganisms in the internal pore spaces area of adsorbent particles, resulting in rapid consumption of pollutants. For activated carbon, it may be valid only for some macropores (> 50 nm), because micropores (< 2 nm) and mesopores (2-50 nm) of activated carbon may not be available for microorganisms (about 1 μm). However, micropores and mesopores contribute to about 95% and 5% of the total surface area of activated carbon, respectively (Bansal and Goyal, 2005). Thus, the assumption of pollutants biodegradation inside the activated carbon is debatable.

Overall, biofiltration models have been useful for research purposes, but have not yet progressed to the point of being reliable and generally accepted tools for design. Further works need to be done in future.

Table 2.7 Summary of existing biofiltration models involving adsorption

Biofilm coverage	Phases	Packing	Important assumptions	Application	Model
Partially	III phases: gas, biofilm and solid surface	Peat + perlite	No biodegradation in the adsorbent	Toluene	(Shareefdeen and Baltzis, 1994)
Partially	III phases: gas, biofilm and solid surface	Compost + GAC	Biodegradation in the adsorbent	BTEX[a]	(Abumaizar et al., 1997)
Partially	III phases: gas, biofilm and adsorbent	Adsorbent	Biodegradation in the adsorbent	VOCs	(Amanullah et al., 1999)
Partially	III phases: liquid, biofilm and solid surface	GAC	No biodegradation in the adsorbent	Atrazine	(Herzberg et al., 2003)
Completely	III phases: liquid, biofilm and solid surface	GAC	No biodegradation in the adsorbent	Phenol	(Speitel et al., 1987)
Completely	III phases: liquid, biofilm and solid surface	GAC	No biodegradation in the adsorbent	Liquid	(Chang and Rittmann, 1987)
Completely	Π phase: gas and solids/water	GAC	Biodegradation in the adsorbent	Ethanol	(Hodge and Devinny, 1995)
Completely	III phases: gas, biofilm and solid support	Bioton + compost	No biodegradation in the adsorbent	MEK[b] /MIBK[c]	(Deshusses et al., 1995a, 1995b)
Completely	III phases: gas, biofilm and solid support	GAC	No biodegradation in the adsorbent	Waste air	(Lim, 2001)
Completely	III phases: gas, biofilm/liquid and solid	GAC	No biodegradation in the adsorbent	TCE[d]	(Den and Pirbazari, 2002)
Completely	III phases: liquid, biofilm and solid surface	GAC	No biodegradation in the adsorbent	DOM[e]	(Liang and Chiang, 2007)

a. Benzene, toluene, ethylbenzene, o-xylene; b. Methyl ethyl ketone; c. Methyl isobutyl ketone; d. Trichloroethylene; e. Aldehydes and ketoacids

2.3 Biological activated carbon application in biofiltration

2.3.1 Activated carbon as adsorbent for odor

Activated carbon has been widely used in the removal of H_2S by adsorption (Turk et al., 1989; Bagreev et al., 2001; Bandosz, 2002; Yan et al., 2002). Virgin activated carbon has maximum physical adsorption, typically with a significant portion of its total pore volume in the micropores. Compared with virgin carbon, impregnated activated carbon for H_2S removal have the advantages in their high efficiency and fast kinetic of reaction (Turk et al., 1989). For a good performance of activated carbon as odor adsorbents, a proper combination of surface chemistry and porosity of carbon is needed (Bagreev et al., 2001; Bandosz, 2002). It was demonstrated that a more acidic environment yielded small H_2S removal capacities. pH should be higher than 5 to ensure the effective removal of H_2S from the gas phase (Bandosz, 2002), and a small increase in pH resulted in a higher H_2S adsorption capacity (Adib et al., 1999b).

The adsorption of NH_3 gas by activated carbon was also studied by few researchers (Stoeckli et al., 2004; Guo et al., 2005). The technology was not used widely in industrial application. In most cases, wet scrubbers are applied for the removal of NH_3 due to its high solubility.

Although adsorption on activated carbon can effectively eliminate odor from contaminated gas, the adsorption removes H_2S by only concentrating contaminants on the vast internal surface area of activated carbon. Thus, contaminants are not permanently treated or destroyed. Once activated carbon column is exhausted, the exhausted carbon may be a hazardous waste, requiring either regeneration or transportation to a hazardous-waste landfill (Hodge and Devinny, 1995). Both regeneration and disposal of exhausted carbon are quite expensive.

2.3.2 Biological activated carbon for odor removal

Biological treatment is relatively inexpensive, but it is subject to system upsets because

of the sensitivity of conventional biological systems to environmental conditions. Fluctuations in influent composition and/or hydraulic loading can disrupt biological activity and reduce removal efficiencies. Compared with biological degradation, activated carbon adsorption is much less sensitive to environmental conditions, with a major disadvantage associated with the cost in replacement or regeneration of exhausted carbon.

The advantages of activated carbon adsorption and biological degradation can be exploited while minimizing their respective disadvantages when the two treatment processes are combined. Research in the area of simultaneous activated carbon adsorption and biological degradation has been directed primarily toward the study of biological activated carbon (BAC) in water and wastewater treatment (Voice et al., 1992; Scholz and Martin, 1997; Zhao et al., 1999; Mason et al., 2000; Xie and Zhou, 2002; Zhou and Xie, 2002). The major function of activated carbon is to not only provide a favorable environment for biofilm growth, but also extends the contact time between the biofilm and contaminants due to its desirable adsorption characteristics (Den and Pirbazari, 2002).

For the treatment of waste gases, activated carbon has been used either alone (Hodge and Devinny, 1995) or as bulking agent in biofilters for the removal of VOCs (Abumaizar et al., 1998). While the adsorption capacity of activated carbon in a biofilter is reduced by the water and biomass on its surface, it remains much higher than other media (Hodge and Devinny, 1995). The biofilter containing activated carbon exhibited a significantly higher removal efficiency and more stable operation than the compost biofilter during sudden VOCs increases (Abumaizar et al., 1998). Adsorption capacity of activated carbon allows biofilters to withstand fluctuations in loading rates without compromising removal rate. When the loads of pollutant compounds are higher than average, they are accommodated on the solid surface. Conversely, microorganisms can gain their carbon or energy requirements during low loading periods from compounds that are then desorbed from the carbon surface.

Activated carbon was also used as packing materials in the biofiltration of gaseous

odor effluents these years (Chung et al., 2004a; Yan et al., 2004; Duan et al., 2005b). It has been demonstrated to be highly effective with the following advantages:

(I) Shorter EBRT and thus smaller bioreactor required;

(II) Higher removal efficiency due to a combination of adsorption and biodegradation;

(III) Strong resistance to fluctuating loadings due to activated carbon adsorption;

(IV) Excellent structural properties of activated carbon for supporting biofilm growth, with uniform particle size and good resistance to crushing;

(V) Good pH buffering capacity;

(VI) Long service lifetime.

This technology is highly promising to become an alternative of the physiochemical treatment in industrial applications. Granular activated carbon has been used in biofilters successfully for full-scale treatment of petroleum hydrocarbons from a refinery (Graham, 1996). However, the cost of activated carbon was high as a packing material in odor biofiltration compared with other conventional packing materials. For example, activated carbon costs about \$900-1000 m^{-3}, while compost costs approximately \$25 m^{-3} (Webster et al., 1997). The high cost currently make the technology unattractive and not practical in most cases (Webster et al., 1997). Therefore, alternative packing media need to be developed and evaluated for the removal of odor in biofiltration application at lower cost while achieving good performance.

2.3.3 Potential of re-using exhausted carbon in biofiltration

As mentioned in section 2.3.1, the exhausted carbon from the H_2S adsorption process may be a hazardous waste, which have to be regenerated or disposed of in a landfill (Hodge and Devinny, 1995). However, the cost of carbon regeneration is generally high and landfill has a limited space.

It has been reported that exhausted carbon, loaded with organic pollutants, can be bio-regenerated by bacterial activity. Some researchers (Speitel et al., 1989; Kim et al.,

1997; Scholz and Martin, 1997; Silva et al., 2004; Aktas and Cecen, 2006) reported that bacteria can use the adsorbed contaminants via exoenzymatic reactions. The micropores in activated carbon that contribute to adsorption are smaller than microbial cells so that adsorbed pollutants are inaccessible to the microorganisms. However, a biofilm containing bacteria can form on the external surface layer of activated carbon, and their "exoenzymes" can go into the micropores to degrade target component. On the other hand, other researchers (Hutchinson and Robinson, 1990; Orshansky and Narkis, 1997; Walker and Weatherley, 1998; Klimenko et al., 2004) believed that contaminants first desorb to the liquid phase, driven by a concentration gradient between the carbon surface and bulk liquid, and then followed by biodegradation.

These phenomena suggest that the pre-adsorbed sulfur compounds on exhausted carbon could possibly be utilized by bacteria as an energy source. The assumption results in two benefits: (1) better biofilm formation during initial period in biofiltration, and (2) recovered active space on carbon for further adsorption in biofiltration. However, it is unclear yet if the pre-adsorbed sulfur compounds on exhausted carbon could be released at the presence of bacteria.

In addition, since the impregnated activated carbon are strong basic (pH above 10), it is necessary to neutralize them to provide a suitable pH for bacteria growth if they are used in biofiltration process (Devinny et al., 1999; Ng et al., 2004). If exhausted carbon is used in biofiltration, the neutralization procedure can be avoided. This results from the fact that exhausted carbon which comes from the H_2S adsorption process using impregnated basic carbon often has near neutral surface pH.

2.4 Summary

Biofiltration have been demonstrated to be cost-effective and environmental friendly for the control of air pollution. Selecting a proper packing material is an important step towards the development of a successful biofiltration system. Activated carbon is an ideal packing material in biofiltration with a lot of advantages. This technology is highly promising to become an alternative of the physiochemical treatment in

industrial applications. However, its disadvantage is high cost. Therefore, alternative packing materials are required to be developed for the removal of odor in biofiltration at low cost while maintaining good performance.

Many studies on biofiltration have been undertaken with a single pollutant that allows an easier and more accurate interpretation of results and phenomena observed. However, at an industrial scale, more than one pollutant will appear in many cases. For example, waste gases emitted from composting facilities in sewage treatment plants contain NH_3 mixed with other odorous compounds such as H_2S. Only recent years, the co-treatment of H_2S and NH_3 by biofiltration was reported. The results showed that simultaneous elimination of H_2S and NH_3 occurred in biofiltration. Long EBRT, low removal performance of NH_3 and nitrification capacity were observed in these co-removal systems. Thus, a more efficient and effective process should be developed for the co-removal of H_2S and NH_3 in biofiltration.

Chapter 3
Materials & Methodology

In this section, materials and methodology employed in the study are summarized and described. Laboratory experimental setup and system operation will be addressed in Chapters 4, 5, 6 and 7.

3.1 Microorganisms and cultivation

Mixed cultures were enriched from a return activated sludge stream at the secondary sedimentation tank in a local wastewater treatment plant. Thiosulfate and ammonium medium (Table 3.1) were used to acclimatize the activated sludge to obtain the enriched sulfur-oxidizing bacteria (SOB) and nitrifying culture. Activated sludge was acclimated to the thiosulfate medium for 5 days, and then transferred to a fresh medium. After acclimatization for about 20 days (4 transfers), the SOB seeds were ready for inoculating into the biofiltration columns. Nitrifying microbial consortium was enriched by refreshing the ammonium medium every day for 30 days. The culture in the phase of stable growth was harvested by centrifugation (3000 rpm for 15 min), and was washed in sterile distilled water three times before they were used.

Table 3.1 Medium composition for cultivation of microorganisms

Chemical	**Thiosulfate medium (g L^{-1})**	**Ammonium medium (g L^{-1})**	**Stored trace element solution (g L^{-1})**	
$Na_2S_2O_3 \cdot 5H_2O$	8.0		Na_2-EDTA	1.0
NH_4Cl	0.4	1.0	$FeCl_2 \cdot 4H_2O$	1.0
KH_2PO_4	3.0	0.2	$CuCl_2 \cdot 2H_2O$	0.1
K_2HPO_4	3.0	0.1	$ZnSO_4 \cdot 7H_2O$	1.1
$MgCl_2 \cdot 6H_2O$	0.46	0.02	$MnCl_2 \cdot 4H_2O$	0.3
$NaHCO_3$	2.0	2.0	$CoCl_2 \cdot 7H_2O$	0.1
Trace element	10 mL	10 mL	$(NH_4)_6Mo_7O_{24} \cdot 4H_2O$	0.1
			$CaCl_2 \cdot 2H_2O$	2.5
			$MgCl_2 \cdot 6H_2O$	0.2

3.2 Biofilm analysis

3.2.1 Bacteria counting and MPN

Standard plate count method (Black, 2005) was used for counting viable SOB cells in the suspended biomass. To enumerate bacteria, carbon-free BactoTM agar was used, which allowed for bacteria to be incubated with only CO_2/HCO_3^- as the sole carbon source. For the preparation of the solid medium, 15 g of BactoTM agar was added into the liquid mineral medium (excluding $Na_2S_2O_3 \cdot 5H_2O$) before autoclaving (for 20 minutes at 15 psi and at 121 °C). The autoclaved agar mineral medium was cooled in a water bath at 60 °C, and concentrated thiosulfate solution was then added into the agar mineral medium through a sterile filter (pore size = 0.20 μm) in a laminar flow chamber. The warm gel liquid medium was poured into Petri dishes to make the agar plate, and the agar plates were left for solidification in the laminar flow chamber. Once cooled and solidified, the agar plates were stored in the refrigerator at 4 °C.

Several ten-fold dilutions of the biomass sample were used. At each dilution rate, three replicate plates were prepared to get the average counts. After the serial dilutions, a volume of 0.1 mL diluted culture broth was spread over the agar plate surface evenly by a sterile spreader and the inoculated plate was sealed by ParafilmTM. After the

liquid had been soaked into the agar, the Petri dishes were placed upside-down in a 30°C incubator for 2-7 days until the colonies appeared. The number of colonies counted on the plate was then multiplied by the number of times of dilution to yield the concentration of bacteria in units of colony-forming units (CFU) per milliliter.

For the concentration of SOB and nitrifying bacteria on carbon surface, the bacterial cells were first de-attached and became suspended following methods described by Chung et al. (2004). Approximately 0.5 g (dry weight) of carbon samples was taken from bioreactors and mixed with 5 mL of sterile 0.8% NaCl solution. The mixed solution with samples was vortexed for 3 min, and then the cell numbers in the solution were enumerated by the method of most probable number (MPN) (Rowe et al., 1977; Page, 1982). The obtained number of bacteria attached on the carbon surface was a conservative estimation since not all the biofilm could be detached from the carbon surface by vortex.

The protocol used for MPN-Griess counting was based on those described previously (Kim et al., 2002; Malhautier et al., 2003). The dispersed packing solution was sub-sampled and inoculated into MPN tubes for a series of dilution (1:10) with autotrophic sterile medium (Table 3.1). Samples were incubated for 6 weeks at 30 °C at 150 rpm in the dark. After incubation, for nitrifying bacteria samples, each tube was scored by adding an indicator (2.2 g of diphenylamine in 100 mL of concentrated H_2SO_4) to indicate the presence of nitrate. An indicator (1 g sulfanilamide and 0.1 g N-(1-naphthyl)-ethylenediamine dihydrochloride in 100 mL water) was added into another batch of tubes to indicate the presence of nitrite. A blue and red color indicated that nitrate and nitrite was formed respectively. For SOB, each tube was scored by adding an indicator (10 g L^{-1} BaCl solution). A white deposit indicated the presence of sulfate. The number of SOB and nitrifying cells per gram of activated carbon was determined with Cochran's Tables (Page, 1982).

3.2.2 Protein and SOUR

The amount of biomass on carbon was quantified based on the measurements of total

protein. Protein was extracted from microorganisms according to the methods of Kim et al. (2005). About 1 g of carbon sample was collected from bioreactors and placed in 5 mL of 1N NaOH solution in a tube, and the tube was pounded for 3 min. The solution with the carbon was then kept in a boiling water bath at 100 °C for 5 min to further extract biomass. The protein content in the solution was determined using the Bradford Protein Assay (Sigma, USA). The "clean" carbon (i.e. without biomass) was dried at 105 °C for 24 h to be ready for weighing. Biomass was reported as mg protein g^{-1} dry carbon. Volatile suspended solids (VSS) and protein concentrations of the different eight suspended biomass were measured in triplicate. A standard calibration curve was obtained. The ratio of protein to VSS in the biomass was 0.47 ± 0.06 g protein g^{-1} VSS. This factor can be used to convert protein concentrations to VSS concentrations. VSS concentrations were measured according to Standard Methods (APHA, 1999).

Biological activities of biofilm were described by determining oxygen uptake rate (OUR) (APHA, 1999). Experiments were conducted in triplicate. About 5 mL of carbon sample from bioreactors was carefully washed with distilled water, and was put in a pre-cleaned BOD bottle. The BOD bottle (70 mL) was then fully filled with the pre-aerated mineral nutrient (excluding thiosulfate or ammonium), and the oxygen-sensing probe with stirring mechanism (YSI 5000, Yellow Springs, OH) was immediately inserted into the BOD bottle. Endogenous respiration was first monitored. The substrate-induced OUR (SOUR) was determined after the addition of a concentrated solution to reach a final concentration of 50 mg L^{-1} of S_2O_3-S and NH_4-N for $(SOUR)_S$ and $(SOUR)_N$, respectively. SOUR values were corrected for the endogenous respiration, and rates were correlated to the protein content of each sample.

3.2.3 Morphological characterization

Biofilm developed on carbon surface were identified and observed using a scanning electronic microscope (SEM) (Stereoscan 420, Leica, Cambridge Instruments). The carbon sample was soaked in a beaker with 2% (v/v) glutaraldehyde for about 2 h in order to fix the microorganisms. The sample was then washed for 20 min three times with 0.1 M sodium cacodylate buffer. The washed sample was then dehydrated in 50%,

70%, 85%, and 95% ethanol each for 15 min before being stored in 100% ethanol. Following dehydration, the sample was dried using critical point drying equipment (E3000 Series). The dried sample was sputter-coated with gold at 20 mA in a high vacuum and low temperature cryo-chamber for 60 s, and then viewed with a SEM at 15 KV.

3.2.4 DNA extraction, PCR and denaturing gradient gel electrophoresis (DGGE)

Genomic DNA of biomass was extracted based on a protocol described previously (Kowalchuk et al., 1997). For sampling of the biofilm in the bioreactors, about 10 g of carbon samples were randomly picked, and was placed into a 20 mL of 0.85% sterile NaCl solution, and then vortexed for 10 min. The mixture was sonicated for 9 min at 42 kHz. The extract was concentrated by centrifugation for 10 min at 5000 rpm and excess supernatant was removed. For DNA extraction, approximately 200-300 mg (wet weight) of biomass was mixed with 50 µL 20% sodium dodecyl sulfate, 600 µL glass bead with a diameter of 0.1 mm and 500 µL saturated phenol in a 2 mL tube and treated in a bead beater at 5000 oscillations/s for 3 min. This involved bead beating followed by extraction with saturated phenol (pH 8.0), phenol:chloroform (1:1), and chloroform. The extracted DNA was precipitated overnight with a sodium acetate-ethanol mix at -20 °C and dissolved in sterile deionized water. Extracted DNA samples were stored in -20 °C freeze before use.

PCR primers P2 (5'-ATT ACC GCG GCT GCT GG-3') and P3 (5'-CGC CCG CCG CGC GCG GGC GGG GCG GGG GCA CGG GGG GCC TAC GGG AGG CAG CAG-3', containing 40 bp of GC clamp) were used to amplify the variable V3 region of the bacterial 16S rDNA gene. Touchdown PCR was performed with a Mastercycler gradient thermal cycler (Eppendorf AG, Germany) using a 50 uL (total volume) mixture containing TaqDNA polymerase (Promega Co., USA), 1 × thermophilic DNA Taq polymerase buffer B, $MgCl_2$, deoxynucleotide triphosphates, primers, and DNA extract. Successful PCR was confirmed by 2.0% agarose gel electrophoresis.

The PCR-amplified fragments were separated by DGGE using a DCode universal mutation detection system (Bio-Rad Laboratories). A 10% (w/v) acrylamide solution (40% acrylamide and bisacrylamide, 37.5:1 stock solution) in 1 × TAE buffer was used, with urea-formamide denaturing gradient gel ranging from 30-70%. Electrophoresis was performed at a constant voltage of 85V for 15 h at 60 °C. After electrophoresis, the gel was stained with ethidium bromide for 30 min and detained in 1 × TAE buffer for 1 h. The gel was viewed and photographed with an EDAS 290 gel imaging system (Eastman Kodak, USA).

GelCompare II (version 1.5) software (Applied Maths, Belgium) was used for DGGE band pattern analysis. Binary coefficient Dice was applied to calculate the similarity of band patterns. The un-weighted pair group method using arithmetic averages (UPGMA) was used to construct the DGGE dendrograms.

3.3 Carbon characterization

3.3.1 Exhausted carbon preparation

Activated carbon with pellet-shaped in 4 mm of diameter, from Jacobi Group (AddSorb VA3, designated as "VA"), was selected. It is chemically impregnated carbon, and is currently the most widely used for the removal of H_2S. The H_2S-exhausted carbon was obtained from the breakthrough capacity test following the standard adsorption method (ASTM-D6646-03). The experimental setup is shown in Figure 3.1.

Activated carbon was packed in a glass tube (4.8 cm i.d.) at a fixed height of 22.9 cm. Glass beads were packed at the bottom and top of the carbon bed to enable a well-mixed gas flow. The 1% (v/v) H_2S together with moist air (RH 80%) was prepared by mixing 5% (v/v) H_2S at 1.05 L min^{-1} and moist air (RH 100%) at 4.15 L min^{-1}. The gas was diverted into the bottom of the carbon bed. The retention time of the gas passing through the carbon bed were kept at 4.8 s. The experiments were carried out at room temperature. The outlet H_2S concentration was monitored until a breakthrough at 50 ppmv concentration. The time taken for breakthrough was recorded, and adsorption

capacity in terms of weight (grams of H_2S per gram of carbon) was calculated from the H_2S concentration in the inlet gas, flow rate, breakthrough time, and mass/volume of carbon. The principal parameters influencing the adsorption result could be the tube diameter, bed height, moist air, carbon pre-humidification, and the total flow rate, etc. The pre-humidification was conducted before the capacity test: moist air (RH100%) passed through the carbon bed for several hours at flow rate 1.5 L min^{-1}.

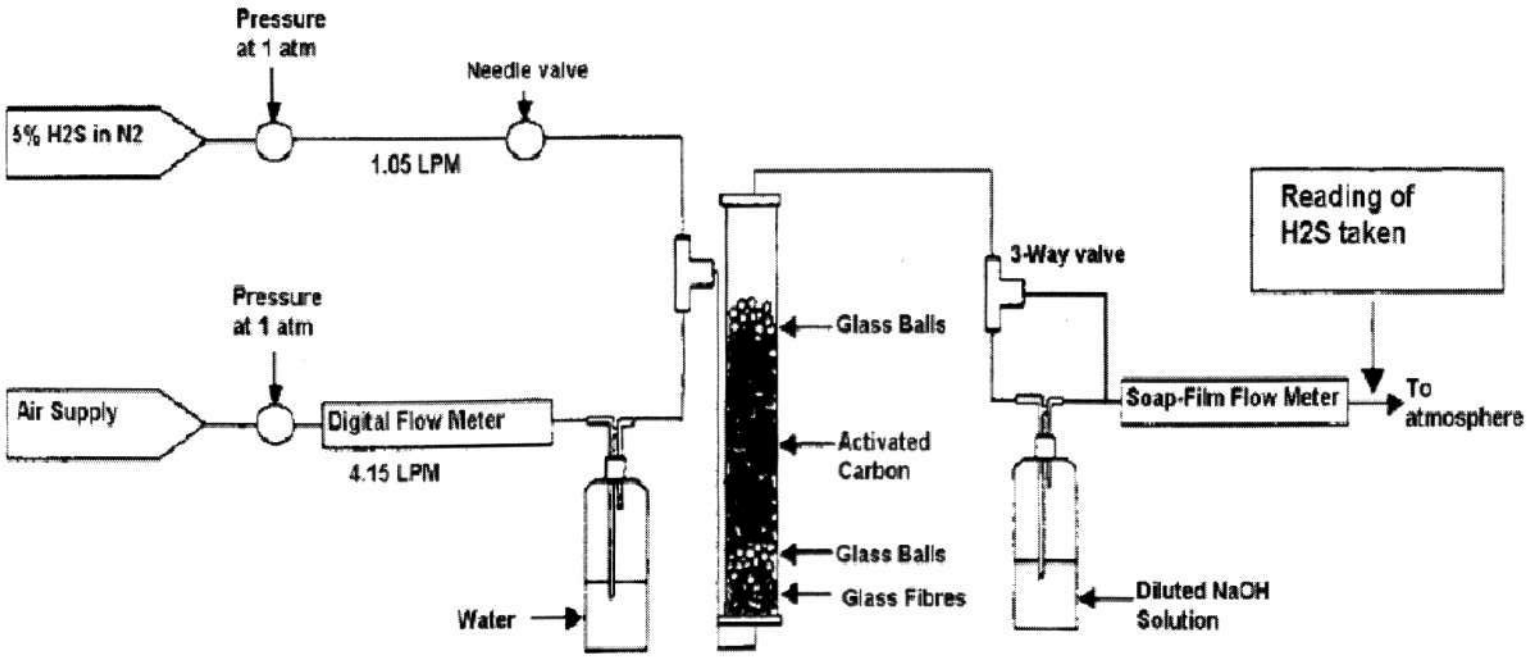

Figure 3.1 Schematics of activated carbon adsorption capacity test

3.3.2 Structure properties

Braunner-Emmett-Teller (BET) tests can indirectly indicate deposited substrates concentration and the effects of microbial growth on carbon. The surface areas and pore volumes of carbon samples were measured by nitrogen adsorption using Micrometrics BET analyzer model ASAP 2010. The carbon samples were pre-dried to remove any adsorbed water through freezing vacuum drying for 24 h before carrying out test. The carbon samples were degassed to 1.33 Pa pressure at 80°C prior to the BET analysis.

3.3.3 Chemical properties

Carbon surface pH: The pH of the carbon surface provides useful information about the average acidity/basicity of carbon surfaces. It was measured in the following way: 0.4 g of carbon sample was soaked in 20 mL of Ultra Pure Water (UPW) and swirled on an auto-shaker for 24 hours to reach equilibrium. The sample was then filtered and the pH of the solution was measured using a Horiba pH meter F-21 (Horiba Ltd. Japan). Two replicate determinations for each sample were carried out for repeatability.

Sulfate on carbon: Sulfate that is soluble would most likely be transferred into the aqueous phase. However, some sulfate, which might remain at the carbon surface after the bioprocess, was measured using the same way as surface pH. Sulfate concentration in the filtered solution were determined by turbidimetric method (APHA, 1999). Two replicate determinations for each sample were carried out for repeatability.

Thermal analysis: Thermal analysis was conducted to evaluate the thermal desorption of different S-species adsorbed on carbon. The thermal gravimetric analyzer (TGA) (Netzsch STA, Germany 409) was used. The carbon pellet was placed onto the pan, and heating was carried out from room temperature to 1000 °C at 10 °C min^{-1}. Nitrogen gas was channeled into the system at 50 mL min^{-1}.

CHNS analysis: CHNS analysis provides information on the contents of combustible

C, N, H and S on the carbon samples. Combustible sulfur species include H_2S and all those intermediates of H_2S oxidation, excluding sulfates (S (VI), the highest oxidation state). The combustible elementary compositions (C, H, N, and S) of carbon samples were measured using a thermo-analytical analyzer (PE2400 series II CHNS/O analyzer, PerkinElmer Instruments, USA). Three analyses for each sample were carried out for consistency.

SEM/EDX: The distribution of sulfur (S) in the surface and cross-section of carbon samples was measured by a scanning electronic microscope (SEM) together with energy dispersive X-ray spectroscopy (EDX) by JEOL model JSM-5310V (Japan).

Total sulfur in carbon: Total sulfur contents in carbon samples were analyzed by X-ray Fluorescence (XRF) technique using PANalytical PW 2400 x-ray spectrometer (Holland). Prior to analysis, carbon samples were ground into fine powder and freeze-dried for 24 h. The manufacture of a pure carbon pellet can hardly be done without the addition of a binder because of the morphology of carbon powder. As boric acid (H_3BO_3) is undetectable for XRF, 0.375 g of carbon powder was mixed with 1.125 g boric acid. The mixture was homogenized in an agate mortar. The mixed powder was pressed at 350 bar pressure for 3 min to obtain the cylindrical pellet of 30.2 mm diameter, which was then used for XRF analysis.

3.4 Gas sampling and measurement

Tedlar bags (SKC Inc., USA) were used to collect the gas samples. Outlet H_2S concentration was measured using a Jerome 631-X H_2S analyzer (Arizona Instruments, USA) and the inlet H_2S concentration was determined using a Finch-com II portable H_2S monitor (Infitron, Seoul, Korea). The outlet and inlet NH_3 concentration were measured using a gas-detection tube (Draeger Safety Asia, Singapore) and a BW NH_3 gas detector (Calgary, AB, Canada), respectively. The Jerome H_2S analyzer (ppb level, up to 30 ppmv) and NH_3 gas-detection tube (0.25-5 ppmv) are capable of measuring low levels of pollutants concentration, while the Finch-com and BW detector are more suitable for higher concentrations (ppmv level, up to 100 ppmv). The analysis of each

gas sample was carried out immediately after sampling to avoid the deterioration of gas sample. To eliminate any effect of residual gas in the Tedlar bags, all sample bags were flushed by clean air after each measurement. Three readings were taken for consistency.

3.5 Liquid analysis

pH: The pH of the solution was measured using a Horiba pH meter F-21 (Horiba Ltd. Japan). The meter was calibrated every day.

Determination of elemental sulfur: Elemental sulfur was determined by reacting with cyanide to produce thiocyanate, which was then quantified as $Fe(SCN)_6^{3-}$ (Schedel and Trtiper, 1980). Elemental sulfur was determined in the following assay system: the solution containing elemental sulfur was filtered through membrane filters of pore size 0.1 μm. The filter that retained elemental sulfur was incubated in 3 mL of 0.1 M NaCN solution at 90°C for 10 min. After cooling, 6.5 mL of distilled water and 0.5 mL of 0.75 M $Fe(NO_3)_3$ in 20 % HNO_3 were added. The optical density was measured at 460 nm against a reagent blank.

Determination of sulfate: Sulfate concentration in liquid were determined by turbidimetric method (APHA, 1999). The principle of this method is the precipitation of sulfate in an acetic acid medium with barium chloride ($BaCl_2$) so as to form barium sulfate ($BaSO_4$) crystals of uniform size. The light absorbance of the $BaSO_4$ suspension was measured by a turbidimeter (HACH, 2100N) using distilled water as a standard. The sulfate concentration was determined, compared with a standard curve.

Determination of sulfide, thiosulfate, ammonium, nitrite and nitrate: The concentrations of these sulfur compounds in liquid were determined according to standard methods (APHA, 1999). The concentrations of sulfide and thiosulfate in liquid were determined in accordance to the iodometric method by titrating an amount of the liquid sample with standard iodine solution, using starch solution as the indicator. Ammonia/ammonium in liquid was determined according to standard Nessler methods. Nitrite and nitrate in liquid was determined according to standard

Colorimetric and Ultraviolet Spectrophotometric Screening methods, respectively (APHA, 1999).

Chapter 4
Feasibility of Re-using H_2S-exhausted Carbon in Biofiltration

4.1 Introduction

Activated carbon has been used as packing material in biofiltration for the removal of odor with high efficiency (Chung et al., 2004; Yan et al., 2004b; Duan et al., 2005a). However, using a large amount of activated carbon has high cost (Medina et al., 1995; Webster et al., 1997).

One of the alternatives to activated carbon could be exhausted carbon from H_2S adsorption process (Duan et al., 2006). Exhausted carbon is a common environmental problem in Wastewater Treatment Plants (WWTPs) (Hodge and Devinny, 1995; Devinny et al., 1999). It is saturated with sulfur, thus requires either costly thermal regeneration or disposal as hazardous wastes (Devinny et al., 1999). Disposal is often done, since thermal regeneration breaks down the carbon resulting in more "fines" and its energy cost has also been increasing. Therefore, economic requirements have driven the re-use of exhausted carbon.

It was reported that exhausted carbon which loaded with pollutants such as phenol and surfactants can be bio-regenerated by bacterial activity (Walker and Weatherley, 1998; Klimenko et al., 2004; Aktas and Cecen, 2006). Based on these phenomena, it is assumed that the pre-adsorbed sulfur compounds on exhausted carbon could be served as energy source for bacteria growth. Meanwhile, the adsorption sites on carbon can be

recovered for further adsorption. Once the assumption is verified, exhausted carbon can be transferred into biological activated carbon (BAC) for the removal of odor in biofiltration.

The main objective of this study is to evaluate the feasibility of using exhausted carbon in biofiltration for the removal of H_2S. The biofilm will be developed on exhausted carbon by off-line (without H_2S supply) and on-line immobilization in biofilters. The performance in biofilters packed with exhausted carbon will also be evaluated. The work will be useful to reveal the suitability of re-using exhausted carbon in biofiltration.

4.2 Experimental setup

4.2.1 Off-line flasks

The exhausted carbons were obtained from the outlet, middle and inlet locations of the adsorption bed after the H_2S breakthrough (section 3.3.1), designated as EC1, EC2 and EC3 respectively. The adsorption capacity of H_2S for the impregnated carbon was 7.8% (w/w) S/carbon. 10 g of exhausted carbon (EC1, EC2 and EC3) was separately added into 500 mL of flasks, which contained 200 mL of sterilized thiosulfate mineral medium (Table 3.1) but excluding thiosulfate. 1 mL of enriched microbial consortium containing 1.9×10^7 cell mL^{-1} of autotrophic sulfide-oxidizing bacteria (SOB) was inoculated into the flasks. Control experiments were also conducted under the same conditions but without adding microbial inoculums. Both experimental and control flasks were covered with cotton stoppers and incubated on a rotary shaker at 150 rpm at room temperature. No external sulfur source was added into the flasks. Three experiments (with bacteria) were referred to BAC1, BAC2 and BAC3 while correspondingly their controls (without bacteria) were CC1, CC2 and CC3, involving the exhausted carbon from the outlet, middle and inlet locations of the adsorption bed (EC1, EC2 and EC3), respectively.

4.2.2 On-line biofilters

Three glass columns (40 mm of diameter; 200 mm of packing height) were used (Figure 4.1). Columns A, B and C were packed with 150 g of the exhausted carbon from the outlet, middle, and inlet location of the adsorption bed (EC1, EC2 and EC3), respectively. The inlet H_2S concentration was maintained at about 20 ppmv by mixing 5% (v/v) standard H_2S (Linda Gas, Singapore) with air adjusted by mass flow controller (The Brooks Model 5850E, USA), except for shock loading and starvation conditions. The peristaltic pump was connected to a spray nozzle to uniformly spray the mineral medium on the surface of columns bed in a counter-flow direction with the inlet gas. 500 mL of mineral medium (Table 3.1) excluding thiosulfate was re-circulated at 100 mL min^{-1} for 2 min once every 6 h to provide the moisture and nutrient to the bacteria. Fresh medium was replaced at the end of every operating stage (i.e. start-up, shock loading and starvation). The experiment was conducted at room temperature of about 25 °C.

An online immobilization was adopted to start the biofiltration. Exhausted carbon was packed into the columns randomly, and then 500 mL of distilled water was re-circulated for 24 h to wash off some sulfur from exhausted carbon. Every 20 mL of concentrated microbial broth at a concentration of 2.32×10^8 cell mL^{-1} of SOB was poured into from the top of the columns. About 20 ppmv of H_2S gas was directed from the bottom into the packing columns at an empty bed residence time (EBRT) of 25 s.

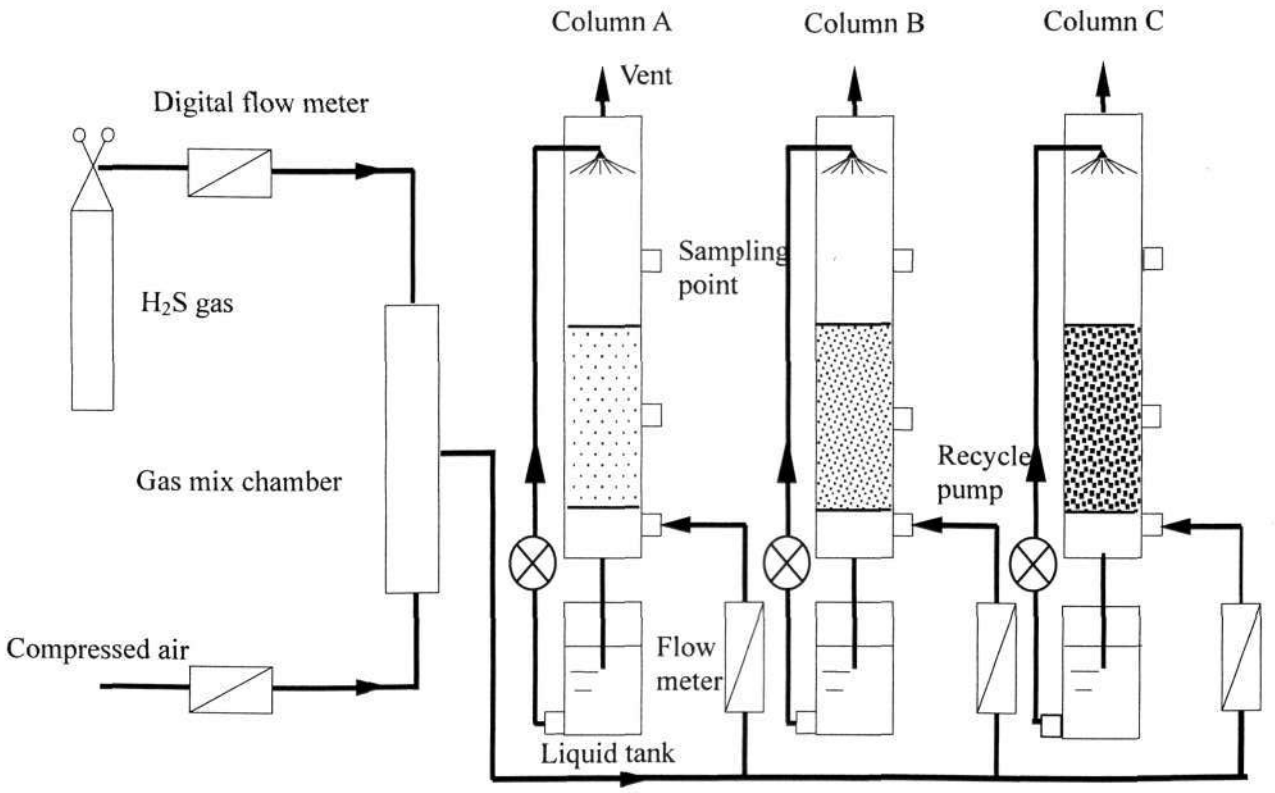

Figure 4.1 Schematic diagram of the biofilters system (Column A: packed with EC1; Column B: packed with EC2; and Column C: packed with EC3)

4.3 Results and discussion

4.3.1 Characteristics of exhausted carbon

The exhausted carbon from different locations of the adsorption bed was characterized for the surface properties, such as sulfur content, pH and structural parameters (Table 4.1). It can be seen that after serving as H_2S adsorbents, the pH values of carbon decreased from the outlet (EC1) to the inlet (EC3) of the adsorption bed. The contents of combustible sulfur and sulfate on carbon increased significantly from EC1 to EC3. The content of combustible sulfur was higher than sulfate on the corresponding exhausted carbon (Table 4.1). It is worthy noted that combustible sulfur is any reduced sulfur species, which might be utilized by SOB.

As shown in Table 4.1, BET surface area (S_{BET}) and micropore surface area (S_{mic}) decreased significantly from EC1 (845 and 378 $m^2\ g^{-1}$) to EC3 (641 and 278 $m^2\ g^{-1}$). Micropore volume (V_{mic}) also decreased from EC1 to EC3, 0.167 to 0.075 $cm^3\ g^{-1}$. This was due to higher content of sulfur adsorbed on carbon pores at the inlet than those at the outlet of the adsorption bed. It indicates that the carbon at the inlet (EC3) was fully used, while the carbon at the outlet (EC1) still remained similar pore structure as fresh carbon (FC) (Table 4.1). External surface area (S_{ext}) of exhausted carbon (466-463 $m^2\ g^{-1}$) did not change significantly, in comparison with that of fresh carbon (510 $m^2\ g^{-1}$). S_{ext} of activated carbon can be used to indicate the available surface for bacteria growth as nearly all internal surface areas are inaccessible, due to the large size of microorganisms (about 1 μm) (Black, 2005). It indicates that a large space is still available for bacterial attachment on exhausted carbon.

Table 4.1 Sulfur content, surface pH and structural parameters of exhausted carbons

Sample	Sulfur content (wt%)		pH	Structural parameters			
	S-combustible	S-sulfate		V_{mic} ($cm^3\ g^{-1}$)	S_{BET} ($m^2\ g^{-1}$)	S_{mic} ($m^2\ g^{-1}$)	S_{ext} ($m^2\ g^{-1}$)
FC	0.26	---	9.9	0.18	910	400	510
EC1	2.85	0.18	8.9	0.167	845	378	466
EC2	5.73	0.56	5.3	0.142	776	322	454
EC3	10.19	1.27	4.2	0.075	641	178	463

FC: fresh carbon; EC1, EC2 and EC3: exhausted carbon from the outlet, middle and inlet part of adsorption bed, respectively; ---: non-detectable; V_{mic}: micropore volume; S_{BET}: BET surface area; S_{mic}: micropore area; S_{ext}: external surface area

4.3.2 Off-line biofilm development

4.3.2.1 Biofilm development

After 15 days of off-line incubation of exhausted carbon, the carbon samples were collected from the experimental flasks for morphological observation. As shown in Figure 4.2, rod-shaped bacteria were distributed partially on carbon surface.

The carbon samples were also collected for plate counts after 15 days of off-line incubation. The results revealed that 1.0×10^5 to 5.8×10^5 cell g^{-1} dry carbon of SOB were attached on these carbons in the experimental flasks. The quantities of bacteria attached on BAC2 and BAC3 were higher than those on BAC1. This could be attributed to higher content of sulfur on EC2 and EC3 than those on EC1 (Table 4.1).

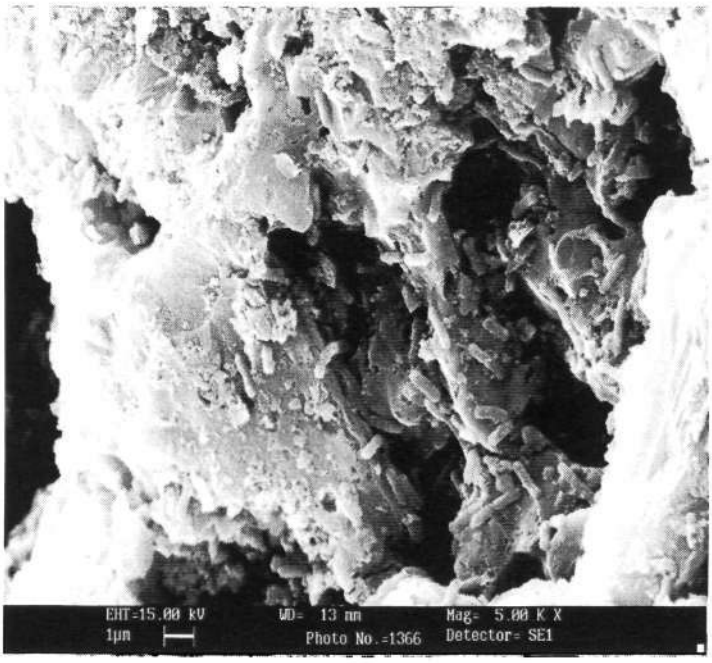

a

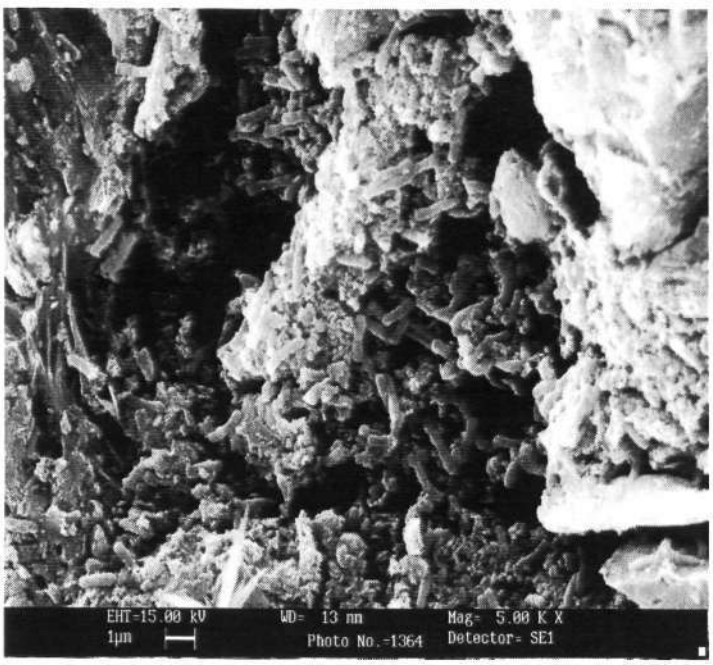

b

Figure 4.2 SEM morphology of biofilm developed on (a) BAC1 and (b) BAC3 after 15 days of off-line incubation (BAC1 and BAC3: experimental samples from EC1 and EC3, respectively)

The biofilm on carbon surface could be formed through the biodegradation of the pre-adsorbed sulfur on exhausted carbon for bacterial growth. The effectiveness of biodegradation can be determined by monitoring the generation of sulfate (Figure 4.3). After 1 day of incubation, sulfate concentration in the solution increased abruptly in all the flasks. It was because sulfate on EC1, EC2 and EC3 (Table 4.1) was washed off into liquid phase. The sulfate concentrations in the control flasks (CC1, CC2 and CC3) were relatively constant from day 1 up to day 28. The sulfate concentrations in BAC1 flask were slightly higher than those in CC1 flask. Nevertheless, sulfate concentrations in BAC2 and BAC3 flasks were significantly higher than those in CC2 and CC3 flasks respectively.

The results indicate that the biodegradation of sulfur occurred in the experiment flasks. It confirmed that the pre-adsorbed sulfur compounds on exhausted carbon were biodegraded for bacterial growth. On day 14, the pH of solution in BAC3 and CC3 flasks was adjusted from 5.2 and 6.2 to 7.0±0.2, respectively. The sulfate concentration in BAC3 flask was higher than that in CC3 flask right after the change (Figure 4.3).

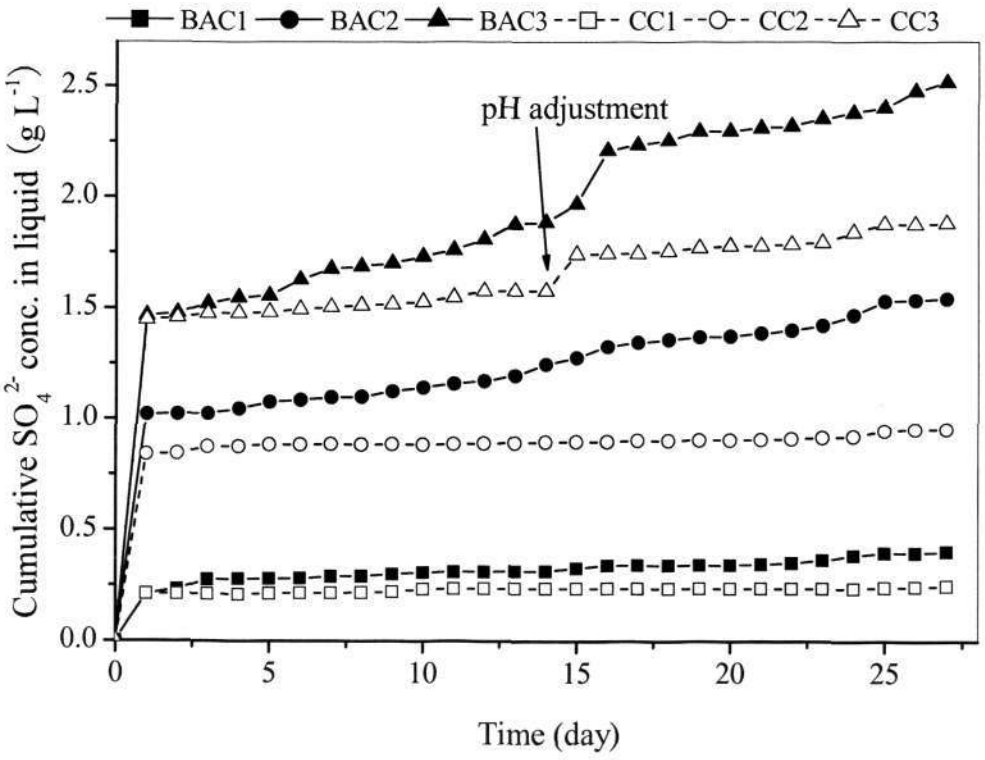

Figure 4.3 Sulfate concentration profiles during biofilm development in off-line incubation (BAC1, BAC2 and BAC3: experimental samples; and CC1, CC2 and CC3: control samples from EC1, EC2 and EC3, respectively)

4.3.2.2 Change of sulfur on carbon after biofilm development

The transformation of pre-adsorbed sulfur species on exhausted carbon is the basis to understand the process of biofilm development. The contents of combustible sulfur on carbon were determined after 28 days of off-line incubation (Figure 4.4). The contents of combustible sulfur increased significantly from CC1 to CC3 and from BAC1 to BAC3. The contents of sulfur on CC1, CC2 and CC3 (2.5-9.4 wt%) were lower than those on EC1, EC2 and EC3 (2.8-10.2 wt%), respectively (Table 4.1). It indicates that some sulfur on exhausted carbon was washed off in the control flasks. Furthermore, the contents of sulfur on BAC1, BAC2 and BAC3 (1.9-8.4 wt%) were much less than those on CC1, CC2 and CC3, respectively. This suggests that the presence of bacteria could help to release more sulfur from exhausted carbon.

The sulfur species on carbon samples were also identified by thermal analysis after 28 days of incubation (Figure 4.5). The peaks of differential thermogravimetric (DTG) represent the weight loss due to desorption of species from activated carbon at the specific temperature range in nitrogen gas. Taller peak means more weight loss. Some weakly attached SO_2 and H_2S can be easily desorbed by raising the temperature to around 130 °C. These species were not discussed because water is also desorbed from carbon surface at the temperature, which contributes to the weight loss and makes the interpretation of the results difficult. According to previous studies (Bandosz, 2002; Yan et al., 2004a), bonded-SO_2 can be desorbed at about 240-300 °C and elemental sulfur can be desorbed at about 380-400 °C.

As shown in Figure 4.5, compared with the case of fresh carbon (FC), the weight loss at the temperature range of about 380-400 °C significantly increased for EC3, CC3 and BAC3. It suggests that elemental sulfur was probably dominated on the three carbons. The weight loss for CC3 was smaller than that for EC3, and a further smaller weight loss for BAC3 was observed. The contents of sulfur on carbon were estimated from the DTG curves via separation of S-SO_2 and elemental sulfur (S^{el}) in different temperature ranges. The contents of S-SO_2 and S^{el} on CC3 were estimated to be 1.6 and 5.4 wt%, and those on BAC3 were 1.1 and 3.9 wt%, respectively. Compared with those on EC3 (2.1 and 7.7 wt%), the contents of S-SO_2 and S^{el} were decreased 26 and

29% in CC3 and 50 and 48% in BAC3, respectively.

A mass balance on sulfur could be evaluated based on the distribution of sulfur in liquid phase and on carbon, because no external sulfur source was added into the flasks, except for the sulfur compounds pre-adsorbed on exhausted carbon (Table 4.1). As shown in Table 4.2, the contents of sulfate in liquid phase of the CC flasks were almost the same as those on exhausted carbon (Table 4.1). This indicates that sulfate on exhausted carbon was washed off into liquid phase in the CC flasks. The contents of combustible sulfur in BAC1, BAC2 and BAC3 flasks were lower while the contents of sulfate were higher than those in CC1, CC2 and CC3 flasks, respectively. This was because some combustible sulfur on exhausted carbon in BAC flasks was biodegraded into sulfate during the incubation. In general, 82-99% of sulfur mass balance was achieved for the carbon samples after 28 days of off-line incubation.

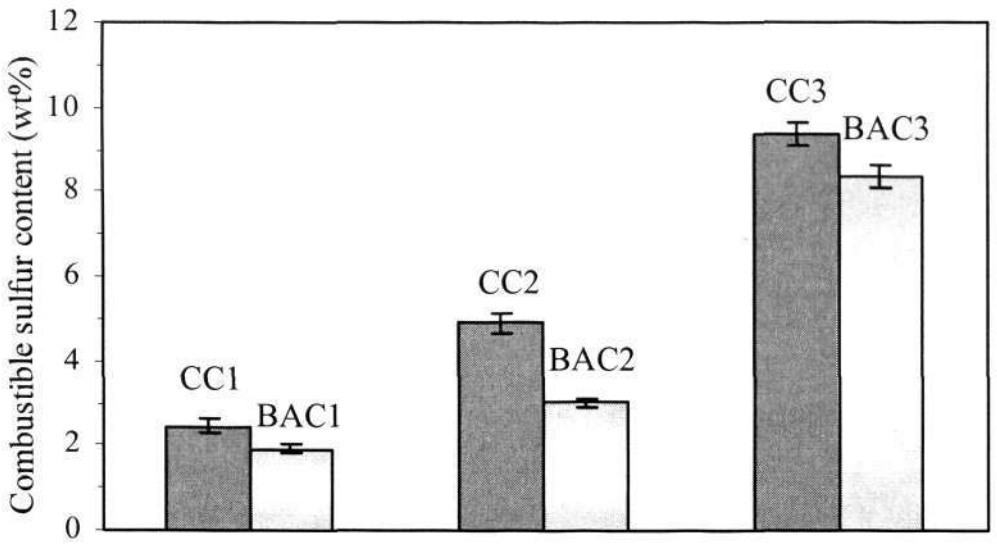

Figure 4.4 Content of combustible sulfur on carbon samples after 28 days of off-line incubation (BAC1, BAC2 and BAC3: experimental samples; and CC1, CC2 and CC3: control samples from EC1, EC2 and EC3, respectively)

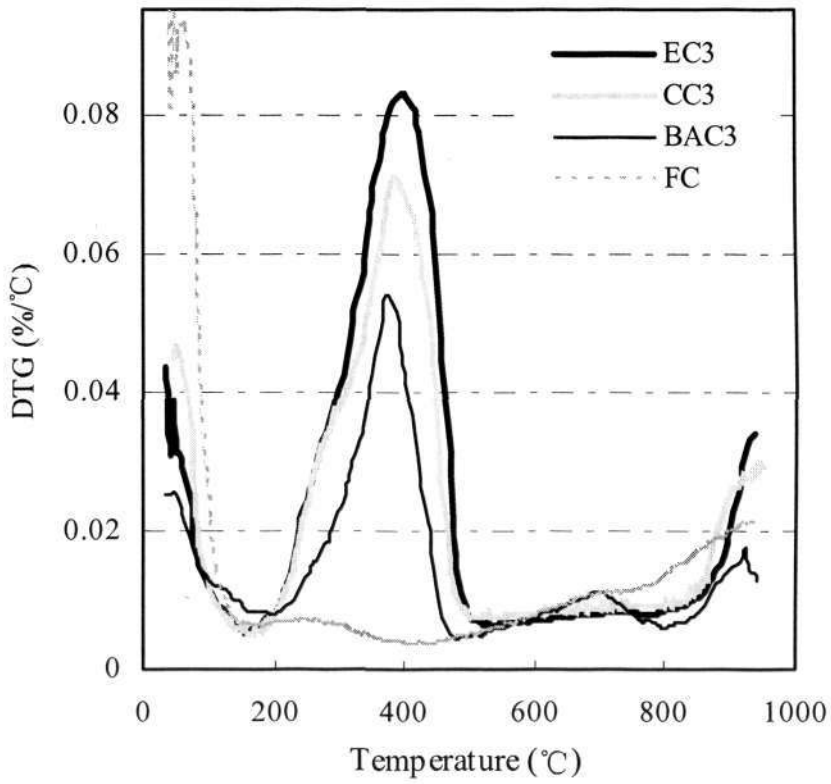

Figure 4.5 DTG curves for carbon samples (FC: fresh carbon; EC3: exhausted carbon at the inlet of adsorption bed; CC3 and BAC3: control and experimental samples from EC3 after 28 days of off-line incubation)

Table 4.2 Analysis of mass balance on sulfur after 28 days of off-line incubation

Sample	Liquid (wt%, g S/100 g carbon)		Carbon (wt%, g S/100 g carbon)	
	S-Combustible sulfur	S-sulfate	S-Combustible sulfur	S-sulfate
BAC1	0.10	0.51	1.92	0.19
BAC2	0.29	1.23	3.02	0.59
BAC3	0.25	1.78	8.36	0.75
CC1	0.15	0.15	2.48	0.05
CC2	0.49	0.50	4.98	0.18
CC3	0.57	1.12	9.44	0.31

(CC1, CC2 and CC3: control samples; and BAC1, BAC2 and BAC3: experimental samples from EC1, EC2 and EC3 after 28 days of off-line incubation, respectively)

4.3.2.3 Bio-regeneration

Bio-regeneration is the recovery of adsorption capacity of activated carbon by the biodegradation of adsorbed compounds on the carbon. It has been generally accepted that bio-regeneration involves desorption of the adsorbed compound from activated carbon to bulk solution, followed by biodegradation. This in turn, induces further desorption of the compound into the bulk solution (Hutchinson and Robinson, 1990). It can be seen that the regeneration of exhausted carbon could also be achieved through desorption without bacteria. In this study, bio-regeneration of activated carbon was evaluated by the method modified from previous studies (Ha and Vinitnantharat, 2000; Putz et al., 2005). The regeneration efficiency was calculated by the following equation:

$$\text{Regeneration efficiency with bacteria (\%)} = 100*(Q_1-Q_2)/Q_1 \qquad \text{Eq. 4.1}$$

$$\text{Regeneration efficiency without bacteria (\%)} = 100*(Q_1-Q_3)/Q_1 \qquad \text{Eq. 4.2}$$

where Q_1 is the initial amount of adsorbate adsorbed on exhausted carbon, g/g; and Q_2 is the amount of adsorbate remained after contact with biomass over a time period, g/g, and Q_3 is the amount of adsorbate remained after desorption without biomass over a time period, g/g.

Thus, in this study, net contribution of bacteria activity should be that regeneration efficiency in BAC flasks subtracts those in control flasks. As shown in Table 4.3, around 18-47% of pre-adsorbed combustible sulfur on carbon was regenerated in BAC flasks, among which about 10-33% was attributed to the bacterial activity.

Micropore volume (V_{mic}) and surface area (S_{mic}) were detected for BAC samples after 28 days of incubation. As shown in Figure 4.6, the V_{mic} of BAC (0.121-0.169$cm^3\ g^{-1}$) was slightly higher than those of exhausted carbon before biofiltration (0.105-0.165 $cm^3\ g^{-1}$). The S_{mic} of BAC (386-336 $m^2\ g^{-1}$) was also higher than those of exhausted carbon (378-278 $m^2\ g^{-1}$). About 40% of the initial V_{mic} and S_{mic} for fresh carbon were remained for EC3. After 28 days of incubation, the V_{mic} and S_{mic} of BAC3 recovered to 67 and 74% of those for fresh carbon, respectively. This indicates that the adsorption sites on carbon were recovered partially due to the biodegradation of pre-adsorbed sulfur on exhausted carbon.

Table 4.3 Regeneration efficiency of combustible sulfur on exhausted carbon

Sample	Regeneration efficiency (%)	Sample	Regeneration efficiency (%)	Net contribution of bacteria (%)
CC1	13.7	BAC1	33.0	19.3
CC2	14.5	BAC2	47.3	32.8
CC3	7.8	BAC3	18.0	10.2

(CC1, CC2 and CC3: control samples; and BAC1, BAC2 and BAC3: experimental samples from EC1, EC2 and EC3 after 28 days of off-line incubation, respectively)

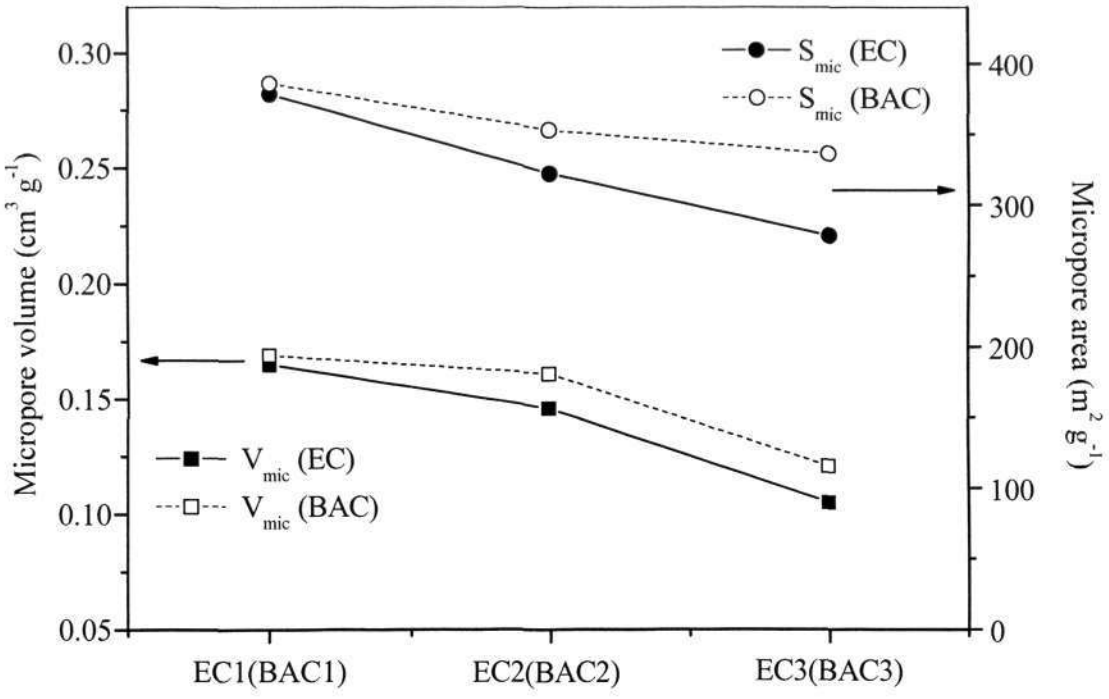

Figure 4.6 Micropore volume (V_{mic}) and area (S_{mic}) of carbon samples (EC: exhausted carbon; BAC: experimental samples; BAC1, BAC2 and BAC3: experimental samples from EC1, EC2 and EC3 after 28 days of off-line incubation, respectively)

4.3.3 On-line biofilters performance

4.3.3.1 Biofilm development

After 240 hours operation of the biofilters packed with exhausted carbon, the carbon samples were taken from the middle of the biofilters for morphological observation. As shown in Figure 4.7, a biofilm was well-formed on the carbon surface in the biofilters. This shows that exhausted carbon was transferred into biological activated carbon successfully in the online biofilters.

The carbon samples were also collected for plate counts after 240 hours of operation. The amounts of attached bacteria on carbon were 4.8×10^8, 9.2×10^8 and 1.4×10^9 cell g^{-1} dry carbon in Columns A, B and C, respectively. The biofilm was better formed on EC2 and EC3 than on EC1. This was possibly attributed to higher content of pre-adsorbed sulfur on EC2 and EC3 (Table 4.1).

4.3.3.2 Biofilters performance

The start-up performance of the biofilters is shown in Figure 4.8. H_2S was removed completely for the first 70 hours in Columns A, B and C. When EBRT decreased from 20 to 10 s at the 70^{th} hour, the removal efficiencies in all columns decreased temporarily. The removal efficiency of H_2S in Column C decreased more significantly than those in Columns A and B. It was possibly resulted from the fact that Column C (packed with EC3) had the limited adsorption capability (Table 4.1) and the biofilm was not well formed on carbon at this stage. When EBRT decreased to 5 s, the removal efficiency in Column A decreased from 99 to 94%. In Columns B and C, the removal efficiencies were relatively stable with decreasing EBRT to 4 s. This relatively stable removal may be attributed to higher amount of SOB in Columns B and C than that in Column A.

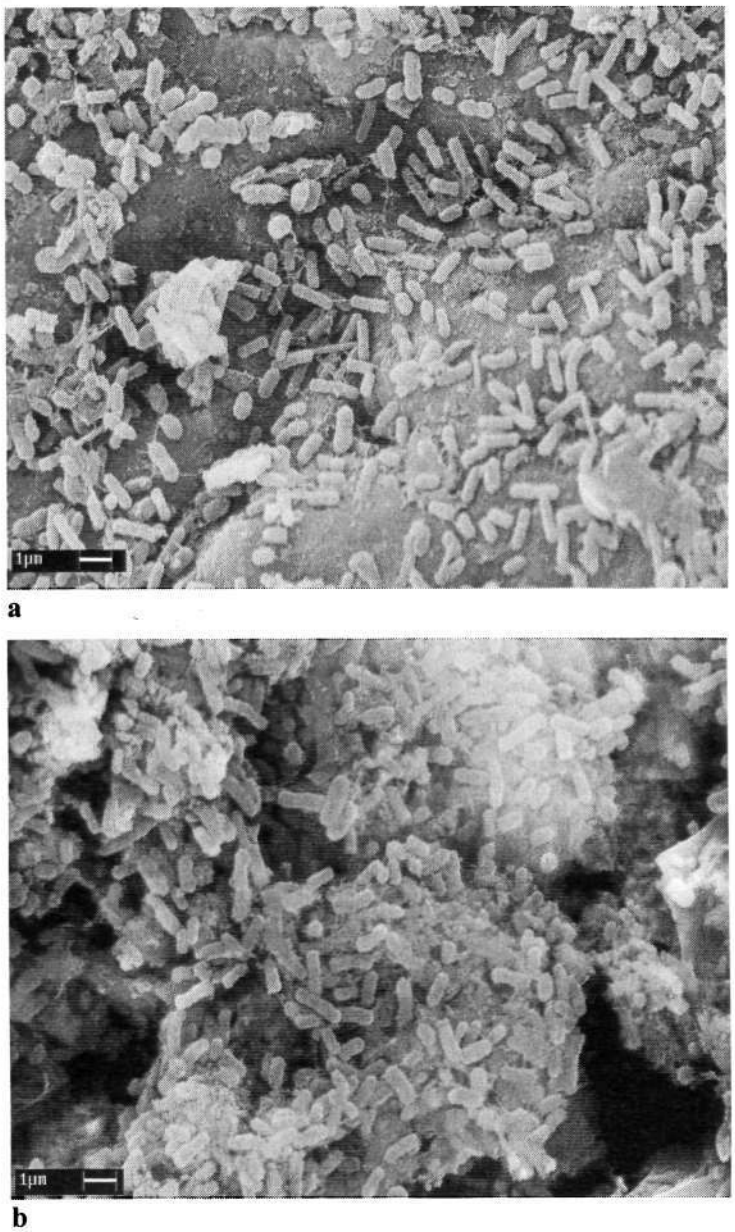

Figure 4.7 SEM morphology of biofilm developed on carbon in (a) Column A and (b) Column C after 240 hours of operation

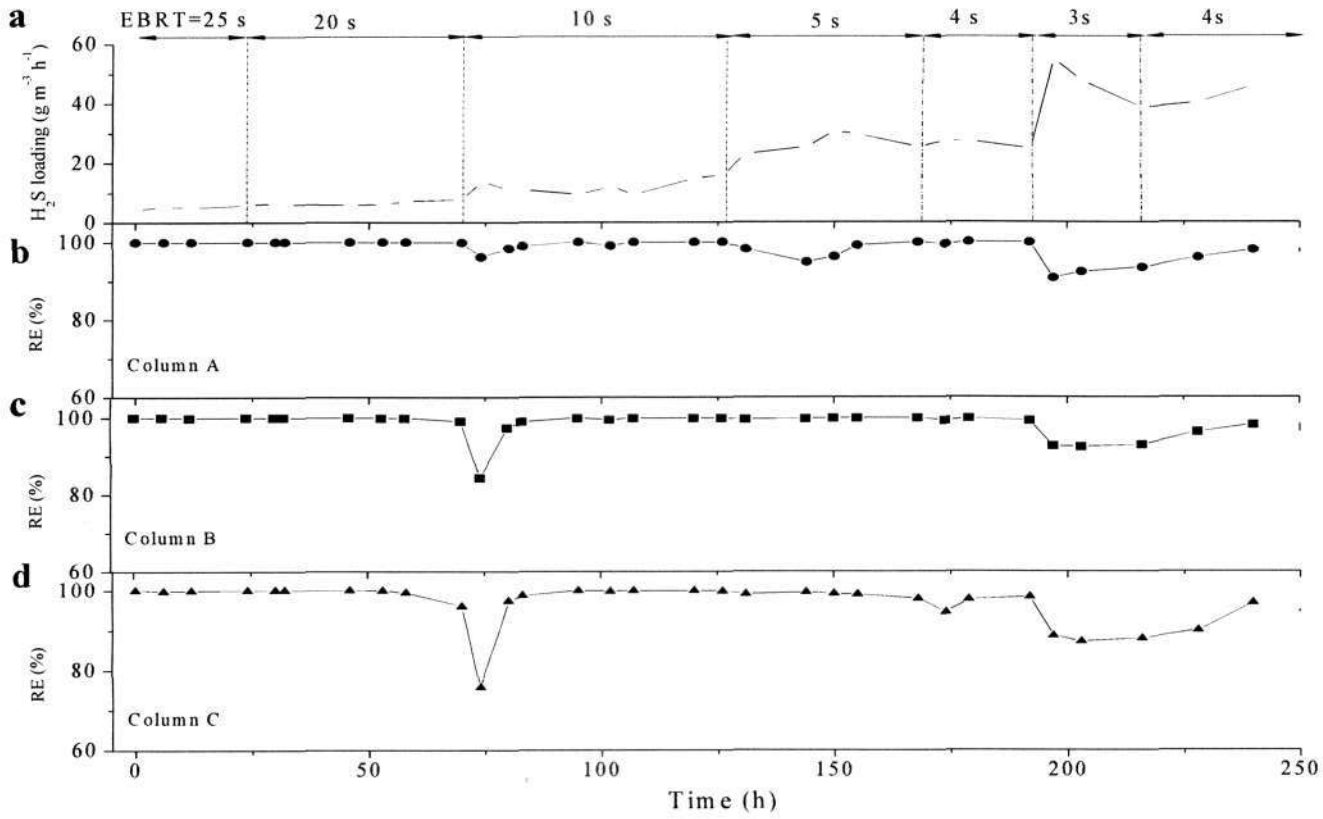

Figure 4.8 Start-up performance of the biofilters: (a) inlet H_2S loading, (b) removal efficiency (RE) in Column A, (c) RE in Column B and (d) RE in Column C

A start-up period of 10 days was needed in a biotrickling filter using polyurethane foam material (Gabriel and Deshusses, 2003). 6 days of start-up period was observed in the biofilter packed with fresh carbon (Duan et al., 2006). In the present study, a fast start-up of about 80 hours was observed in all the columns packed with exhausted carbon (Figure 4.8). This was possibly attributed to the pre-adsorbed sulfur on exhausted carbon, which could act as an additional sulfur source for microbial growth. This indicates the prospect of applying exhausted carbon in a biofilter for H_2S treatment.

After 240 hours of operation, three columns were subjected to a sudden increase in H_2S concentration (Figure 4.9). The inlet concentration varied from 20 up to 160 ppmv (i.e. 27 to 219 g m^{-3} h^{-1}) over 2 hours at EBRT of 4 s, and later the H_2S concentration was brought down to 20 ppmv. When the inlet H_2S concentration increased from 20 to 60 ppmv, the removal efficiencies dropped to 90, 91 and 70% in Columns A, B and C, respectively. When the inlet H_2S concentration decreased to about 20 ppmv, the outlet concentrations decreased rapidly to below 1 ppmv in all the columns. The response to other shock loadings was similar (Figure 4.9). Overall, the removal efficiencies recovered to the original level within 2 hours.

As shown in Figure 4.9, the performance in Columns A and B was higher than that in Column C during shock loadings. This was likely due to the high adsorption capability (i.e. buffering capacity) of the carbons in Columns A and B. From Table 4.1, it was expected that Column A packed with EC1 should have a better adsorption capacity than Column B packed with EC2. However, buffer capacities Columns A and B were almost identical (Figure 4.9). It suggests that part of the adsorption capacity of EC2 in Column B was recovered. In comparison, the recovery in the adsorption of EC3 in Column C was not satisfactory. The adsorption capacity of Column C could possibly be recovered better with a longer period under low inlet H_2S concentration or non-H_2S supply.

After 465 hours of operation, H_2S was not supplied while air and mineral medium was added in the columns. From the 575th hour, about 20 ppmv of H_2S was re-directed into the columns at EBRT of 4 s. The removal efficiencies rapidly recovered within 5 hours, with a shorter recovery time (1 hour) observed in Column C.

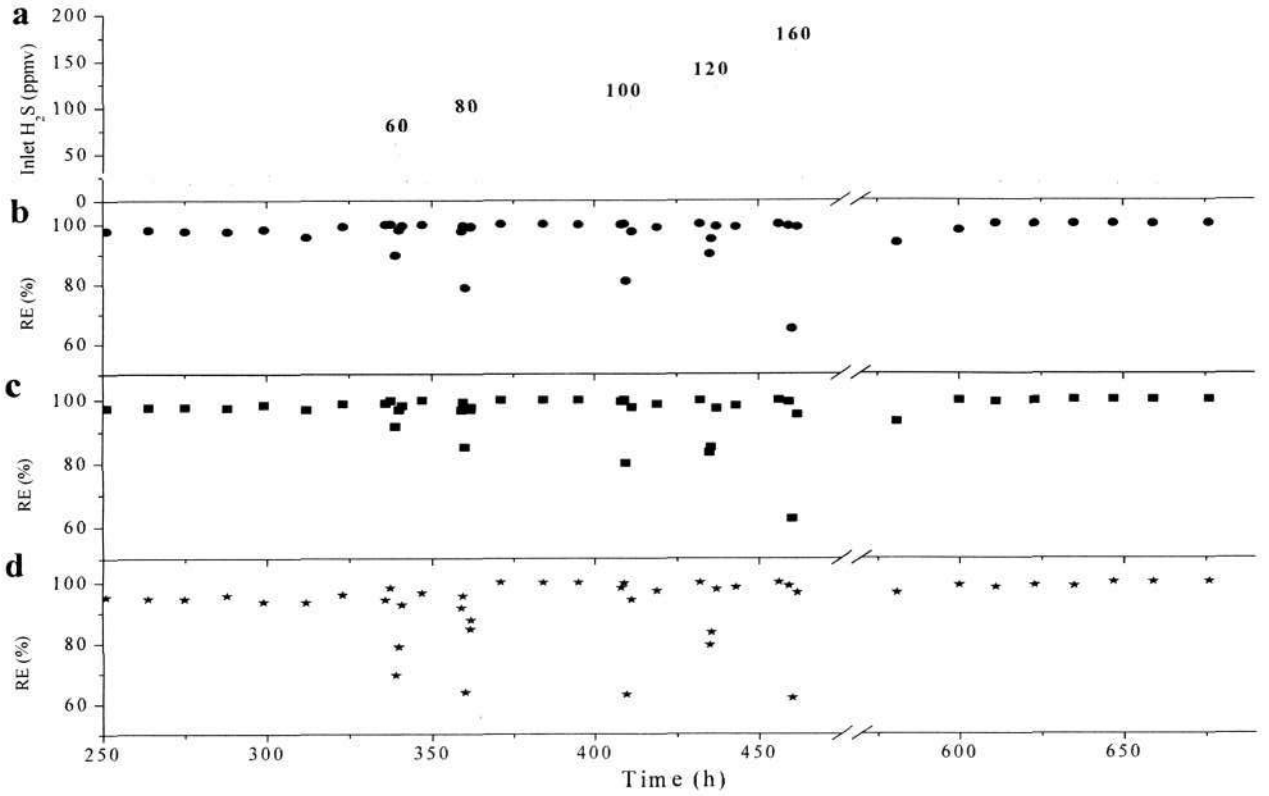

Figure 4.9 Response of the biofilters to shock loading and starvation of H_2S: (a) inlet H_2S concentration, (b) removal efficiency (RE) in Column A, (c) RE in Column B and (d) RE in Column C (EBRT = 4 s)

4.3.3.3 Sulfide biodegradation product

Sulfate and pH in liquid phase were monitored over the biofilters operation to determine the biodegradation of H_2S (Figure 4.10). At the end of the start-up period, sulfate concentration increased significantly to 2.8, 5.3 and 9.0 g L^{-1} in Columns A, B and C respectively (Figure 4.10a). The sulfate in liquid phase will be approximately 5.6 g L^{-1} if all removed H_2S (0.94 g S) are biodegraded into sulfate and totally existed in the liquid phase (0.5 L). This indicates that part of sulfate in Column C resulted from the biodegradation of the pre-adsorbed sulfur on carbon in addition to supplied H_2S. However, the sulfate in Column A was less than the theoretical sulfate from removed H_2S. Meanwhile, the pH value in Column C decreased from around 7 to 3, while the pH value in Column A remained almost constant (Figure 4.10b). The results indicate that there were more biodegradation of sulfur happening in Column C than in Column A during the start-up period. In addition, the high sulfate concentration (7.0-9.0 g L^{-1}) and low pH (about 3) during the 200-240th hour in Column C could be one of reasons for the low removal of H_2S (85%) at the short EBRT (3 s) (Figure 4.8).

During the shock loading period, sulfate concentrations increased and pH values decreased significantly in the three columns (Figure 4.10). Sulfate concentrations were higher and pH values were lower in Column C than those in Columns A and B. This might be attributed to both high amount of SOB (14×10^8 cell g^{-1} AC) and high content of sulfur on EC3 in Column C (Table 4.1). After 390 hours, the sulfate concentration and pH values in Column C remained at stable. It showed the incomplete biodegradation of H_2S, possibly due to low pH at 3 and high sulfate concentration in Column C at this period.

During the starvation period, sulfate concentrations still increased and pH dropped in all the columns (Figure 4.10). The sulfur adsorbed in biofilm or on carbon surface was biodegraded. Sulfate concentration was higher and pH value was lower in Column C than those in Columns A and B, which shows a higher biodegradation activity in Column C. This can explain that Column C could recover more quickly than Columns A and B after 110 hours of starvation period (Figure 4.9).

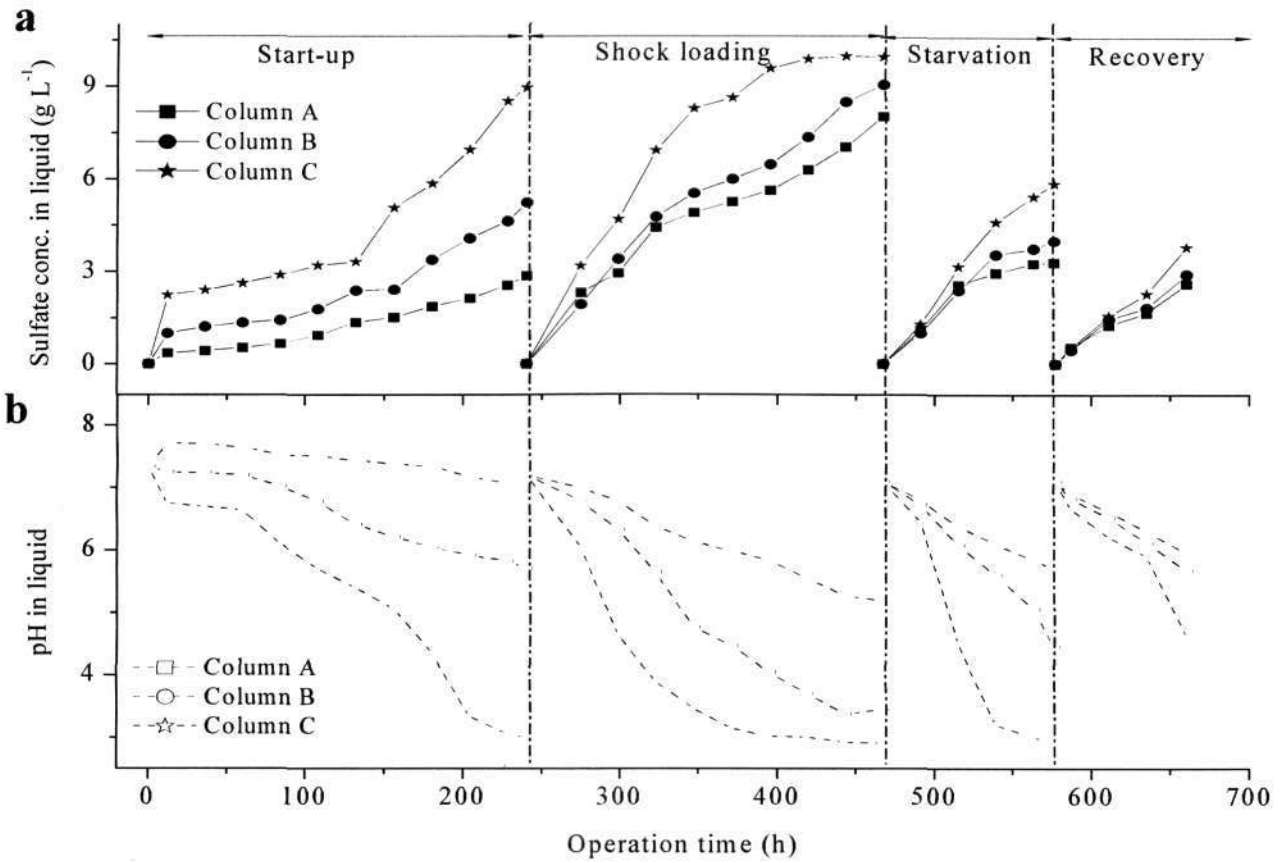

Figure 4.10 Profiles of sulfate concentration (a) and pH (b) in liquid phase of Columns A, B and C

The content of combustible sulfur on carbon samples from each column was also determined during the biofiltration (Figure 4.11). Overall, the contents of sulfur on carbon in all the columns decreased, compared with those on exhausted carbon before the biofiltration. During the start-up stage of biofiltration, the content of sulfur in Column C significantly decreased from 9.4 to 5.5 wt%. This indicates that the pre-adsorbed sulfur on EC3 in Column C was released significantly as energy source for bacteria. In Column A, the content of sulfur on carbon did not change significantly. It suggests that H_2S in gas phase served mainly as the energy source for bacteria. The sulfur contents in three columns slightly increased after the shock loading period, and decreased after the starvation period.

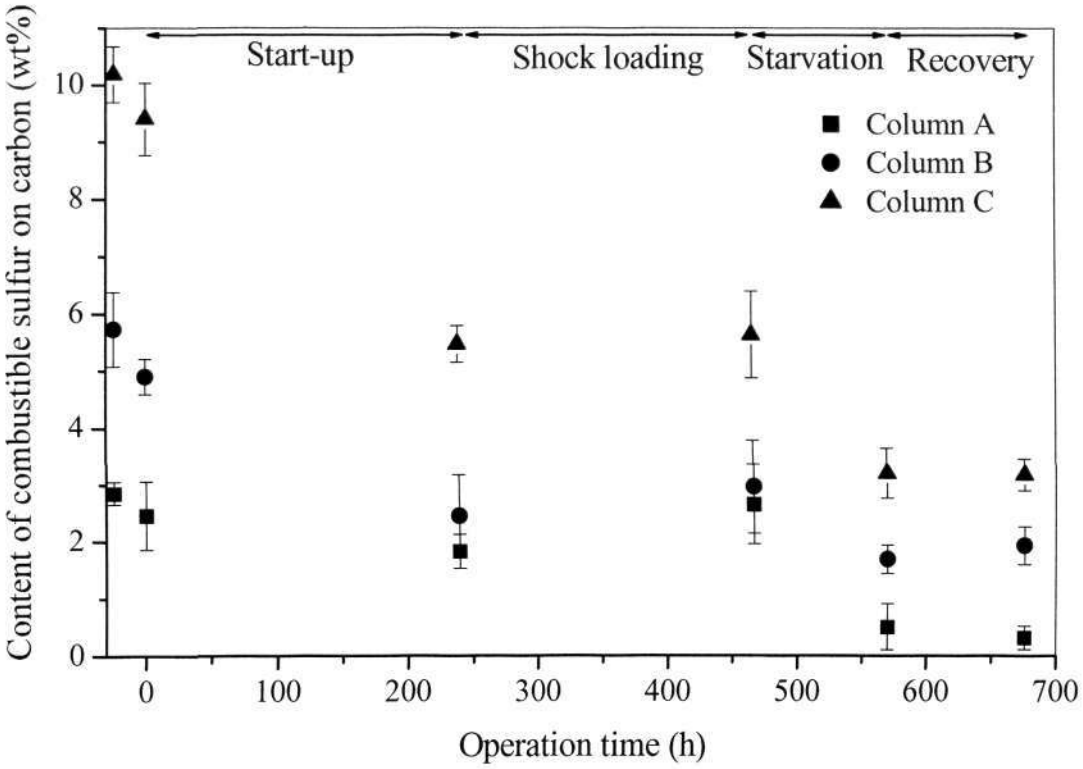

Figure 4.11 Content profiles of combustible sulfur on carbon in Columns A, B and C

4.3.3.4 Characterization of carbon after biofiltration

After the biofiltration, carbon samples (BAC1, BAC2 and BAC3) in Columns A, B and C were characterized (Table 4.4). The contents of sulfate on carbon slightly increased from 0.18-1.27 wt% before the biofiltration (Tables 4.1) to 0.58-1.35 wt% after the biofiltration (Tables 4.4). The contents of combustible sulfur on carbon significantly decreased from 2.85-10.19 wt% before the biofiltration (Tables 4.1) to 0.31-3.17 wt% on BAC (Tables 4.4). Compared with the case of off-line incubation (Figure 4.4), the contents of sulfur on carbon from the biofilters were much lower. It could be because the initial biofilm could be formed on carbon by utilizing the supplied H_2S as the energy source. Attached bacteria then facilitated the release of pre-adsorbed sulfur from exhausted carbon.

After the biofiltration, the surface pH values of carbon decreased (Table 4.4). This was attributed to the accumulation of H^+ produced by the biodegradation of sulfur compounds. The pH value of carbon in Column C was lower than those in Columns A and B. The low pH was not good for adsorption, which could affect the buffer capacity in Column C during shock loading period (Figure 4.9). Hence, necessary measures should be adopted to increase surface pH of EC3 when it is applied in biofiltration.

Table 4.4 Sulfur content, surface pH and structural parameters of carbon samples after biofiltration

Sample	Sulfur content (wt%)		pH	Structural parameters			
	S-combustible	S-sulfate		V_{mic} ($cm^3\ g^{-1}$)	S_{BET} ($m^2\ g^{-1}$)	S_{mic} ($m^2\ g^{-1}$)	S_{ext} ($m^2\ g^{-1}$)
BAC1	0.31	0.58	3.8	0.132	817	360	457
BAC2	1.93	0.87	3.1	0.148	698	333	366
BAC3	3.17	1.35	2.5	0.090	564	264	300

BAC1, BAC2 and BAC3: carbon samples from Columns A, B and C after biofiltration; V_{mic}: Micropore volume; S_{BET}: BET surface area; S_{mic}: Micropore area; and S_{ext}: External surface area

After the biofiltration, the pore structure of carbon samples was determined. As shown in Table 4.4, the values of all structure parameters decreased from BAC1 to BAC3. BET surface area (S_{BET}) of BAC in all the columns (564-817 m^2 g^{-1}) slightly decreased after the biofiltration, compared with the case of exhausted carbon (642-845 m^2 g^{-1}) (Tables 4.1). Micropore volume (V_{mic}) and surface area (S_{mic}) of BAC (0.09-0.13 cm^3 g^{-1} and 264-360 m^2 g^{-1}) did not change significantly from those of exhausted carbon (0.07-0.17 cm^3 g^{-1} and 178-378 m^2 g^{-1}). External surface area (S_{ext}) of BAC (300-457 m^2 g^{-1}) was slightly lower than exhausted carbon (463-466 m^2 g^{-1}). This may result from the bacterial attachment on carbon.

4.4 Conclusions

The results demonstrate that the biofilm can be formed on the surface of exhausted carbon using the pre-adsorbed sulfur as the sole energy source for bacterial growth in off-line trials. Around 18-47% of the pre-adsorbed sulfur on exhausted carbon was regenerated. The part of adsorption sites on carbon were recovered due to the biodegradation of the pre-adsorbed sulfur on exhausted carbon.

The biofilm can also be formed very well on the surface of exhausted carbon in on-line biofilters. During the biofiltration, the pre-adsorbed sulfur compounds on exhausted carbon were also biodegraded, with the sulfur contents decreased from 2.8-10.2 wt% to 0.3-3.2 wt% after 680 hours of biofilters operation. The biofilters packed with exhausted carbon demonstrated a quick start-up (about 80 hours) and worked well (> 95%) at a short EBRT of 4 s. Therefore, it is highly feasible and economical to transfer exhausted carbon into biological activated carbon for the removal of H_2S in biofiltration.

Chapter 5
Removal Mechanisms of H_2S Using Exhausted Carbon in Biofiltration

5.1 Introduction

Chapter 4 demonstrates that exhausted carbon is a promising and effective packing material in biofiltration for the removal of H_2S. Biofilm was developed on carbon surface (Figures 4.2 and 4.7) and part of the adsorption sites on carbon was recovered (Figure 4.6).

However, it is still unclear concerning the removal mechanisms of H_2S using exhausted carbon in biofiltration. The removal capacity of exhausted carbon in biofiltration could be attributed to the role played by the biofilm in metabolizing both pre-adsorbed sulfur compounds on carbon surface and supplied H_2S (Ng et al., 2004; Yan et al., 2004). The mechanisms include desorption of pre-adsorbed sulfur, biodegradation of desorbed sulfur, adsorption and biodegradation of supplied H_2S. It is very difficult to experimentally understand and integrate the subtle details of the phenomena occurring during the treatment. Mathematical models help to build a fundamental understanding of the biofiltration process (Shareefdeen and Singh, 2005).

Therefore, the main objective of this chapter is to explore and explain the mechanisms of H_2S abatement employing exhausted carbon in biofiltration by mathematical model simulation together with experimental data. This study is useful to provide an understanding of different mechanisms of H_2S removal in the biofilters using

exhausted carbon and fresh carbon.

5.2 Experimental setup

The exhausted carbons from different locations, the outlet, middle and inlet of the carbon adsorption bed, have different physical and chemical characteristics (Table 4.1). Biological activity on the exhausted carbon which was located at the inlet of adsorption bed has by far the most significant effect on process performance (Chapter 4). Thus, in the study, the inlet exhausted carbon was chosen as the packing material in biofiltration. Two parallel columns (80 mm diameter; 400 mm packing height) were packed with about 1.2 kg of exhausted carbon and fresh carbon, designated as Column EC and Column FC, respectively (Figure 5.1). They were operated in the same mode.

The inlet H_2S concentration was adjusted by mixing 5 % (v/v) standard H_2S (Linda Gas, Singapore) with air adjusted by mass flow controllers (The Brooks Model 5850E, USA). Four sampling ports were located along the bed from the top (inlet) to bottom (outlet) of the columns for gas sampling. The peristaltic pump was connected to a spray nozzle to uniformly spray the mineral medium on the surface of column bed in a concurrent-flow direction with the influent gas. A 1.5 L of mineral medium (g L^{-1}: KH_2PO_4, 4.08; K_2HPO_4, 10.44; $NaHCO_3$, 2.00; $MgCl_2 \cdot 6H_2O$, 0.46) was used at 100 mL min^{-1}. 0.5 L of recirculation liquid was replaced with fresh medium every day to prevent a toxic accumulation of sulfur compounds in the system.

An online immobilization was adopted to start the biofiltration. After exhausted carbon was packed into Column EC, 1.5 L of distilled water was re-circulated in the column for 24 hours to wash off some sulfur from exhausted carbon. 100 mL of concentrated sulfide-oxidizing bacteria (SOB) culture at 2.2×10^7 cell mL^{-1} was poured into from the top of the two columns. About 35 ppmv of the synthetic H_2S gas was directed from the top into the packing columns at an empty bed residence time (EBRT) of 10 s.

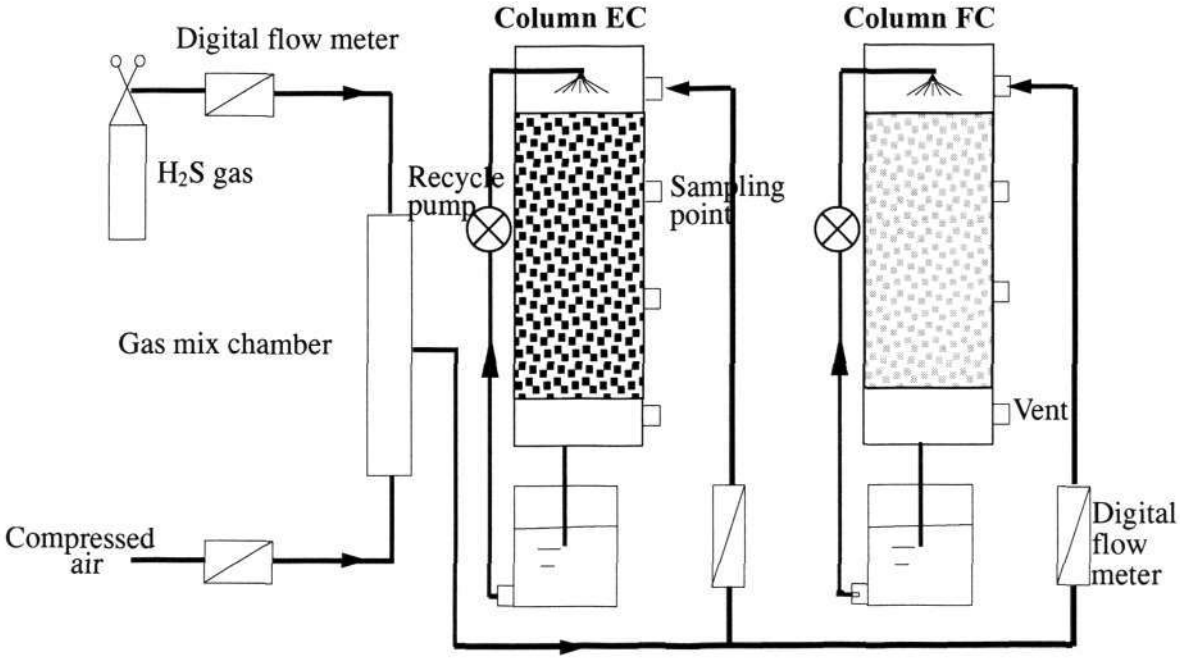

Figure 5.1 Schematic diagrams of Column EC and Column FC biofiltration system

5.3 Model development

5.3.1 Model description

A mathematical model is developed based upon some fundamental mechanisms. They include biofilm transport from the bulk gas, biodegradation within the biofilm, diffusion through the biofilm immobilized on carbon surface to the carbon particles, adsorption within the carbon, and growth of the biofilm (Figure 5.2).

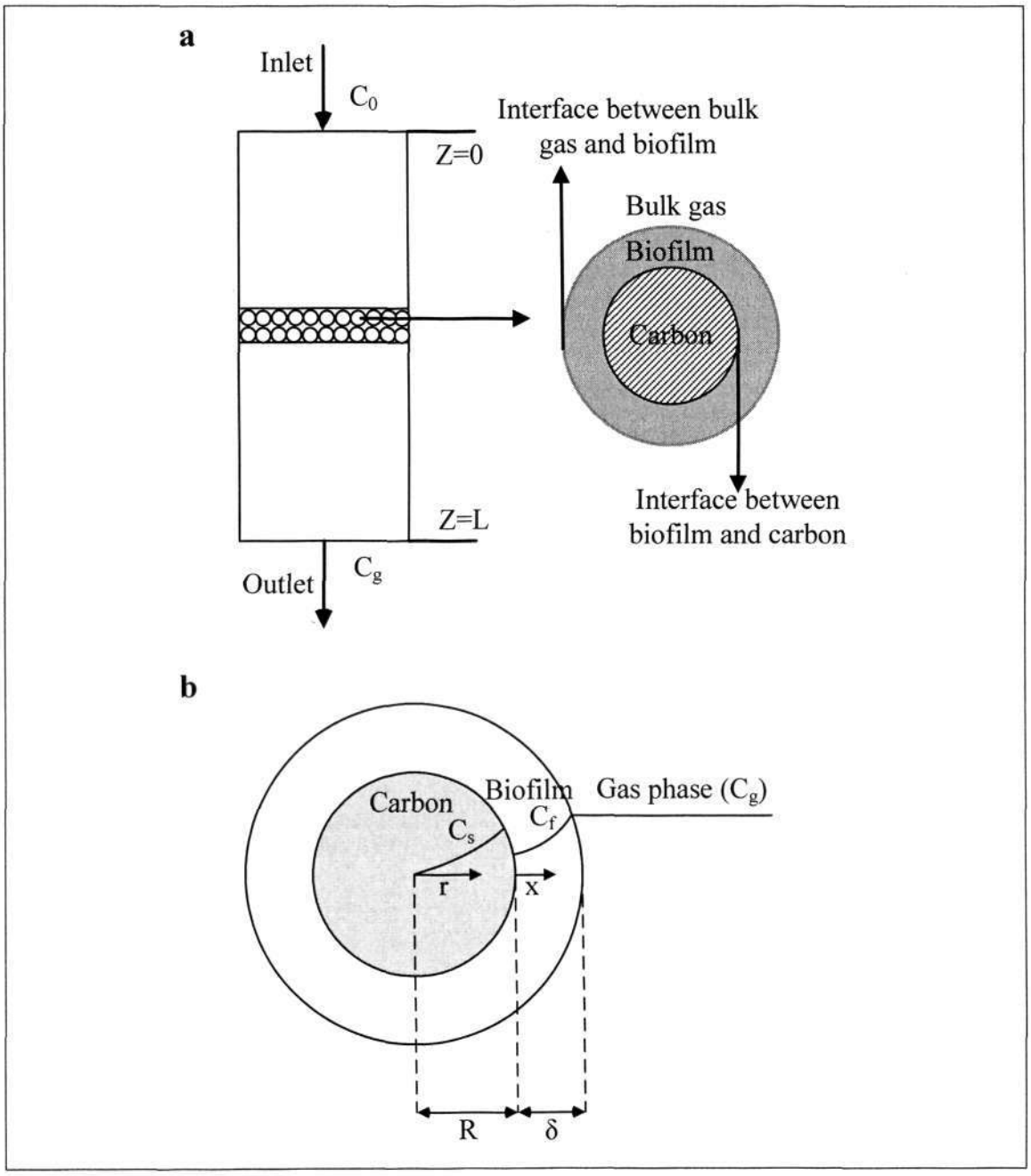

Figure 5.2 Conceptual basis (a) and concentration profile (b) of biological activated carbon system

It is assumed that part of the adsorption sites on exhausted carbon can be recovered by desorption and biodegradation of pre-adsorbed sulfur on the carbon after the start of biofiltration. The recovered adsorption sites can be used for additional adsorption during biofiltration system.

Several simplified assumptions are made in developing the theoretical model and listed as follows:

1. An axially dispersed plug flow is assumed for the gas flow through the packed bed, and gas flow rates are sufficiently high to neglect axial dispersion.
2. Oxygen limitation is not considered in this study.
3. The biodegradation is described by the Monod kinetics.
4. The biofilm is modeled as a flat plate, because the thickness of the biofilm is much smaller compared with the diameter of the carbon pellet. The biofilm is assumed as a homogeneous layer with uniform cell density. The substrate is assumed to contact the biofilm and transport within the biofilm through diffusion only and characterized by Fick's law (Montgomery, 1985).
5. The granular carbon particles are assumed to be spherical. The intra-particle substrate concentration inside carbon pellet is considered to be radically uniform.
6. The rate of mass transfer around the boundary of the carbon pellet is approximated by a linear driving force (LDF) model.
7. Adsorption is a reversible process driven by concentration gradients, and its equilibrium is characterized by the Freudlich isotherm. First order adsorption kinetics is applied to describe the adsorption on carbon particles.
8. The biofilm is formed on the external surface of the carbon pellets. Biomass does not grow in the pores of the pellets and thus no biodegradation occurs in the pores.
9. The external surface of the carbon is completely covered with the biofilm.
10. The water layer in the biofilters represents a negligible barrier to gas contaminant transfer, and so it is ignored (Alonso et al., 1997; Kim and Deshusses, 2003).

Based on the above assumptions, the transient biofilter operation is described using the following equations.

Gas phase

The mass balance of the substrate (H_2S) concentration in gas phase of the carbon filter, which considers the dispersion, advection, reactions in the biofilm and solid phases can be modeled as described previously (Liang et al., 2007):

$$\frac{\partial C_g}{\partial t} = D_g \frac{\partial^2 C_g}{\partial z^2} - V\frac{\partial C_g}{\partial z} - \frac{1-\varepsilon}{V_p \varepsilon}\int_0^{\delta} X_f \frac{\mu_m C_f}{K_s + C_f} 4\pi (x+R)^2 dx - \frac{1-\varepsilon}{\varepsilon}\rho_p \frac{\partial C_s}{\partial t} \qquad \text{Eq.5-1}$$

Initial condition:

$$C_g\big|_{t=0} = 0 \qquad \text{Eq.5-1a}$$

Boundary condition 1:

$$C_g\big|_{z=0} = C_{g0} \qquad \text{Eq.5-1b}$$

Boundary condition 2:

$$\left.\frac{\partial C_g}{\partial z}\right|_{z=L} = 0 \qquad \text{Eq.5-1c}$$

where C_g =substrate concentration in air phase at a position z along the filter, $g \cdot m^{-3}$; D_g =dispersion coefficient of substrate in air phase, $m^2 \cdot s^{-1}$; z =distance of travel in the filter, m; V = axial interstitial gas velocity, $m \cdot s^{-1}$; ε =bed porosity of the filter column; V_p =volume of a carbon particle, m^3; X_f = biomass density in the biofilm, $g \cdot m^{-3}$; μ_m = maximum degradation rate, s^{-1}; K_s = half-saturate constant, $g \cdot m^{-3}$; C_f = substrate concentration in biofilm, $g \cdot m^{-3}$; R =equivalent radius of carbon pellet (spherical), m; x =distance in biofilm, 0 ~δ m; δ =biofilm thickness, m; ρ_p =carbon particle density, g m^{-3}; C_s =substrate concentration in the solid particle, g g^{-1}; t =time, d; and L =length of the filter, m.

Biofilm phase

The substrate reaction in the biofilm surrounding the carbon pellets is characterized by the Monod biodegradation kinetics. H_2S is the only rate-limiting substrate. The

equation combining mass transport and biodegradation can be written as follows (Liang et al., 2007):

$$\frac{\partial C_f}{\partial t} = D_f \frac{\partial^2 C_f}{\partial x^2} - X_f \frac{\mu_m C_f}{K_s + C_f} \qquad 0 \le x \le \delta \qquad \text{Eq.5-2}$$

Initial condition:

$$C_f\big|_{t=0} = 0 \qquad \text{Eq.5-2a}$$

Boundary condition 1:

$$D_f \frac{\partial C_f}{\partial x}\bigg|_{x=0} = D_s \rho \frac{\partial C_s}{\partial r}\bigg|_{r=R} \qquad \text{Eq.5-2b}$$

Boundary condition 2:

$$C_f\big|_{x=\delta} = \frac{C_g}{H} \qquad \text{Eq.5-2c}$$

where D_f =diffusivity coefficient of substrate in the biofilm, $m^2 \cdot s^{-1}$; D_s =diffusivity coefficient of substrate within carbon pellet, $m^2 \cdot s^{-1}$; H = Henry's Law constant; and r = radius distance in carbon pellets, m. The first boundary condition establishes that the mass flux into the solid/biofilm interface must be equivalent to that leaving the interface. The second boundary condition describes the interface equilibrium between the biofilm and gas phase.

The biodegradation rate by a single carbon particle can be derived by integrating the Monod reaction expression and the amount of biofilm volume (Liang et al., 2007):

$$\int_0^{\delta} X_f \frac{\mu_m C_f}{K_s + C_f} 4\pi (R + x)^2 dx \qquad 0 \le x \le \delta \qquad \text{Eq.5-3}$$

Solid phase

Substrates that diffuse to the bottom of the biofilm can be adsorbed into the carbon, particularly during the early stages of biofiltration when the biofilm is thin (Devinny and Ramesh, 2005). The adsorbed substrate is subsequently transported to the inner pore-wall of the carbon, driven by the concentration gradient along the carbon radius. The transport is described by the classic 1-D diffusion equation (Traegner and Suidan,

1989):

$$\frac{\partial C_s}{\partial t} = \frac{D_s}{r^2}\frac{\partial}{\partial r}(r^2\frac{\partial C_s}{\partial r}) \qquad 0 \le r \le R \qquad \text{Eq.5-4}$$

Initial condition: $C_s|_{t=0} = 0$ (Fresh carbon) Eq.5-4a

$C_s|_{t=0} = Q_0$ (Exhausted carbon) Eq.5-4b

Boundary condition 1:

$$\left.\frac{\partial C_s}{\partial r}\right|_{r=0} = 0 \qquad \text{Eq.5-4c}$$

Boundary condition 2:

$$C_s|_{r=R} = K_F C_f^{\,n}|_{x=0} \qquad \text{Eq.5-4d}$$

where Q_0 = adsorbed substrate concentration in the exhausted carbon before biofiltration process, g g^{-1}; K_F and n represent the Freundilich isotherm constants. The first boundary condition describes a symmetric concentration profile over the entire carbon particle, with no concentration gradient at its center. An adsorption isotherm is used to relate the concentration adsorbed in solid phase at the biofilm-solid interface, as the second boundary condition. First order adsorption kinetics was applied: $\rho_p \frac{\partial C_s}{\partial t} = k_{ad} C_f|_{x=0}$, where k_{ad} is the first order reaction rate constant that describes adsorption on carbon particles, s^{-1}.

Substrate molecules accumulate within as they penetrate deeper into the carbon particle. In this regard, the accumulated or adsorbed quantity of contaminants per particle can be computed from the following equations.

$$M = \int_0^R C_s dV_p = 4\pi \int_0^R C_s r^2 dr \qquad \text{Eq.5-5}$$

System solution

The proposed model consists of a set of coupled partial differential equations (PDEs). The governing equations of the substrate concentrations in the gas phase (Eq.5-1),

within the biofilm (Eq.5-2) and in the carbon particle (Eq.5-4) were solved by MATLAB (partial differential equation toolbox).

5.3.2 Determination of model parameters

The bio-kinetic and adsorption parameters for H_2S in this model were determined independently from a series of mini-biofilter and mini-adsorption column experiment. They were specifically designed to simulate the actual biofilter operational regimes in a miniature scale. The set of model parameters are tabulated in Table 5.1. Details of determination of the model parameters are provided as follows.

Mass-transfer parameters (D_g, D_f and D_s)

The mass transfer parameters include the intra-particle surface diffusion coefficient (D_s), the substrate diffusion coefficient in air (D_g) and in biofilm (D_f). The D_s was independently estimated by adopting the parameter-search technique involving the homogeneous surface diffusion model (HSDM) (Kim and Pirbazari, 1989; Pirbazari et al., 1993). The parameter D_s, which represents the diffusion of the compound along the pore-wall surfaces, determines the uptake rate of a compound by activated carbon. Its value was validated by simulating the mini-column adsorption breakthrough profiles using the non-bioactive version of the biofiltration model (Ravindran et al., 1999).

The D_g can be estimated from the correlation method proposed by Fuller et al. (1966) based on molecular diffusivity:

$$D_g = \frac{0.001T^{1.75}\sqrt{\frac{1}{M_1}+\frac{1}{M_2}}}{P\left[(\Sigma v)_1^{1/3}+(\Sigma v)_2^{1/3}\right]^2} \qquad \text{Eq.5-6}$$

where v represents the molar volume, M is the molar mass, and the subscripts 1 and 2 correspond to H_2S and air molecules, respectively. The constants T and P denote the

absolute temperature (K) and pressure (atm), respectively.

Diffusion of contaminants in biofilm is generally slower than that in water due to the additional resistance attributed to the microorganisms. The D_f was estimated from the diffusivity of H_2S in water (D_w) using the correlation of Williamson and McCarty (1976): $D_f/D_w = 0.8$. The diffusivity of H_2S in water was estimated at 1.61×10^{-9} m^2 s^{-1} (Perry and Green, 1999).

Adsorption rate constant (k_{ad})

Adsorption rate constant was determined from a series of mini-column adsorption experiments. The column (i.d. 20 mm) (Figure 3.1) was filled with activated carbon to a height of 2 cm. Different concentrations of H_2S gas stream (10, 20, 30 and 50 ppmv) were passed through the column at a superficial velocity of 2 $cm{\cdot}s^{-1}$. Measuring the removal rate prior to exhaustion time yields a theoretical rate constant. The outlet concentration profiles against time revealed an exponential increasing function. Therefore, the first-order adsorption rate constant (k_{ad}) for the varied inlet H_2S concentrations could be estimated by performing a linear regression analysis of the constant pattern profiles. k_{ad} value was obtained at 0.21 ± 0.08 s^{-1}.

Adsorption equilibrium parameters (K_F and n)

Adsorption equilibrium parameters were also determined from a series of mini-column adsorption experiments. Different concentrations of H_2S gas stream (10, 20, 30, and 50 ppmv) were passed through the column (i.d. 20 mm) (Figure 3.1) filled with different quantities of activated carbon (2, 3, 4 and 6 g). The breakthrough profile for each operating condition was determined by periodic analysis of samples from effluent streams. The mini-column adsorption experiments generated a series of H_2S breakthrough profiles corresponding to different influent concentrations and carbon masses. The Freudlich isotherm was found to provide the most appropriate

representation of equilibrium data. The logarithmic version of the Freudlich relation is expressed as follows:

$$InC_s = InK_F + nInC_0 \qquad \text{Eq. 5-7}$$

The values of the Freundlich isotherm constants, K_F and n, were determined to be 2.16 g g^{-1} $(m^3\ g^{-1})^n$ and 0.71, respectively.

Biofilm thickness (δ)

The biofilm thickness (δ) was estimated as described previously (Herzberg et al., 2003).

$$\delta = \frac{\rho_p V_p X_b}{\pi d_p^{\ 2} X_f} \qquad \text{Eq. 5-8}$$

where d_p = particle's diameter, m; and X_b = biomass concentration in the biofilm on carbon, g g^{-1} carbon.

Biodegradation parameters (K_s and μ_m)

The column experiments (internal diameter of 40 mm; packing depth of 200 mm) were used (Figure 4.9) to provide an accurate and realistic approach for estimating bio-kinetic parameters. The column was packed with plastic discs (Ng et al., 2004) as a non-adsorbing medium to simulate H_2S removal solely attributed to biodegradation. The medium was seeded with an enriched SOB culture prior to packing into the column. Various inlet concentrations (10, 20, 30 and 50 ppmv) were investigated at EBRT of 10 s. The column was operated for at least 5 days under steady-state removal for each set of inlet concentration.

The Monod half-saturation constant (K_s) and maximum substrate utilization rate (μ_m) were estimated by using the linear version of mass balance equations for a plug-flow reactor under steady-state conditions.

$$\frac{X_f T_g}{C_0 - C_e} = \frac{K_s}{\mu_m} \frac{In(C_0 / C_e)}{C_0 - C_e} + \frac{1}{\mu_m} \qquad \text{Eq. 5-9}$$

The plot of $X_f T_g / (C_0 - C_e)$ and $In(C_0 / C_e) / (C_0 - C_e)$ shows a good linear correlation (R^2=0.978), from which K_s and μ_m were estimated as 0.039 g m^{-3} and 3.61 d^{-1}, respectively. T_g is the gas residence time for the column, s.

Table 5.1 Values of model parameters preset

Parameters	**Description**	**Symbol**	**Input Value**
Mass-transfer parameters	Effective diffusion coefficient in biofilm	D_f, $m^2\ s^{-1}$	1.28×10^{-9}
	Dispersion coefficient of substrate in air	D_g, $m^2\ s^{-1}$	1.8×10^{-5}
	Internal pore diffusivity of substrate within carbon	D_s, $m^2\ s^{-1}$	4.16×10^{-13}
Physicochemical parameters	Equivalent radius of carbon particle	R, m	2.7×10^{-3}
	Particle's diameter	d_p, m	5.4×10^{-3}
	Particle density	ρ_p, $g\ m^{-3}$	0.49×10^{6}
	Typical particle volume	V_p, m^3	0.083×10^{-6}
	First-order adsorption rate constant	k_{ad}, s^{-1}	0.21
	Distribution coefficient between biofilm & air	H	0.42
	Freundlich isotherm constant	K_F, $g\ g^{-1}\ (m^3\ g^{-1})^n$	2.16
	Freundlich isotherm constant	n	0.71
	Material bed porosity	ε	0.37
	Adsorbed substrate concentration in the exhausted carbon before biofiltration process	Q_0, $g\ g^{-1}$	0.1
Biological parameters	Maximum substrate utilization rate	μ_m, d^{-1}	3.61
	Half-saturation constant	K_s, $g\ m^{-3}$	0.039
	Microbial yield coefficient	Y, $g\ g^{-1}$	0.28
	Biofilm thickness	δ, μm	2-52
	Biofilm density	X_f, $g\ m^{-3}$	0.028×10^{6}

Y (Rittmann and McCarty, 2001); X_f (Den and Pirbazari, 2002); H (Perry and Green, 1999); D_s, D_g and D_f was independently estimated by the methods described previously (Fuller et al., 1966; Williamson and McCarty, 1976; Kim and Pirbazari, 1989; Pirbazari et al., 1993); ε was calculated by the equation described previously (Hodge and Devinny, 1995); δ was calculated by the equation described previously (Herzberg et al., 2003).

5.4 Results and discussion

5.4.1 Biomass concentration

The biomass concentration in a bioreactor is one of the most important parameters governing the overall removal of waste gases in biofiltration (Liang et al., 2003). In the biofiltration process, as the substrate (H_2S) diffuses into and through the bioreactor, H_2S is utilized for the growth of biofilm. Mathematically, the growth rate of microbial cells is frequently expressed as (Rittmann and McCarty, 2001):

$$\frac{dX_a}{dt} = Y(-r) - bX_a \qquad \text{Eq.5-10}$$

where dX_a/dt represents the net growth rate (mg m^{-3} h^{-1}) of active organism (X_a, mg m^{-3}); Y is the yield coefficient of biomass, 0.28 mg cells mg^{-1} H_2S-S (Rittmann and McCarty, 2001) ; t is operation time, h; -r represents the rate of elimination of H_2S, mg $m^{-3}.h^{-1}$; and b is the loss rate of the organisms due to endogenous decay, 0.0028 h^{-1} (Lin and Leu, 2008). Since the rate of the re-circulating liquid stream is very low in the biofiltration system, the biofilm detachment is negligible. Integration of Eq.5-10 gives:

$$X_a = (X_{a0} - \frac{Y(-r)}{b})e^{-bt} + \frac{Y(-r)}{b} \qquad \text{Eq.5-11}$$

where X_{a0} is the initial biomass concentration at t=0, and assume X_{a0}=10 mg m^{-3}.

The protein (biomass) concentration profiles in Column EC and Column FC are shown in Figure 5.3. The biomass concentration in Column EC was higher than that in Column FC. Compared with the prediction from Eq.5-11, the biomass concentration in Column EC was higher while that in Column FC was relatively lower during the start-up period.

The un-similar biomass development in the two columns could be because they

received different loads of sulfur source even though the same loading of H_2S gas was supplied. Column EC was supplied with higher sulfur load: H_2S feeding + pre-adsorbed sulfur on carbon. The concentration of sulfur on exhausted carbon significantly decreased from 10.2 to 4.5 wt% after 30 days of biofiltration. In contrast, Column FC was supplied with only H_2S feeding as sulfur source. In addition, the slow biomass development was also due to the significant adsorption capacity of fresh carbon. The growth of biomass on fresh carbon only occurred in response to substrate in gas adjacent to the carbon particles.

It should be noted that this advantage of Column EC takes place only under the conditions of low inlet concentration of H_2S. At this time when the substrate is limited, the extra sulfur source from exhausted carbon is beneficial. At most of WWTPs, H_2S concentration in the sewage air stream is typically less than 40 ppmv (Devinny et al., 1999; Shareefdeen and Singh, 2005). Hence, biofilters packed with exhausted carbon should be able to perform efficiently for the removal of H_2S during the start-up period of biofiltration.

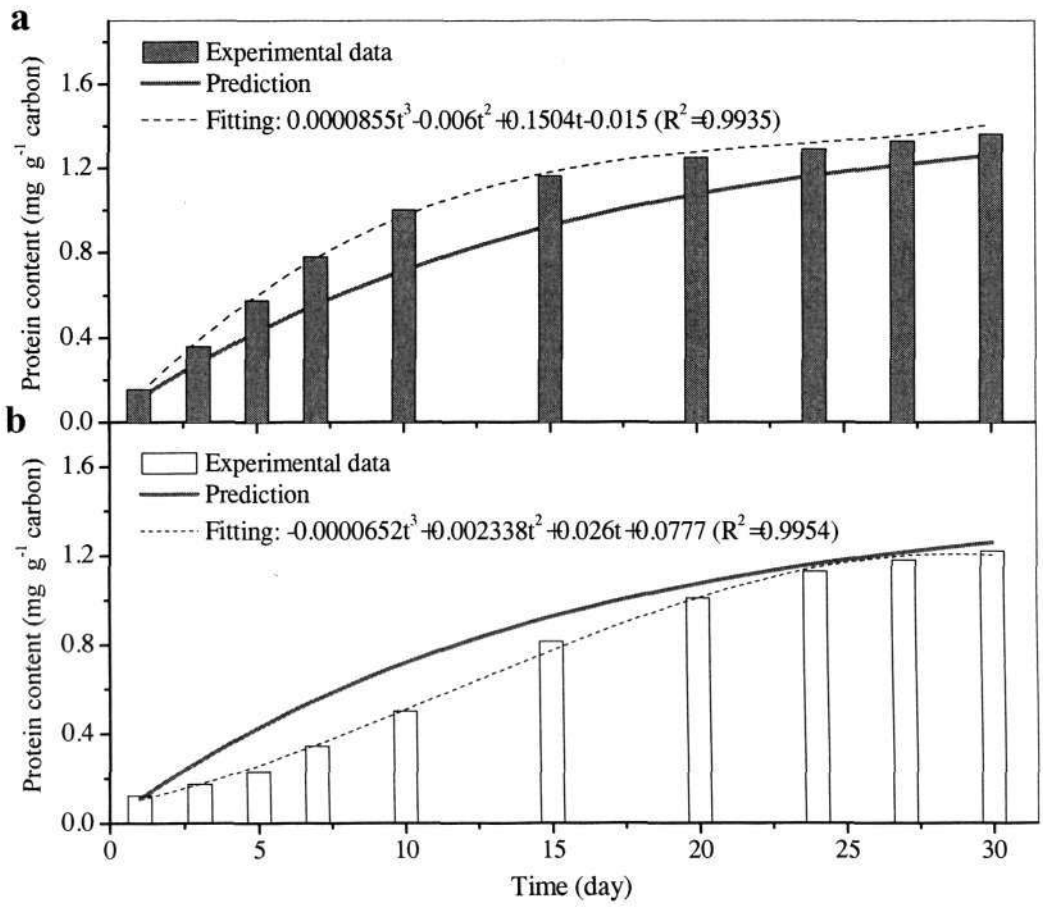

Figure 5.3 Protein concentration profiles in (a) Column EC and (b) Column FC

5.4.2 Distribution of sulfur in carbon

The scanning electronic microscope (SEM) together with energy dispersive X-ray spectroscopy (EDX) was used to determine the distribution of sulfur on the surface and inside carbon samples. They included fresh carbon (FC), exhausted carbon (EC) and biological activated carbon (BAC) which was collected randomly from the top of the two columns bed after 30 days of operation. Figure 5.4 shows the cross section of a carbon particle. The distribution of sulfur along the cross of carbon particles is shown in Figure 5.5.

It can be seen that the content of sulfur increased significantly along the cross section of EC (Figure 5.5). The contents of sulfur at the locations close to the surface were higher than those close to the centre section of EC. Compared with that along the cross section of EC (4-15 wt%), the distribution of sulfur on the carbon surface (13.8±1.5 wt%) was relatively more homogeneous. This was probably because the quantity of impregnated chemicals were much higher at the carbon surface (Yan et al., 2002).

After 30 days of biofiltration, the distributions of sulfur along the cross section of BAC changed significantly from EC and FC before biofiltration (Figure 5.5). The content of sulfur on the outer portion (0-0.7 mm from the surface) of BAC from EC was much lower than those of EC, while those inside (1-2 mm from the surface) the carbon remained stable. This indicates that the sulfur compounds on the outer portion of exhausted carbon were readily available to microorganisms. Because of their sizes, bacteria can remain only on the carbon surface (i.e. macropores). Thus, the effect of microorganisms is confined to maintaining the concentration of sulfur on the carbon external surface at the minimum level. Some sulfur into deep internal pores of activated carbon were not available (i.e., irreversible adsorption), as described for other

pollutants previously (Hutchinson and Robinson, 1990; Klimenko et al., 2004).

In the case of BAC from FC (Figure 5.5), H_2S was only adsorbed in the outer portion (0-1.2 mm from the surface) of carbon at the presence of biodegradation. The results indicate that the unavailable sulfur that was pre-adsorbed inside EC pores might not affect the performance of H_2S removal just as if the adsorbed substrate did not exist.

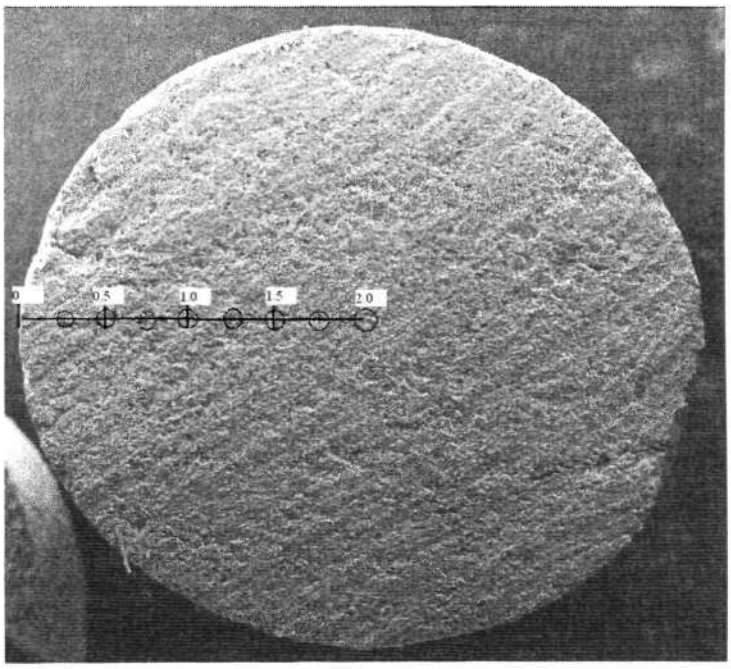

Figure 5.4 Cross section of activated carbon

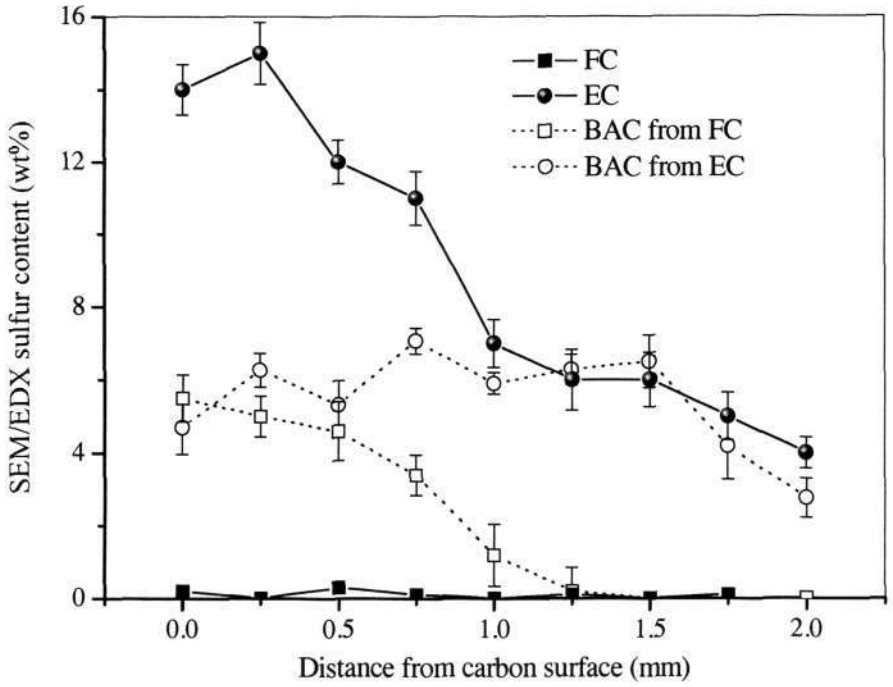

Figure 5.5 SEM/EDX sulfur content from the surface to center of carbon sample

5.4.3 Model simulation of H_2S removal

In this proposed model (Eq.5.1-5.5), the growth of biofilm was considered by introducing the time-dependent value of the biomass concentration in the two columns (Figure 5.3). Generally, it was assumed that the net growth in the biofilm is zero in biofilters for air pollutants previously (Shareefdeen and Baltzis, 1994; Lim, 2001; Den and Pirbazari, 2002), due to the difficulty in describing the actual phenomena as well as the complexity of the model itself. However, bacterial growth is a crucial phenomenon in biofiltration process (Alonso et al., 1998; Song and Kinney, 2002). Due to bacterial growth, the thickness of biofilm will increase with operation time. Therefore, the developed model considering the growth of biofilm may accurately predict the performance of a biofilter.

The experimental data and model prediction profiles of H_2S removal efficiency in

Column FC and Column EC are presented in Figure 5.6. It can be seen that H_2S was almost completely removed (95-100%) with 35 ppmv of inlet concentration at 10 s of EBRT in the two columns over 30 days of operation. In both cases, a good agreement was observed between the experimental data and the predicted model profiles.

The ratios of the H_2S removal by the adsorption and biodegradation were also simulated in the biofilters operation, respectively (Figures 5.6). The ratios of H_2S removal by the biodegradation in Column EC were higher than those in Column FC during the start-up period. In Column EC (Figure 5.6a), the removal of H_2S during the initial stage (about 5 days) was significantly attributed to the adsorption mechanism. The adsorption capacity could be resulted from water dissociation and recovered carbon adsorption due to desorption and biodegradation of pre-adsorbed sulfur compounds on EC. It was observed that the removal efficiency in Column EC was slightly lower than the model prediction, even though high removal performance ($>$ 95%) was still obtained (Figure 5.6a). This could be because the recovered adsorption capacity of EC was probably limited at this stage. After 5 days, biodegradation mechanism mainly contributed to the removal of H_2S in Column EC (biodegradation ratio >0.9). At this time, the removal efficiency of H_2S in Column EC can be predicted by the developed model very well.

In Column FC (Figure 5.6b), the adsorption capacity of fresh carbon was significantly responsible for 100% removal of H_2S during the first 15 days of operation. Afterwards, the biodegradation effect increased and displaced the adsorption as the primary removal mechanism (biodegradation ratio >0.9).

The results show that the steady-state biodegradation was obtained earlier in Column EC than in Column FC (Figure 5.6). This was mostly attributed to higher biomass concentration in Column EC than those in Column FC (Figure 5.3).

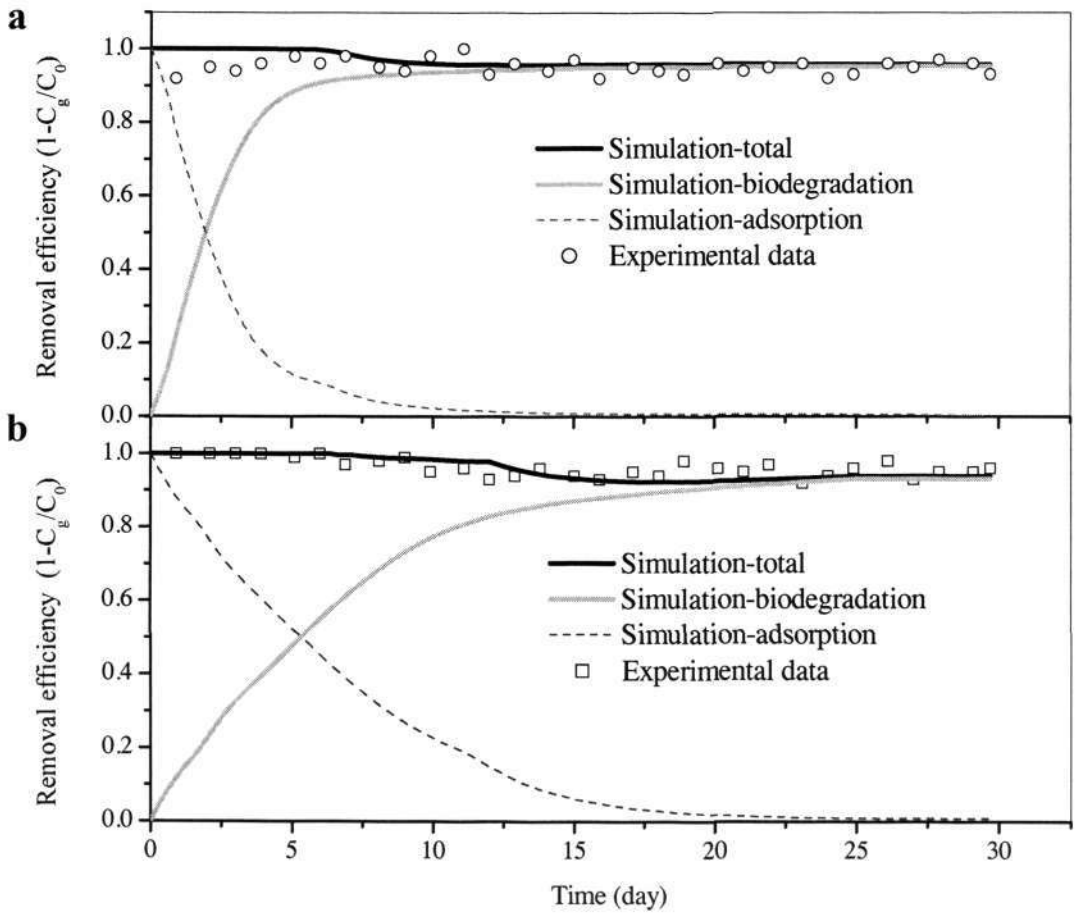

Figure 5.6 Experimental data and simulation removal ratios of total, adsorption and biodegradation for H_2S in Column EC (a) and in Column FC (b)

5.4.4 Effect of biodegradation on H_2S removal by adsorption

The biodegradation of H_2S within biofilm and sequentially the adsorption into carbon were simulated, respectively (Figures 5.7 and 5.8). It can be observed that H_2S concentration profiles within biofilm and in carbon were different in Column EC and Column FC with operation time. In Column EC, the H_2S concentration gradients within biofilm were bigger while the H_2S loading into carbon were smaller than those

in Column FC. During the initial operating stage, a small concentration gradient within biofilm was observed in the two columns (Figure 5.7). This resulted in a large amount of H_2S into carbon (Figure 5.8). Gradually, the concentration gradients within biofilm became bigger. As a result, the H_2S loading into carbon was significantly decreased.

The results show that biodegradation in biofilm significantly influenced the removal of H_2S by adsorption of carbon in the bioreactors. During the initial period (about 5 days), a very thin biofilm was formed on the surface of FC (3-8 μm) and EC (3-19 μm) (Figure 5.9). At this time, little biodegradation happened, which resulted in high H_2S concentrations at the interface of biofilm/carbon. As a result, activated carbon was adsorbing substrate without significant resistance to the diffusion of H_2S posed by biofilm. In Column EC, H_2S concentration at the interface of biofilm/carbon was lower than those in Column FC, due to higher biofilm thickness in Column EC. Thus, the ratio of H_2S removal by the adsorption in Column EC was lower than that in Column FC (Figure 5.6).

After 5 days, as the biofilm thickness increased, the H_2S concentration at the interface of biofilm/carbon decreased rapidly due to the biodegradation (Figure 5.9). After 15 days, the H_2S concentration at the interface of biofilm/carbon was below 1% of C_g/H (the interface of biofilm/gas) in Column EC, while the concentration was obtained in Column FC after 24 days. It indicates that H_2S was biodegraded almost completely within biofilm and the adsorption became insignificant.

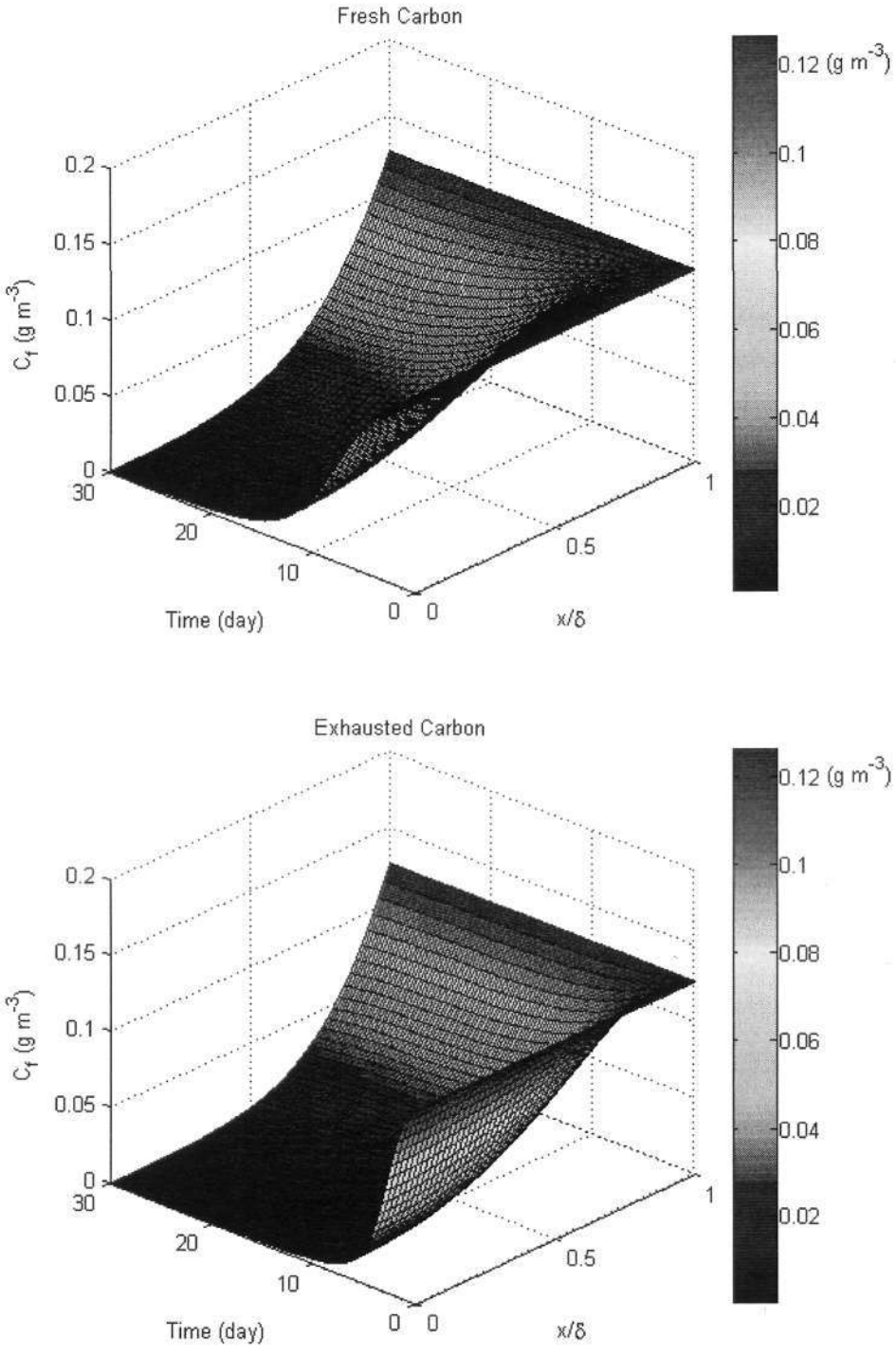

Figure 5.7 Model simulation of H_2S concentration profiles along the biofilm in the inlet section of Column EC and Column FC

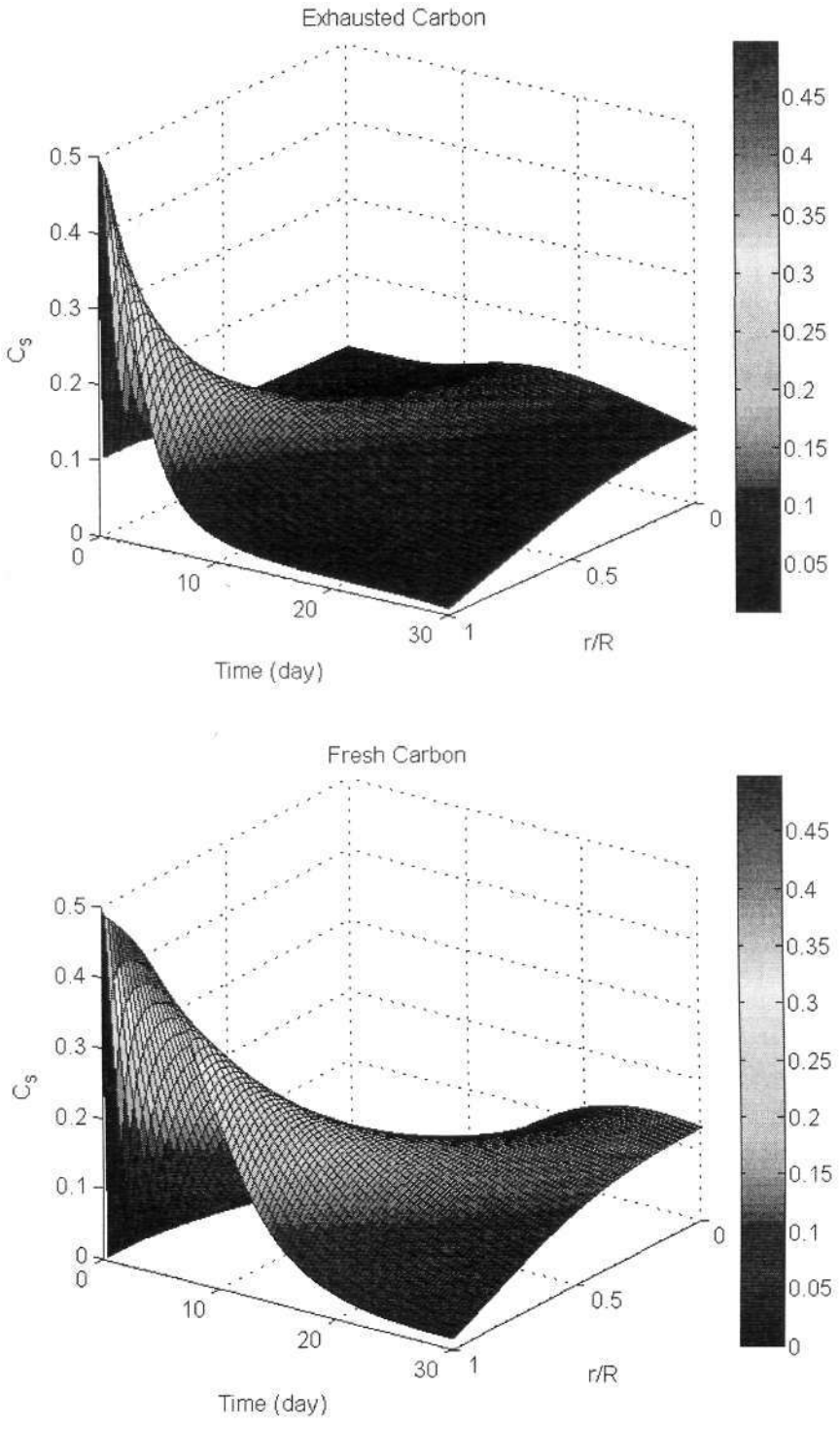

Figure 5.8 Model simulation of H_2S concentration profiles along the carbon radius in the inlet section of Column EC and Column FC

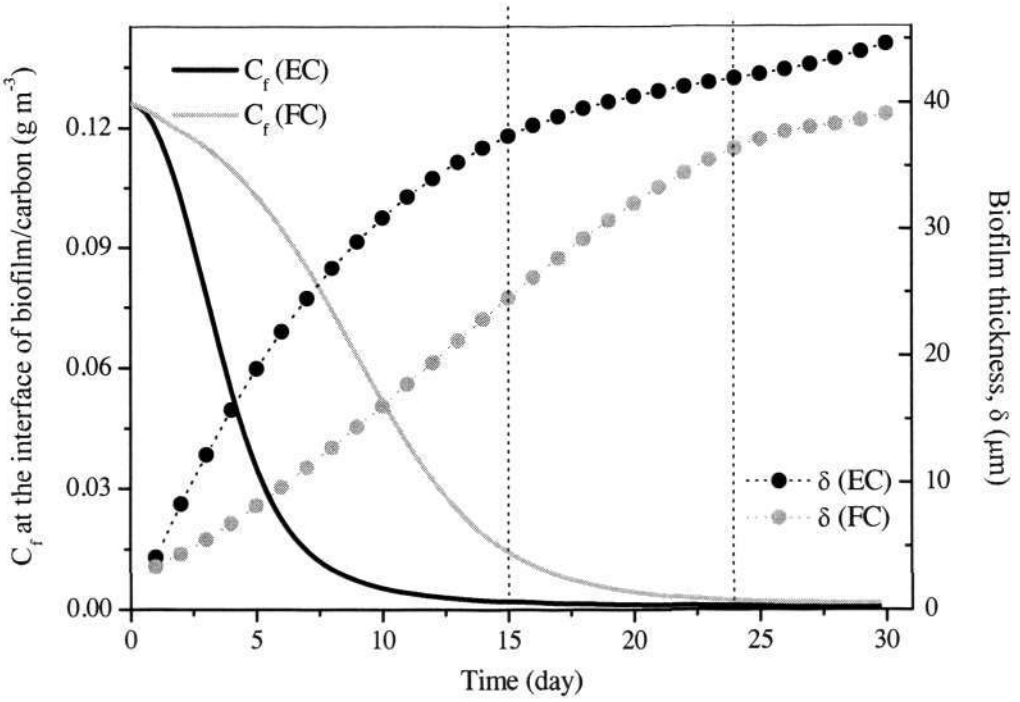

Figure 5.9 Model simulated profiles of H_2S concentration at the interface of biofilm and carbon in the inlet section of Column EC and Column FC

The effective biofilm thickness was about 38 μm in this study, based on the approach described by Shareefdeen et al. (1993). A further increase in the biofilm thickness will not affect the biodegradation removal anymore. This suggests that the system become diffusion-controlled when the biofilm thickness was above 38 μm. At this time, the effectiveness of carbon adsorption is limited by the biofilm thickness. 30-100 μm of effective biofilm thickness has been reported (Amanullah et al., 1999).

During 30 days of operation, about 19% and 9% of removed H_2S were attributed to the adsorption mechanism in Column EC and Column FC, respectively. It indicates that the higher biodegradation in Column EC significantly decreased the adsorption

effect in biofilters, compared with Column FC. In addition, when H_2S concentration at the interface of biofilm/carbon would gradually become lower than the concentration in carbon, sulfur compounds which deposited on carbon will diffuse into the surrounding biofilm for degradation. This desorption phenomenon can recover the adsorption sites on the carbon for more pollutant uptake. Eventually, a flux balance between the substrate concentrations in the gas and solid phases is attained as the process approaches equilibrium.

5.4 Conclusions

The experimental results show that the removal efficiency of H_2S in Column EC and Column FC was almost identical. The biomass concentration in Column EC was higher than that in Column FC. This was because Column EC has higher sulfur load (H_2S feeding +desorption of pre-adsorbed sulfur) while Column FC was supplied with H_2S feeding only and has significant adsorption of fresh carbon.

The developed model can predict very well the experimental data of removal efficiency in the two columns. The adsorption mechanism significantly contributed to the removal of H_2S at the start-up stage in Column EC (about 5 days) and Column FC (about 15 days). The removal of H_2S by the adsorption was significantly affected by the biodegradation. The ratios of H_2S removal by the biodegradation in Column EC were higher than those in Column FC during the start-up period. The steady-state biodegradation was obtained in a shorter time in Column EC than in Column EC. Under steady-state conditions, the elimination of H_2S was mainly attributed to the biodegradation mechanism. The adsorption into carbon could be ignored.

Chapter 6
Effect of Substrates Acclimation Strategies on Simultaneous Biodegradation of H_2S and NH_3

6.1 Introduction

Biofiltration of single pollutant, such as H_2S or NH_3, has been studied extensively (Gracian et al., 2002; Duan et al., 2006; Kim et al., 2007). However, both NH_3 and H_2S are found in waste gases emitted from Wastewater Treatment Plants (WWTPs) (e.g. composting facilities) (Shareefdeen and Singh, 2005). Only recent years, co-removal of H_2S and NH_3 by biofiltration was reported (Malhautier et al., 2003; Chung et al., 2005; Galera et al., 2008).

When biofilters were supplied with a mixture of H_2S and NH_3, both substrate and microbial interactions were observed during the start-up period (Malhautier et al., 2003; Chung et al., 2005; Galera et al., 2008). NH_3 biodegradation (i.e. nitrification) happened after 3-7 weeks of operation while H_2S biodegradation was carried out at the beginning. Nitrification was much more difficult than H_2S biodegradation in the co-removal systems. The poor nitrification caused relatively low elimination capacity of NH_3 gas under high loadings of H_2S and NH_3 (Kim et al., 2002; Malhautier et al., 2003; Chung et al., 2005). Moreover, the removal of NH_3 gas was mostly attributed to the absorption, adsorption or chemical reaction (Kim et al., 2002; Lee et al., 2005; Shanchayan et al., 2006; Galera et al., 2008). Since NH_3 gas was only transferred into liquid phase, liquid effluent from the biofiltration system requires a further treatment.

Thus, a more efficient and effective process need to be developed to promote nitrification for the improvement of NH_3 gas removal and for the elimination of NH_4^+ effluent from the co-removal biofiltration system.

It was reported that suitable acclimation strategy was significantly important for biodegradation of mixed substrates successfully (Kar et al., 1996). Acclimation is a period required for the development of the optimum population of substrate-consuming microorganisms before they started the vigorous biodegradation (Jones et al., 2004). The time needed for such acclimation will depend on the severity of the stress imposed and the diversity of the organisms capable of performing the required degradation. Once an adequate culture is established, the level of substrate interactions was somewhat reduced (Rozich and Colvin, 1986). It was observed that phenol was removed more effectively in bioreactors that had the longest interim prior to glucose addition (Rozich and Colvin, 1986; Kar et al., 1996). A bioreactor that was acclimated to volatile organic compounds (VOCs) in a sequential manner achieved high performance (Park, 2004). However, few studies have been found to systematically investigate how substrates acclimation strategy affects the simultaneous biodegradation of H_2S and NH_3.

Therefore, the main objective of this study is to evaluate the effect of substrates acclimation strategy on simultaneous biodegradation of H_2S and NH_3, especially on nitrification. The polymerase chain reaction (PCR) and denaturing gradient gel electrophoresis (DGGE) was used to investigate the effect of acclimation strategies on the composition of the microbial population in the co-removal bioreactors.

6.2 Experimental setup

Three identical glass columns (40 mm of diameter; 200 mm of packing height) were used (Figure 6.1). They were packed with about 150 g of the mixed exhausted carbon and operated in an identical mode except for the composition of the waste gas to each column (Table 6.1). The first column (mixture feeding column, MFC) was fed with both H_2S and NH_3 gas and inoculated by sulfide-oxidizing bacteria (SOB) and

nitrifying culture. The second column (NH_3 feeding column, NFC) was fed with NH_3 and inoculated by nitrifying culture firstly, and followed by feeding H_2S. The third column (H_2S feeding column, SFC) was supplied with H_2S gas and SOB firstly, and then NH_3 and nitrifying culture.

The inlet concentration of H_2S and NH_3 was adjusted by mass flow controller (The Brooks Model 5850E, USA) at the outlet of a standard 5% H_2S and NH_3 gas cylinder (Soxal Gas, Singapore) respectively, through mixing with air supplied by an air blower. The peristaltic pump was connected to a spray nozzle to uniformly spray the mineral medium on the surface of filter bed in a concurrent-flow direction with the influent gas. A 1.5 L of mineral medium (g L^{-1}: KH_2PO_4, 4.08; K_2HPO_4, 10.44; $NaHCO_3$, 2.00; $MgCl_2 \cdot 6H_2O$, 0.46) was used at 30 mL min^{-1}. After 9 days of operation, recirculation liquid was replaced with 0.5 L of fresh medium every day to prevent a toxic accumulation of S and N compounds in the system. On day 36, 1.5 L of recirculation liquid was exchanged with fresh medium. The experiments were conducted at room temperature of about 25 °C.

The H_2S-exhausted carbon (AddSorb VA3, pellet-shaped in 4 mm of diameter, Jacobi Group) was obtained as described in section 3.3.1. The main properties of the exhausted carbon were as follows: S content (w/w %), 7.8; pH value, 6.15; surface area (m^2 g^{-1}), 776; bulk density (kg m^{-3}), 778. An online immobilization was adopted to start the biofiltration. Exhausted carbon was stuffed into the columns randomly, and then 1.5 L of distilled water was re-circulated for 24 hours to wash some sulfur from exhausted carbon. 20 mL of concentrated microbial broth at 4.1×10^8 cell mL^{-1} of SOB and 3.4×10^8 cell mL^{-1} of nitrifying culture were poured into from the top of MFC/SFC and MFC/NFC respectively. The synthetic foul gas with 60 ppmv of H_2S and/or NH_3 was directed from the top into the packing columns at an empty bed residence time (EBRT) of 10 s.

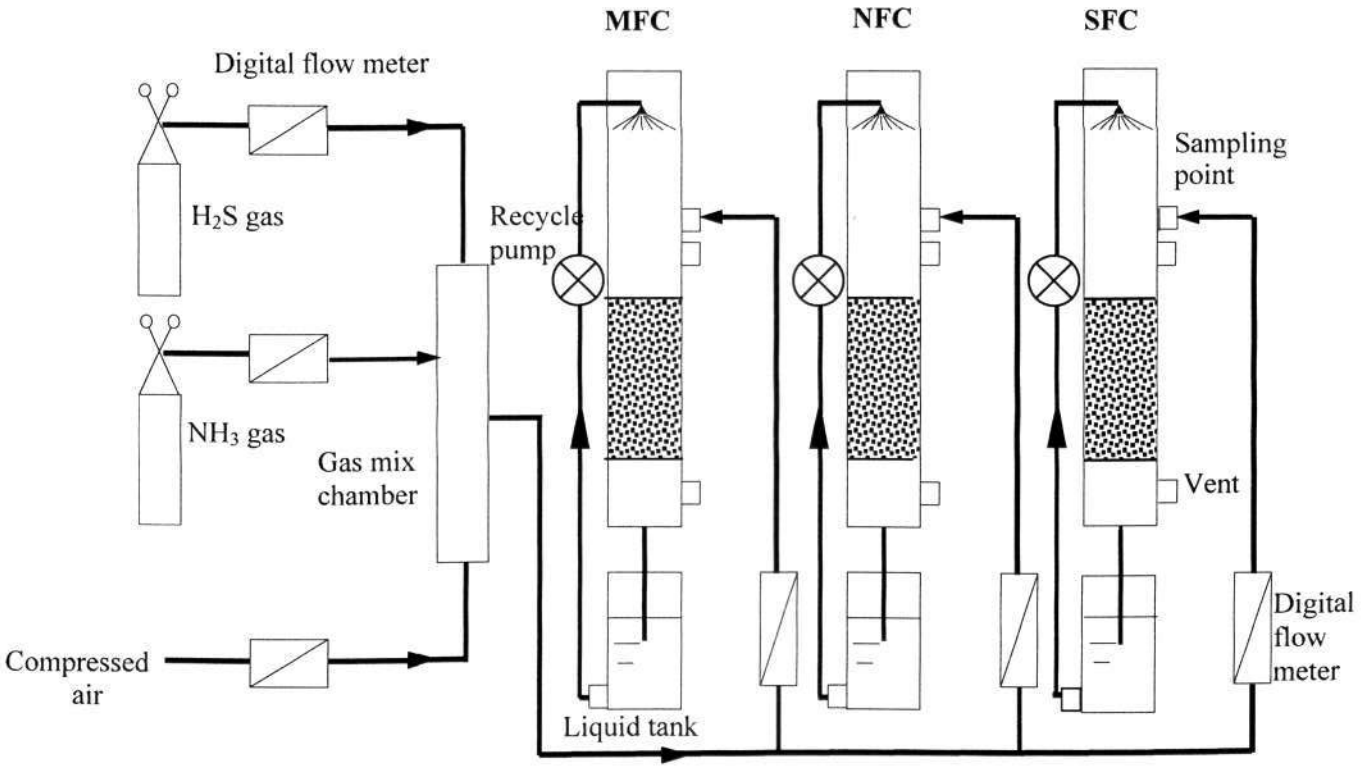

Figure 6.1 Schematic diagram of the biotrickling filters system

Table 6.1 Pollutant feed composition and loading during biofiltration

Days	Pollutant	EBRT (s)	Pollutant loading (g m^{-3} h^{-1})		
			MFC	NFC	SFC
1-17	H_2S	5-10	33-66	0	33-109
	NH_3	5-10	16-33	16-55	0
17-43	H_2S	5	109-164	109-164	109-164
	NH_3	5	55-82	55-82	55-82

6.3 Results and discussion

6.3.1 System performance evaluation

Figure 6.2 shows the profiles of inlet loadings and removal efficiency of H_2S and NH_3 in MFC. It can be seen that H_2S was completely removed from the beginning at the loading of 33 g m^{-3} h^{-1}. The complete removal of NH_3 was achieved only during the first two days at the loading of 16 g m^{-3} h^{-1}. After that, the removal efficiency of NH_3 decreased gradually to 83% on day 6, with the steady-state at 98% obtained till day 10. The removal efficiencies of H_2S and NH_3 remained at > 90% till day 29. On day 30, the removal efficiencies rapidly dropped to 74 and 63%, when the loading of H_2S and NH_3 increased to 164 and 82 g m^{-3} h^{-1}, respectively. As the loading of H_2S and NH_3 decreased to 109 and 55 g m^{-3} h^{-1} on day 33 respectively, the removal performance recovered gradually.

The removal performance in NFC is shown in Figure 6.3. During the first 17 days, NH_3 was completely removed, only with a slight drop of removal efficiency on day 13 at the loading of 55 g m^{-3} h^{-1}. On day 17, when 109 g H_2S m^{-3} h^{-1} was introduced to the system, the negative effect was not observed for the removal of NH_3. H_2S was also removed immediately (> 95%), even though the column was inoculated with nitrifying culture only. The removal efficiency of H_2S and NH_3 were stable at over 95 and 97% respectively through the entire operation, except for lower removal efficiency (87-90%) for H_2S at the high loading of 164 g m^{-3} h^{-1} on day 30-33.

For the performance in SFC (Figure 6.4), H_2S was almost completely removed at the beginning. The removal efficiencies of H_2S decreased from 99 to 90% as the loading increased to 109 g m^{-3} h^{-1} on day 13. The removal of H_2S was not influenced negatively by the introduction of 55 g NH_3 m^{-3} h^{-1} on day 17. In contrast, the removal of H_2S became more stable, possibly because NH_3 supplied N nutrient in the system. NH_3 was also removed immediately. As nitrifying culture was added into the column on day 26, the removal efficiency of NH_3 slightly increased. From day 30, the removal efficiencies of H_2S and NH_3 dropped due to the further increased loadings.

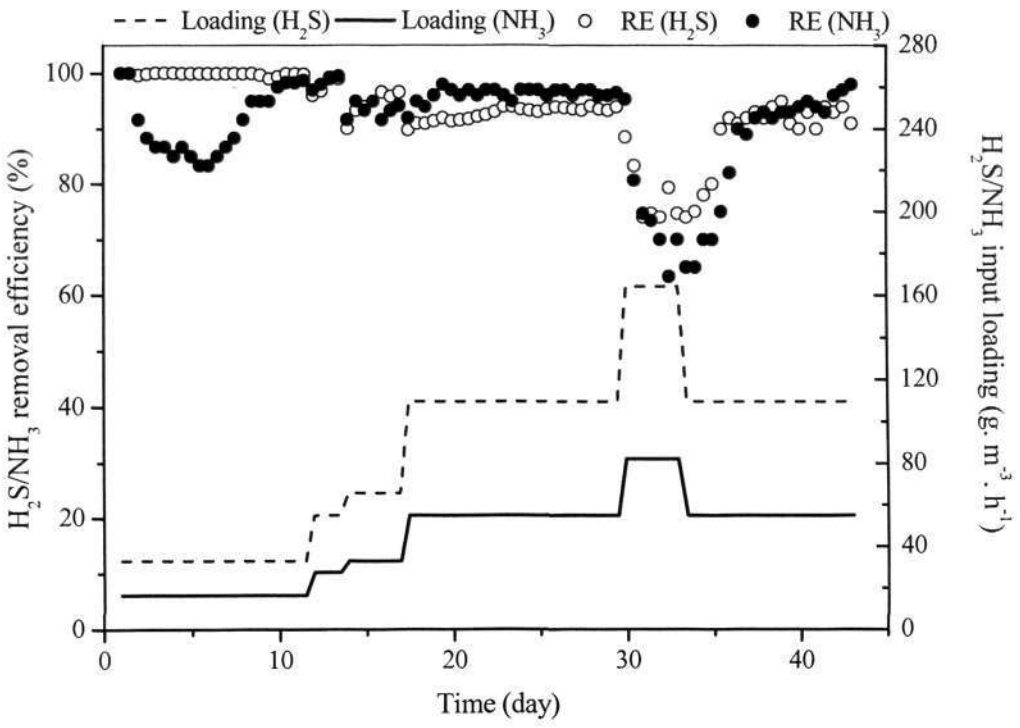

Figure 6.2 Removal performance of H_2S and NH_3 in MFC

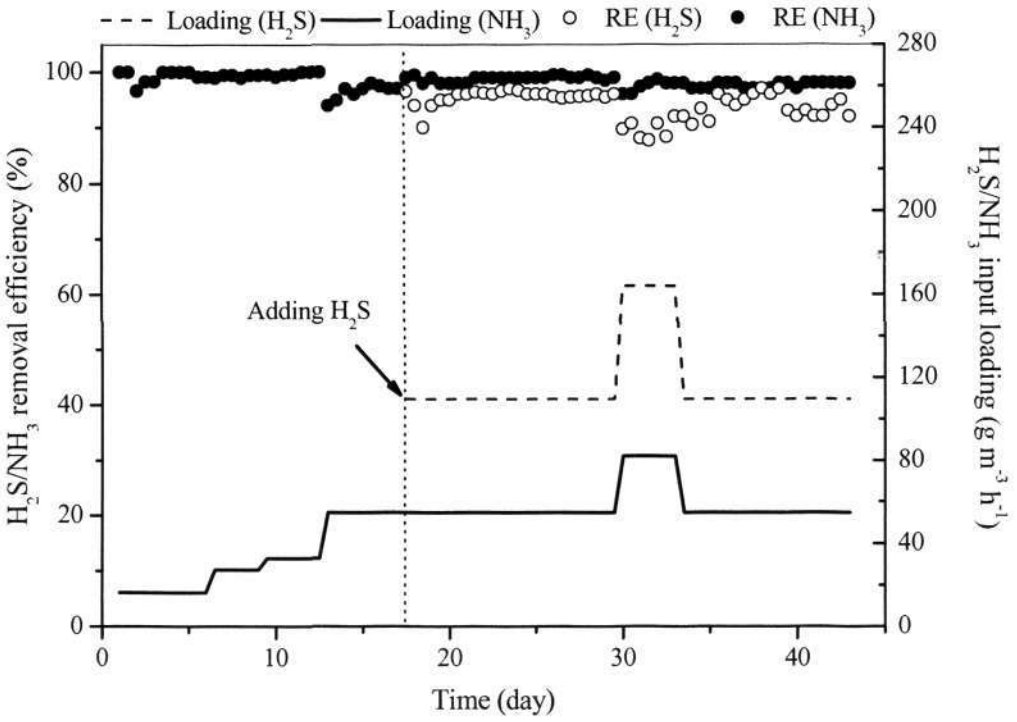

Figure 6.3 Removal performance of H_2S and NH_3 in NFC

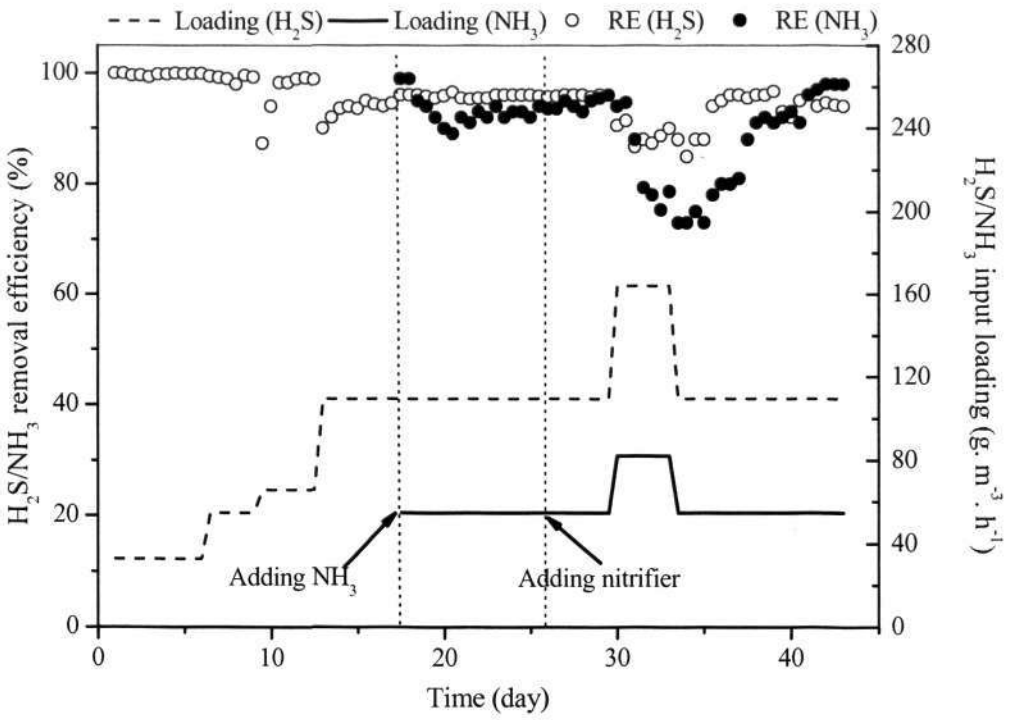

Figure 6.4 Removal performance of H_2S and NH_3 in SFC

6.3.2 Performance comparison of the different strategies

The above results (Figures 6.2-6.4) show that removal performances of H_2S and NH_3 were different in the three columns with various substrates acclimation strategies. Removal efficiencies of H_2S were more stable in SFC and NFC than MFC. At the high H_2S loading of 164 g m^{-3} h^{-1} on day 30-33, the lowest removal efficiency was found in MFC (Figures 6.2-6.4). A delay of H_2S removal in NFC would have been expected, because SOB has not been inoculated. However, about 95% of H_2S was removed from the beginning. This may be attributed to both the recovered adsorption of carbon and biodegradation by SOB. The SOB culture might be enriched by the pre-adsorbed sulfur on exhausted carbon. Through consuming the pre-adsorbed sulfur, some adsorption sites on carbon were possibly recovered. Still, further research was warranted to understand the mechanism behind.

For the removal of NH_3 (Figures 6.2-6.4), NFC has a shorter acclimation period and higher removal efficiency at high loading of H_2S and NH_3 than those in MFC and SFC. During the first 17 days, over 95% of NH_3 was removed in NFC (Figure 6.3), while a clear drop followed by an increase of removal was observed in MFC (Figure 6.2). The initial 2 days of high removal in MFC could be attributed to the adsorption/dissolution of NH_3. From day 6, the increased removal of NH_3 was due to the nitrification by nitrifying culture which adapted to the environment in MFC. The acclimation in NFC was fast so that the biological activity was established before the adsorption capacity of the bed was exhausted. From day 30, removal efficiencies of NH_3 decreased greatly to 63 and 75% in MFC and SFC respectively. In contrast, over 97% of NH_3 was removed in NFC. High removal performance in NFC was most likely caused by the acclimation strategies used.

6.3.3 Biodegradation pathways

In order to understand the biodegradation pathways of NH_3 and H_2S, NH_4^+, NO_2/NO_3^- and SO_4^{2-} in liquid phase were monitored (Figure 6.5). The concentration of NH_4^+ was higher than that of NO_2/NO_3^- in MFC during the first 10 days. This indicates that NH_3

gas was mainly removed by the adsorption/absorption and chemical reaction. From day 10, the concentration of NO_2/NO_3^- increased gradually (Figure 6.5b). The increased nitrification was consistent with the increased removal of NH_3 gas from day 10 (Figure 6.2). As high loadings of NH_3 at 55-82 g m^{-3} h^{-1} were applied from day 17, the concentration of NH_4^+ increased again till recirculation liquid exchanged on day 36 (Figure 6.5a).

NO_2/NO_3^- was the main product in NFC before day 17 (Figure 6.5b), which suggests that nitrification contributed mostly to the removal of NH_3. From day 17, the production rate of NO_2/NO_3^- decreased, and NH_4^+ increased gradually (Figure 6.5a). It indicated that the introduction of 109 g m^{-3} h^{-1} of H_2S negatively influenced the nitrification, even though the removal of NH_3 gas was not inhibited (Figure 6.3). During days 30-36, the concentration of NH_4^+ further increased (Figure 6.5a), possibly resulting from high loadings of H_2S and NH_3.

In SFC, NH_4^+ became the main product through the operation (Figure 6.5a). This indicates that the removal of NH_3 was mainly attributed to the adsorption and chemical reaction. Although the inoculation of nitrifying culture on day 26 indeed enhanced the nitrification (Figure 6.5b), the function was limited during day 30-33. It suggests that the effective establishment of nitrifying culture have been prevented because H_2S biodegradation was established firstly. As a result, NH_3 gas would be readily removed as $(NH_4)_2SO_4$ (Figures 6.5a).

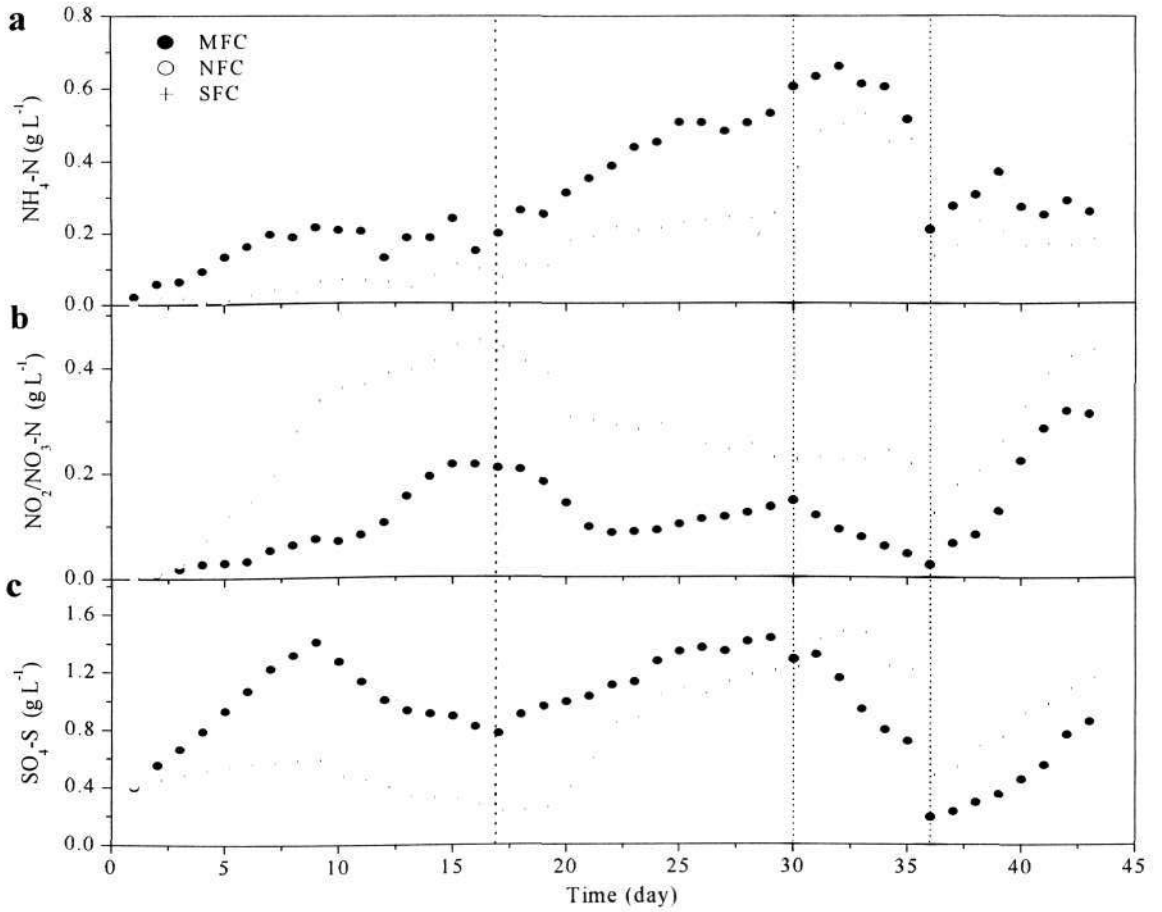

Figure 6.5 Concentration profiles of NH_4-N (a), NO_2/NO_3-N (b) and SO_4-S (c) in liquid of MFC, NFC and SFC

Figure 6.5c shows the concentration profiles of sulfate, i.e. the biodegradation product of H_2S. During the first 17 days, the concentration of SO_4^{2-} in SFC was higher than that in MFC. Sulfate cumulated at 1.39 g S in NFC (without H_2S supply). This gave the evidence that the pre-adsorbed sulfur on exhausted carbon was biodegraded. This resulted in SOB enrichment and the recovery of adsorption sites on carbon in NFC. This indicates that the inoculation of SOB was not required when H_2S-exhausted carbon was used as the packing material under this acclimation strategy.

From day 30, the production rate of SO_4^{2-} decreased in the three columns (Figure 6.5c). White deposits on the carbon surface were observed, which indicate the existence of other S species (e.g. elemental S) due to the high loading of H_2S at 164 g m^{-3} h^{-1}. Meanwhile, the production rate of NO_2/NO_3^- was low (Figure 6.5b). It suggests that the incomplete H_2S biodegradation products have negative effect on nitrification.

pH and sulfide concentration in liquid phase was also monitored. It was found that during day 30-36 pH remained at neutral in NFC, while it ranged between 8.2 and 9.3 in MFC and SFC even though the pH was adjusted to 7.5±0.2 every day. The sulfide concentration in MFC and SFC was higher than that in NFC (Figure 6.6b). From day 36, the pH started to drop and sulfide concentration decreased in MFC and SFC, corresponding with the recovery of NH_3 removal (Figure 6.6a).

The results indicate that the removal of NH_3 gas and nitrification was negatively influenced by high pH and sulfide concentration. The high pH was caused by not only the accumulation of NH_4^+ from day 30 (Figure 6.5a), i.e. $NH_3 + H_2O \rightarrow NH_4^+ + OH^-$, but also incomplete biodegradation of H_2S in MFC and SFC (Figure 6.5c). High pH does not benefit the H_2S biodegradation while it is good for the adsorption of H_2S. As a result, more sulfides (H_2S/HS^-) were produced in MFC and SFC. Sulfide has been reported to inhibit nitrifying bacteria in biofilm reactors (Srna and Baggaley, 1975; Aesoy et al., 1998). Moreover, high pH brought high concentration of free NH_3, consequently inhibited nitrification (Ford et al., 1980; Villaverde et al., 1997). In addition, high pH will not benefit the adsorption of NH_3 gas, resulting in limited mass

transfer of NH_3 from gas phase to liquid phase.

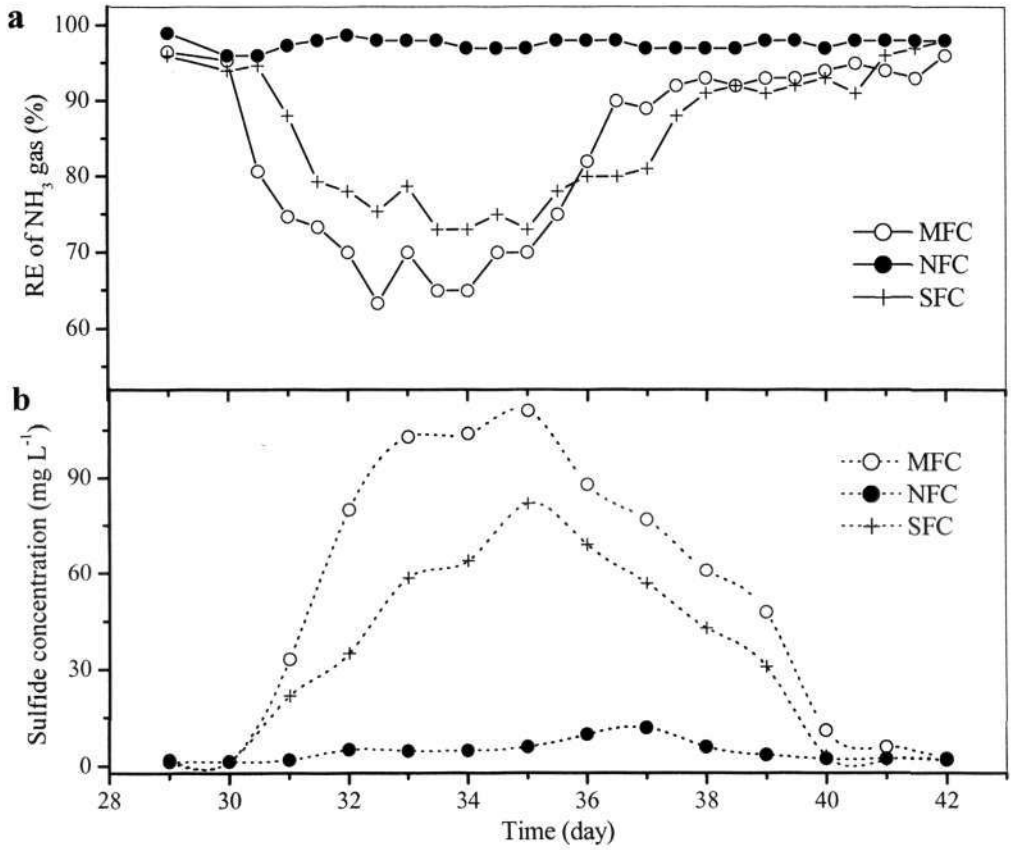

Figure 6.6 Relationship between removal efficiency of NH_3 (a) and sulfide concentration (b)

A total balance of sulfur and nitrogen in the three columns was evaluated during 17 and 43 days of operation, respectively (Figure 6.7). As shown in Figure 6.7a, totally, about 90, 98 and 90% of input NH_3 gas were removed in MFC, NFC and SFC during 43 days of operation, respectively. The ratios of NH_4-N cumulated in liquid reached 39 and 53% of input NH_3 in MFC during 17 and 43 days of operation respectively. Ratios of NH_4-N in NFC were lower, i.e., 10 and 32% during 17 and 43 days, respectively. SFC has the highest ratio of cumulated NH_4-N at 65% during 43 days of running. For ratios of NO_2/NO_3-N cumulated in liquid, they were the highest at 67

and 49% of input NH_3 in NFC during 17 and 43 days respectively. SFC showed the lowest biotransformation efficiency at 12% of NO_2/NO_3-N during 43 days. It demonstrated that the adsorption and chemical reaction mainly contributed to the removal of NH_3 in MFC and SFC, while the removal of NH_3 in NFC was largely attributed to nitrification. Other removed N was assumed to exist on the carbon surface in terms of organic N or adsorbed N.

As shown in Figure 6.7b, the total removal of H_2S gas in the three columns was almost identical and most of removed H_2S was biodegraded into sulfate. For the first 17 days, the amounts of sulfate in both MFC and SFC were more than those of sulfate that was produced from the removed H_2S. It was because that pre-adsorbed sulfur on exhausted carbon was also biodegraded, in addition to the H_2S fed to the columns. Totally, the conversion ratio of H_2S to sulfate was the highest in NFC over 43 days of operation. It might result from better bio-regeneration of pre-adsorbed sulfur on exhausted carbon and different enrichment methods for SOB in NFC. Other removed S was supposed on the carbon surface in terms of organic S and elemental S.

The results demonstrated that a higher nitrification was achieved in NFC. The improved nitrification in NFC was most likely attribute to the substrates acclimation strategies applied. Nitrifying culture that was immobilized on carbon firstly in NFC could effectively overcome or reduce the inhibitions of H_2S or SOB, due to the sensitivity and lower growth rate of nitrifying culture than other bacteria.

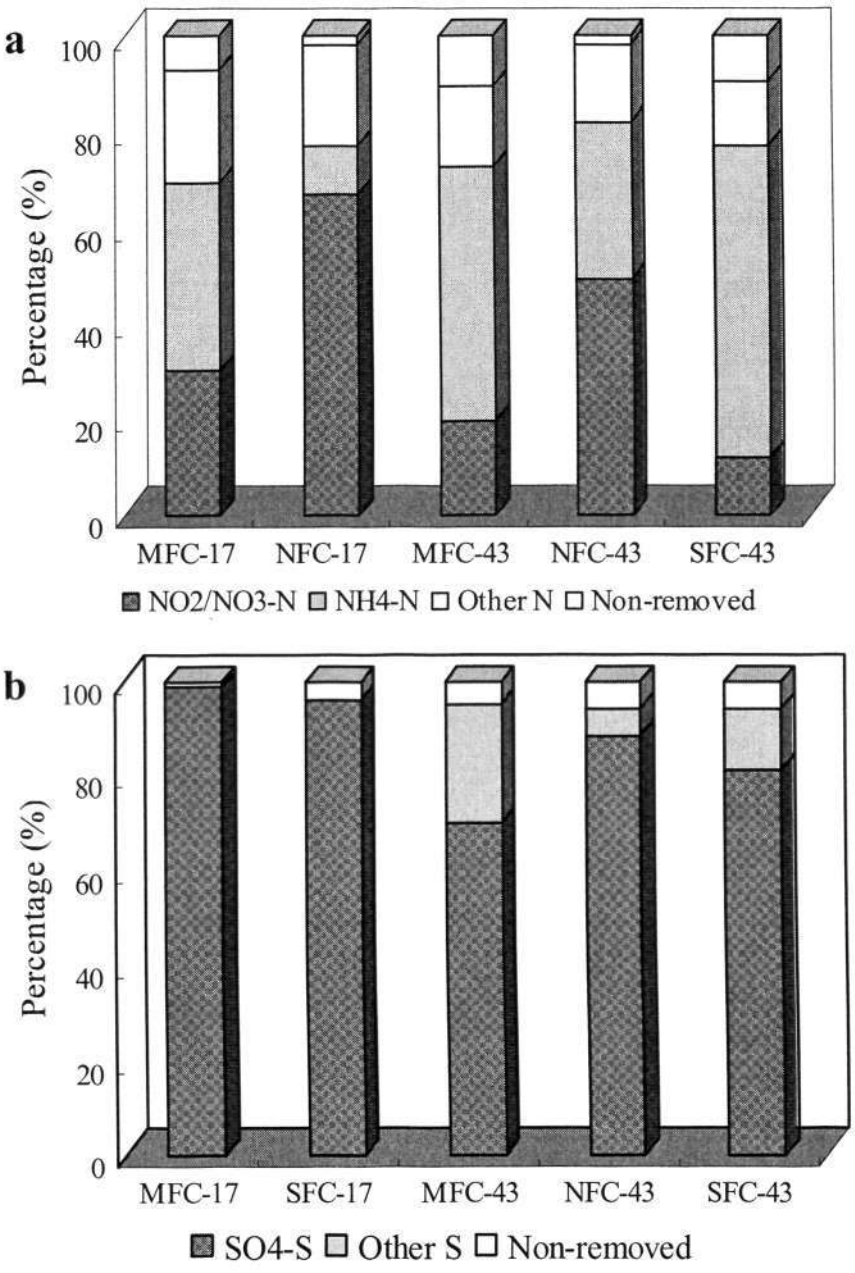

Figure 6.7 Distribution of biodegradation products of NH_3 (a) and H_2S (b) in MFC, NFC and SFC during 17 and 43 days of operation

6.3.4 Microbial communities

The diversity of microbial communities of biofilm samples from the three columns was analyzed and compared by the DGGE profiles of 16S rRNA gene fragments (Figure 6.8). Each band on the DGGE represented a gene fragment of unique 16S rRNA sequences and accordingly represented a specific species in the microbial community. The intensity of a band represents the relative abundance of the corresponding microbial species (Casamayor et al., 2000). The Dice coefficient (Cs) was used to quantify the similarity of these community fingerprints in the three columns (Table 6.2). A Cs value of 0% indicates that the samples are completely different, and Cs value of 100% indicates that the samples are identical.

As shown in Figure 6.8, the inoculated cultures (IN and IS) were predominantly bacteria in NFC (N) and SFC (S) on day 17 respectively. 4 and 5 new species appeared in N and S compared with IN and IS respectively. N and IN showed moderate similarity at 78%, and the similarity of S and IS was at 75% (Table 6.2). It suggests that the biomass established in the columns was subjected to further enrichment, possibly due to the different environmental conditions in the batch flasks and the bioreactors.

In MFC on day 17 (M), most of bacterial species in both the IN and IS were appeared, while 4 species present in the IN were disappeared (Figure 6.8). The inoculated culture (IN and IS) were selectively enriched without competition from microorganisms by growing the cultures separately. However, when the culture was combined in MFC, the microorganisms would be determined not only by the environmental conditions in the bioreactor but also by their ability to compete with microorganisms in degrading another component. Hence, microorganisms that can grow in stressful conditions (e.g. IS) would have a competitive advantage over the organisms sensitive to environmental conditions (e.g. IN). It may explain the delayed NH_3 gas removal and nitrification in MFC during the start-up period (Figures 6.2 and 6.5b).

On day 43, microbial species changed in the three columns (Figure 6.8). Similarity

was obtained at 45-82% in the three columns, and the ME (in MFC) and NE (in NFC) have higher similarity at 82% (Table 6.2). Microbial community structures in MFC and NFC differed in relative abundance of each species (Figure 6.8).

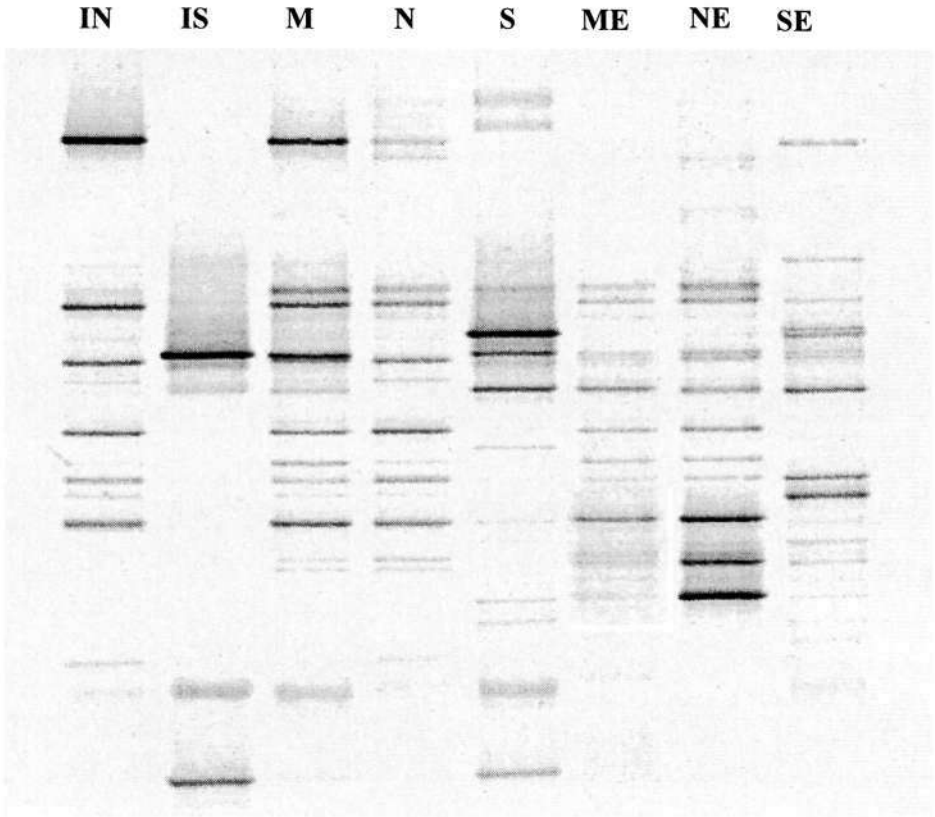

Figure 6.8 DGGE profiles of the bacterial population in MFC, NFC and SFC (IN: Nitrifying inoculums; IS: SOB inoculums; M: MFC on day 17; N: NFC on day 17; S: SFC on day 17; ME: MFC on day 43; NE: NFC on day 43; and SE: SFC on day 43)

Table 6.2 Dice coefficients (Cs) comparing the similarities of PCR-DGGE fingerprints in MFC, NFC and SFC on days 17 and 43

Case	IN	IS	M	N	S	ME	NE	SE
IN	1.00							
IS	0.25	1.00						
M	0.58	0.50	1.00					
N	0.78	0.21	0.74	1.00				
S	0.30	0.75	0.50	0.26	1.00			
ME	0.53	0.27	0.69	0.64	0.42	1.00		
NE	0.52	0.32	0.67	0.77	0.43	0.82	1.00	
SE	0.43	0.42	0.59	0.38	0.43	0.45	0.46	1.00

(IN: Nitrifying inoculums, IS: SOB inoculums, M: MFC on day 17, N: NFC on day 17, S: SFC on day 17, ME: MFC on day 43, NE: NFC on day 43, and SE: SFC on day 43)

6.4 Conclusions

The results show that substrates acclimation strategy is a crucial step when a biofiltration process is applied for co-treatment of H_2S and NH_3. Different removal performances of H_2S and NH_3 were obtained in the three biofilters with various substrates acclimation strategies. NFC has a shorter acclimation time for the removal of NH_3 gas and nitrification than that in MFC. Moreover, under high loading of H_2S and NH_3, NFC exhibited high removal efficiency of NH_3 (> 95%), while the removal efficiencies of NH_3 were obtained at 63 and 75% in MFC and SFC respectively. The removal performance of H_2S was more stable in SFC and NFC than MFC.

In terms of biodegradation pathways, H_2S was removed almost completely by biodegradation into sulfate in the three columns. The removal of NH_3 gas in NFC was attributed to nitrification, while adsorption and chemical reaction significantly contributed to the removal of NH_3 in MFC and SFC. The different biodegradation capacities could be explained by the dissimilarity in the microbial population present in each column due to different substrates acclimation strategies. A microbial

population capable of degrading NH_3 which was acclimatized firstly in NFC benefited the fast acclimation and high removal of NH_3 in the co-removal system. These findings provide important new insights into simultaneous biofiltration of gaseous H_2S and NH_3.

Chapter 7
Long-term Operation of a Biotrickling Filter for Simultaneous Biodegradation of H_2S and NH_3

7.1 Introduction

H_2S and NH_3 could be removed simultaneously in biofilters (Kim et al., 2002; Malhautier et al., 2003; Chung et al., 2005). A long empty bed residence time (EBRT), e.g., 20-180 s, was usually required to achieve high removal efficiency (>90%). Nitrification capacity of NH_3 was relatively low at high loadings of H_2S and NH_3. The low nitrification was caused by either the accumulation of S and N compounds on the packing (Kim et al., 2002), or acidification of the biofilter system (Chung et al., 2001). However, in biotrickling filters, the recirculation liquid can remove metabolic products on the packing, and the packing acidification can be avoided due to better control of pH (Fortin and Deshusses, 1999). Moreover, biotrickling filter is an attractive technology for the removal of NH_3 because of its high water solubility.

It has been demonstrated that the nitrification capacity of NH_3 was improved when a biotrickling filter was used with optimal substrates acclimation strategy in a co-treatment system (Chapter 6). In order to compete with conventional technologies, long-term operation of a bioreactor with reliable and efficient removal of gas pollutants should be pursued (Diks et al., 1994). Low removal efficiencies occurred due to either the

accumulation of substrates and metabolite on packing materials (Smet et al., 2000; Kim et al., 2002; Gabriel et al., 2007), or the change of surface characteristics of packing materials in biofilters (Chung et al., 2001; Duan et al., 2005a). Next to physical-chemical parameters, microbiological parameters could also be used as indicators for the functioning or stability of a bioreactor. Microbial indicators could include biomass concentration, biological activity of biofilm and microbial diversity (Fernandez et al., 2000; Song and Kinney, 2005; Sercu et al., 2007). However, very few studies have been found on investigating long-term performance in a biotrickling filter for the co-removal of H_2S and NH_3.

Therefore, the main objective of this chapter is to investigate the long-term operation of a biotrickling filter packed with exhausted carbon for simultaneous biodegradation of H_2S and NH_3. The results will be useful to understand the key parameters influencing long-term performance in a biotrickling filter and establish a knowledge base presently lacking in the literature.

7.2 Experimental setup

As some Wastewater Treatment Plants (WWTPs) still use horizontal chemical scrubbers, information on performance in a horizontal biotrickling filter (HBTF) will be useful when these horizontal chemical scrubbers are to be converted into biotrickling filters. The studied HBTF (Figure 7.1) has three segments, each with dimensions of 15×15 cm with 10 cm in length. The general properties of the bed are summarized in Table 7.1. The air stream containing H_2S and NH_3 was directed from the left to right through the packing bed. The H_2S and NH_3 inlet concentration was adjusted by mass flow controller (The Brooks Model 5850E, USA) at the outlet of a standard 5% H_2S and NH_3 gas cylinder (Soxal Gas, Singapore) respectively, through mixing with air supplied by an air blower. Four sampling ports were located along the bed the HBTF for gas sampling.

The recirculation solution was trickled down from the top of each segment, and the flow rate of the solution was controlled at 1.2 L min^{-1}. The sump was maintained at 10 L. The recirculation solution was refreshed once every 5 days to prevent a toxic accumulation of S and N compounds in the system after 30 days of operation. The solution contained (g L^{-1}): KH_2PO_4, 4.08; K_2HPO_4, 10.44; $NaHCO_3$, 2.00; $MgCl_2 \cdot 6H_2O$, 0.46. The pH of the recirculation solution was controlled at the desired value (6.0-8.0) with an automatic pH controller (ON/OFF type, SIKO, PR75-C, Singapore) after 30 days of operation, except for specific need. The system was operated at room temperature (about 25 °C) throughout the experiments.

An online immobilization of microorganisms was conducted. The H_2S-exhausted carbon (AddSorb VA3, Jacobi Group) was obtained as described in section 3.3.1. About 1.7 kg of exhausted carbon was stuffed into the HBTF randomly, and then 200 mL of enriched nitrifying microbial consortium (2400 mg L^{-1}) was poured into from the top of the HBTF. This inoculation was performed by continuously trickling the ammonium growth medium (Table 3.1) over the bed. The nitrifying culture was then grown and attached on the carbon surface. After 20 days, the reactor showed a good ability of biodegrading ammonium in the liquid medium. Separately, about 1.7 kg of exhausted carbon was soaked in a 2 L of sulfide-oxidizing microbial consortium (SOB) (1100 mg L^{-1}) in a 5 L of container for 24 h. The carbon was then taken out and packed into the HBTF, after mixing with the carbon which was immobilized with nitrifying culture. The operating conditions are tabulated in Table 7.2.

The kinetics of the system can be expressed by a Michaelis-Menten type relationship by assuming that oxygen limitation was not present in the system and the conversion was in the reaction-controlled regime (i.e. the biofilm was fully active). At steady-state, the growth rate of microorganisms was balanced by its own decay rate, resulting in the biological equilibrium of the system. The degradation kinetic parameters in the HBTF were calculated using the following equation derived from the Michaelis-Menten equation (Hirai et al., 1990; Wani et al., 1999):

$$\frac{1}{R} = \frac{K_s}{V_m} \times \frac{1}{C_{ln}} + \frac{1}{V_m} \qquad \text{Eq. 7-1}$$

where R is apparent removal rate, g S or g N day^{-1} kg^{-1} dry AC; $C_{ln} = (C_0-C_e)/\ln(C_0/C_e)$, is logarithmic mean concentration of H_2S or NH_3 at the inlet and outlet of the HBTF, ppmv; V_m is maximum apparent removal rate, g S or g N day^{-1} kg^{-1} dry AC; and K_s is apparent half-saturation constant, ppmv. From the linear relationship between $1/C_{ln}$ and 1/R, V_m and K_s were calculated from the slope and intercept.

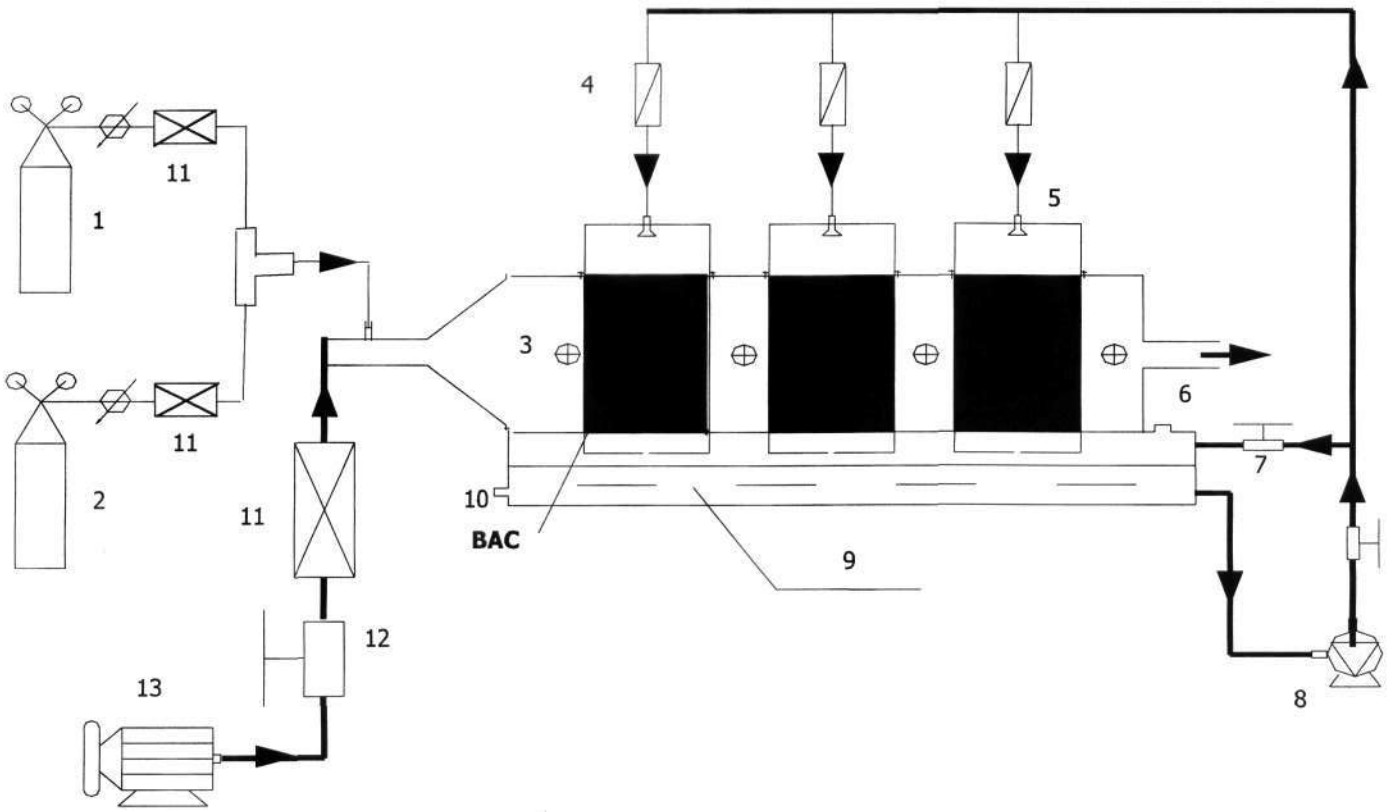

Figure 7.1 Schematic diagram of the horizontal biotrickling filter (HBTF) system (1 H_2S cylinder; 2 NH_3 cylinder; 3 sampling ports; 4 liquid flow meter; 5 nozzle; 6 nutrient feeding port; 7 water valve; 8 water pump; 9 water tank; 10 water sampling port; 11 gas flow meter; 12 air valve; 13 air blower)

Table 7.1 Physical properties of the HBTF

Physical Property	**Parameters**
Packing material	Exhausted carbon (Section 3.3.1)
Immobilization bacteria	Autotrophic SOB and nitrifying culture (Section 3.1)
Wet carbon weight, W_1 (g)	5,214
Dry carbon weight, W_2 (g)	3,300
Moisture content, m $=(W_1-W_2)/W_1$ (%)	36.7
H_2S adsorption capacity, (w/w, %)	8.3
Bed dimensions, (cm)	15×15×10×3 [a]
Segment length, L (cm)	3×10
Packing volume, V (L)	6.75
Initial pH of exhausted carbon	6.15
Bulk density, $d=W_1/V$ ($kg \cdot m^{-3}$)	772
Surface area, $m^2 \cdot g^{-1}$	776
External surface area, $m^2 \cdot g^{-1}$	454
Diameter of carbon pellet, mm	4
Bed porosity, %	37
Apparent density of carbon, ρ ($kg \cdot m^{-3}$)	490

a. Three segments in total

Table 7.2 Experimental designs in the HBTF

Phase	**Period (d)**	**Inlet loading ($g\ m^{-3}\ h^{-1}$)**		**EBRT (s)**	**Purpose**
		H_2S	NH_3		
1	0-30	2-18	1-9	30-60	Start-up
2	31-112	4-137	2-68	4-20	EBRT effect
3	113-124	0	0	8	Starvation
4	125-196	27-137	14-137	8	Substrates interaction
5	197-244	0	0	8	Starvation
6	245-316	55	27	4	Constant condition

7.3 Results and discussion

7.3.1 System performance evaluation

7.3.1.1 Start-up performance

As shown in Figure 7.2, the removal efficiencies of H_2S and NH_3 were approached 100% in the HBTF over the first 30 days of operation. The inlet loadings varied under 2-19 and 1-10 g m^{-3} h^{-1} for H_2S and NH_3, respectively. The concentration ratio of H_2S and NH_3 was maintained at around 1:1 (molar ratio).

The recirculation solution was analyzed to evaluate the biodegradation behavior in the HBTF. As shown in Figure 7.3, the concentration of NO_3^- and SO_4^{2-} increased with operation time. This indicates that NH_3 and H_2S were biodegraded. The HBTF was characterized by nearly full conversion of NH_3 to nitrate (>90%) and H_2S to sulfate (> 95%). High degradation capacity of NH_3 was attributed to the pre-established nitrifying biofilm (Chapter 6). High biodegradation of H_2S was possibly due to the pre-adsorbed sulfur on exhausted carbon which could act as the extra sulfur source for bacteria growth (Chapters 4 and 5). It was observed that biofilm was formed very well on the carbon surface in the HBTF after 30 days of operation (Figure 7.4). The pre-adsorbed sulfur compounds on exhausted carbon did not show any negative effect on the development of nitrifying biofilm.

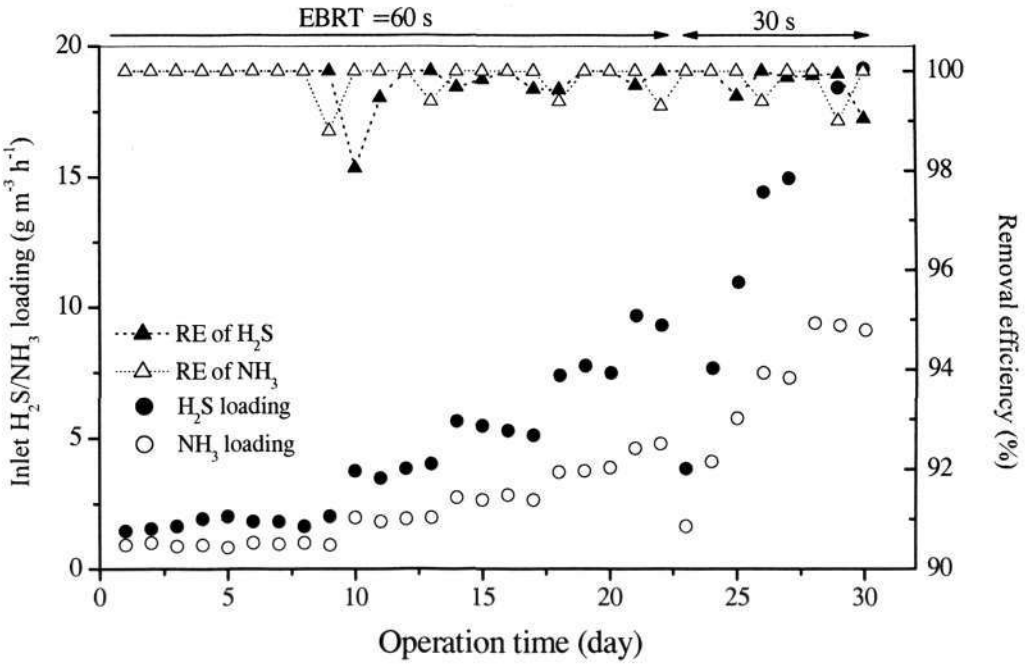

Figure 7.2 Start-up performance in the HBTF

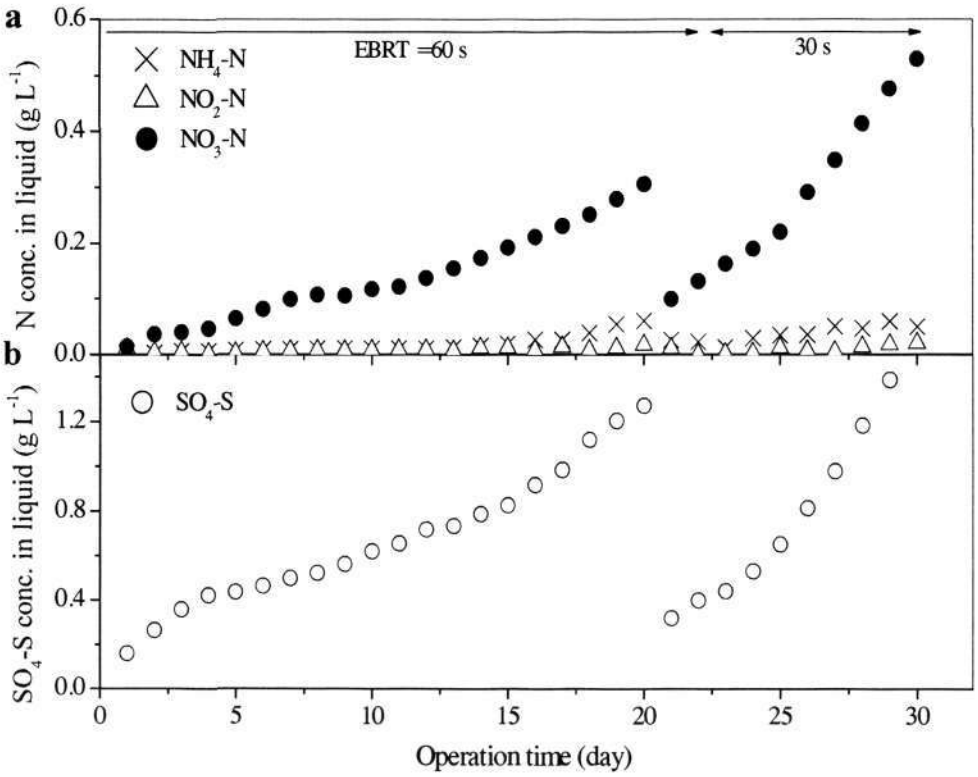

Figure 7.3 Biodegradation products profiles in liquid during the start-up period: (a) NH_4, NO_2/NO_3-N and (b) SO_4-S (Recirculation solution was replaced by fresh medium on day 20)

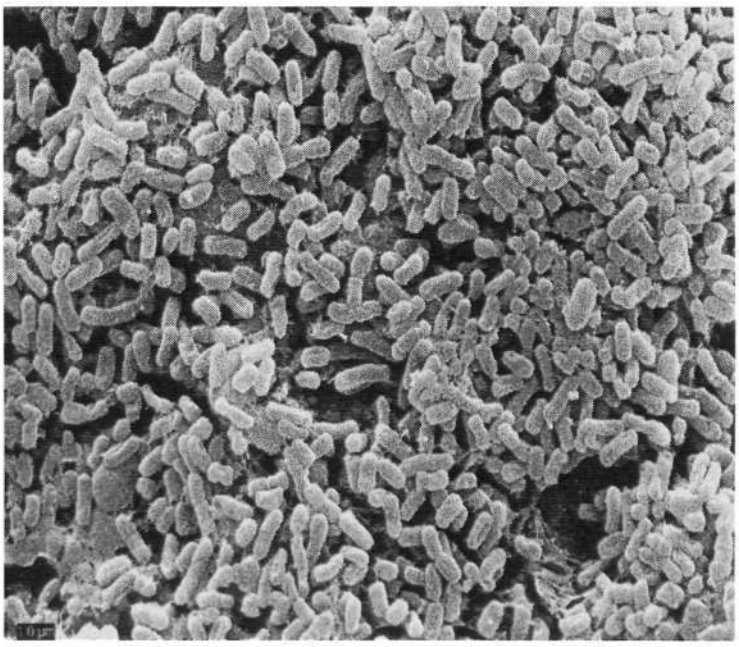

Figure 7.4 Biofilm developed on exhausted carbon for 30 days in the HBTF

7.3.1.2 Overall performance

The long-term performance of the HBTF (Table 7.1) is shown in Figure 7.5. After 30 days of start-up (Figure 7.2), the removal efficiencies of H_2S were ranged from 80 to 100% at the loadings of 4-137 g m^{-3} h^{-1}, while 95-100% of NH_3 was removed at inlet loadings of 2-137 g m^{-3} h^{-1} (phases 2 and 4). Removal efficiency of H_2S and NH_3 recovered within 1-3 days after 11 and 48 days of substrates starvation period (phases 3 and 5). During phase 6 when the system was operated under the constant loading (i.e. 4 s of EBRT with 40 ppmv each), average over 92 and 98% of H_2S and NH_3 were removed, respectively.

The results show that simultaneous removal of H_2S and NH_3 was achieved in the HBTF during 316 days of operation (Figure 7.5). The removal efficiencies at over 90% of H_2S and 95% of NH_3 were obtained in most cases. Low removal efficiencies were observed

during high loadings and after substrates starvation period. The removal of H_2S was more sensitive than NH_3 regarding the high loadings and after substrates starvation period. It is better to run the HBTF below the loading of 137 g H_2S m^{-3} h^{-1} to achieve high removal performance ($> 90\%$). In addition, it was observed that the removal performance deteriorated on day 100, 190, 264 and 294 (Figure 7.5). Carbon in each section in the HBTF was then washed by 5 L of tap water to remove loosely attached biomass. The actions resulted in an immediate improvement of the removal of H_2S and NH_3 (Figure 7.5). This phenomenon indicates that the deterioration in removal performance was due to the accumulation of biomass in the HBTF over an extended running. Thus, it is necessary to periodically remove some biomass to maintain a good performance over long-term operation.

Kinetic data is an important parameter for comparing the performance and characteristics of various biofiltration systems which have different seeding sources, packing materials and reactor configurations (Yani et al., 1998). Biodegradation rate parameters include maximum apparent removal rate (V_m) and apparent half saturation constant (K_s). They were estimated from the modified Michaelis-Menten (Eq.7-1) fitting of the experimental results in the HBTF. The linear form of 1/R vs $1/C_{In}$ of NH_3 and H_2S biodegradation was obtained and the K_s and V_m values were calculated, respectively (Figures 7.6). The V_m was 6.93 and 5.72 g kg^{-1} carbon day^{-1} for H_2S and NH_3 in the HBTF respectively. The K_s was 46.8 and 67.4 ppmv for H_2S and NH_3, respectively.

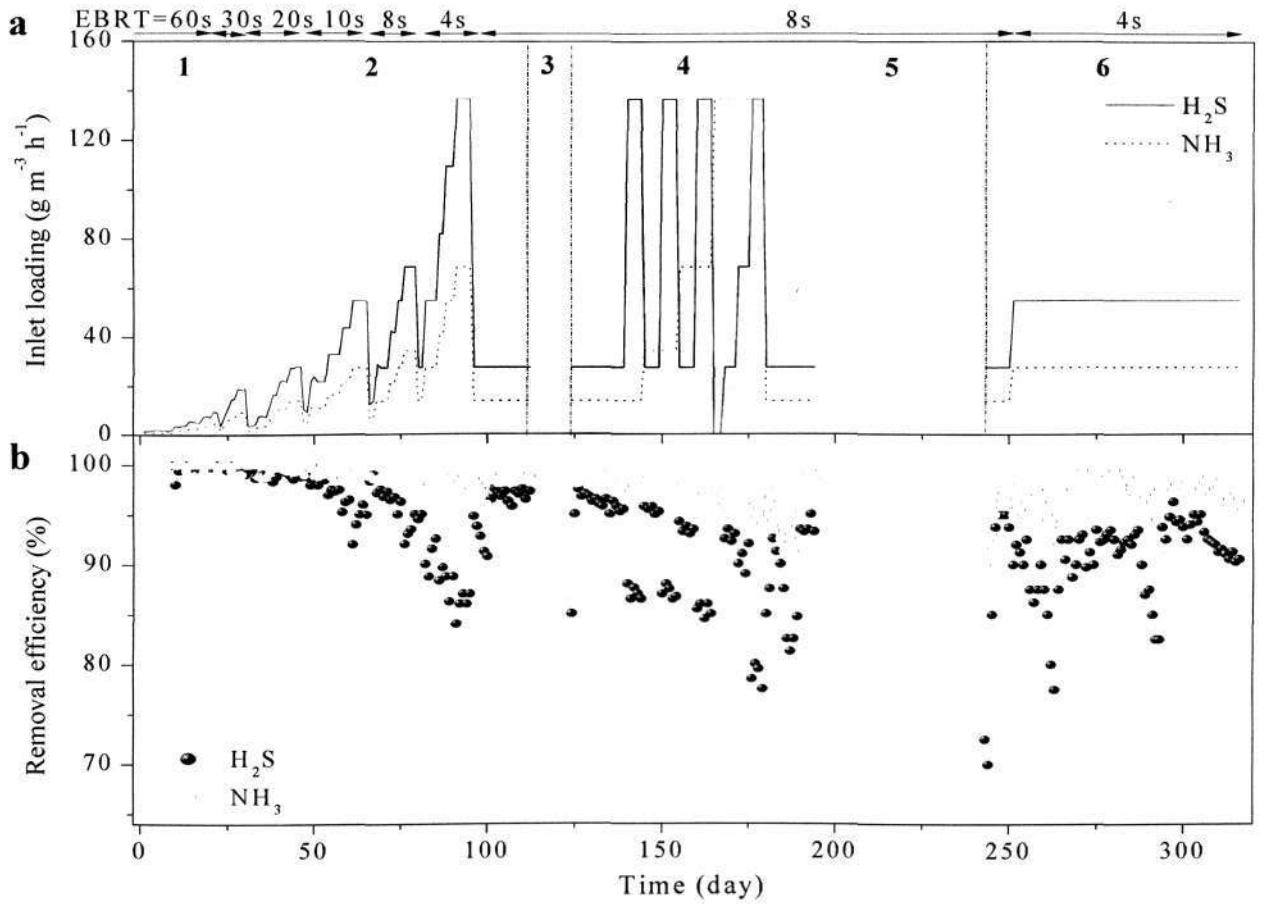

Figure 7.5 Inlet loading (a) and removal efficiency profiles (b) of H_2S and NH_3 in the HBTF

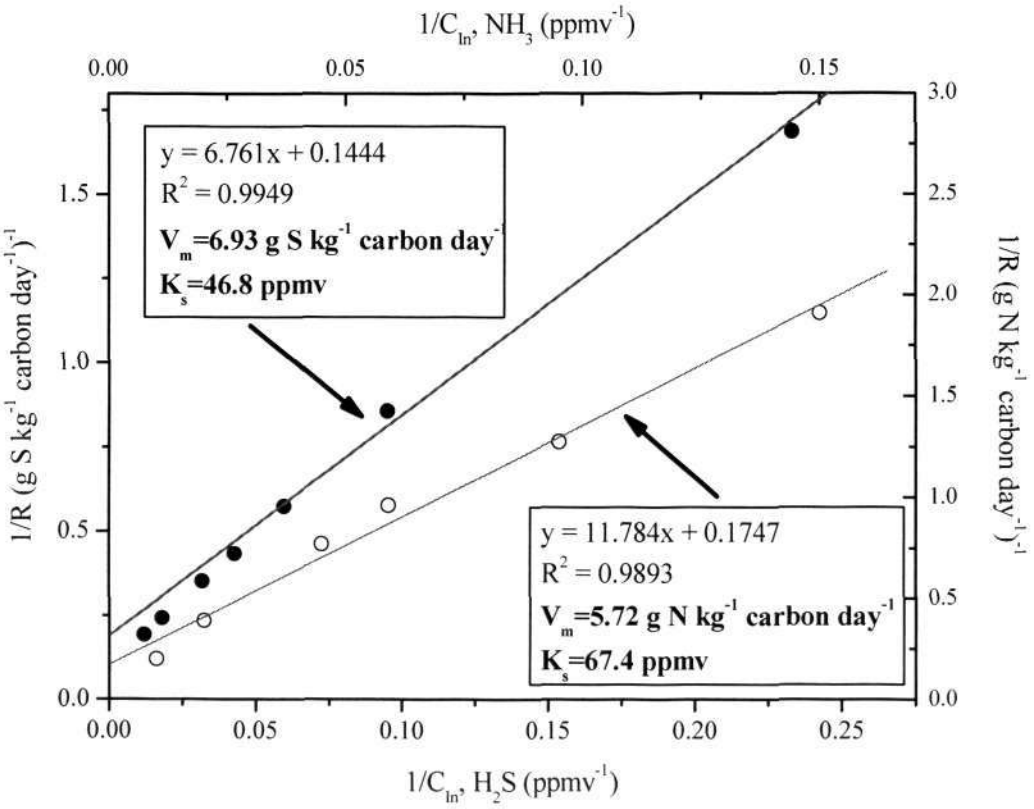

Figure 7.6 Relationships between 1/R and $1/C_{In}$ of NH_3 and H_2S degradation in the HBTF (Conditions: 20 to 400 ppmv of NH_3 at EBRT of 8 s with 100 ppmv of H_2S; 20 to 200 ppmv of H_2S at EBRT of 8 s with 100 ppmv of NH_3)

7.3.1.3 Effects of EBRT

Figure 7.7 shows the relationship between EBRT (4-20 s) and removal efficiency of NH_3/H_2S under varied inlet concentration (20-100 ppmv) in the HBTF. As shown in Figure 7.7a, NH_3 was almost completely removed when the EBRT were over 4 s, even when 100 ppmv of NH_3 was supplied. For the removal of H_2S (Figure 7.7b), almost completely removal was obtained when the EBRT were > 8 s. At a shorter EBRT of 4 s, 93% of H_2S was removed when 40 ppmv of H_2S was supplied.

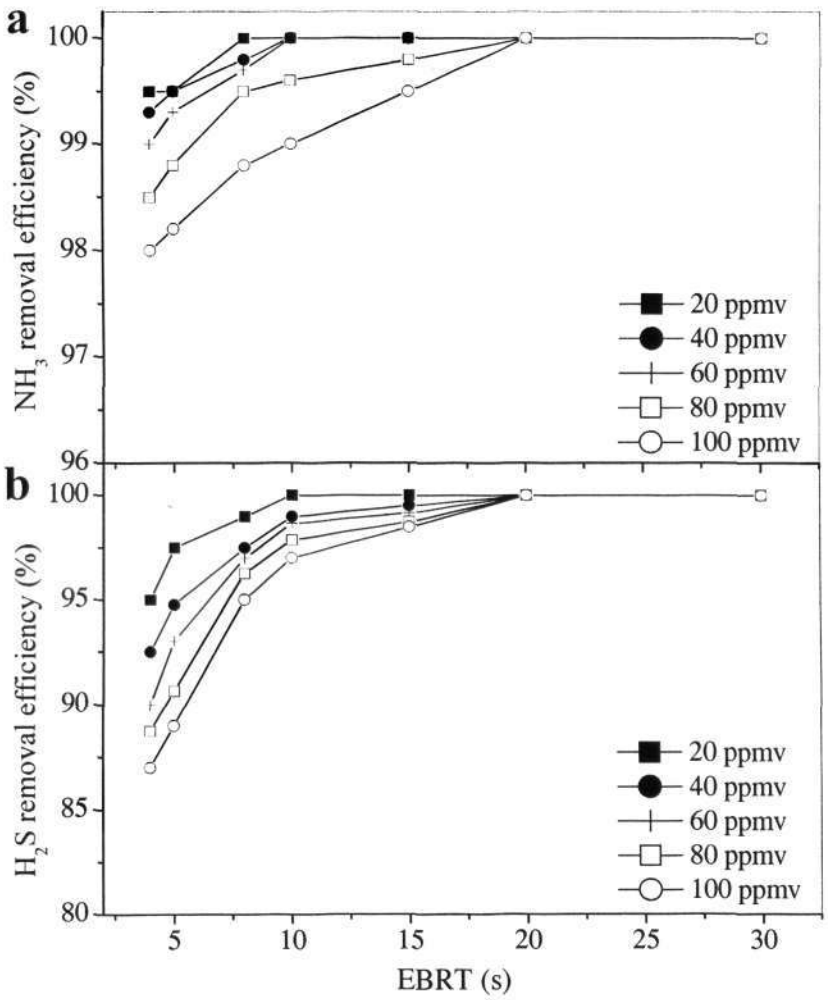

Figure 7.7 Removal efficiencies under different EBRTs and inlet concentrations: (a) NH_3 and (b) H_2S

The results show that the removal efficiencies of NH_3 were higher than those of H_2S at short EBRT (Figure 7.7). This indicates that the removal of H_2S was more sensitive at the short EBRT than NH_3. This is possibly due to a slower diffusion of H_2S from gas phase into liquid/biofilm phase (lower solubility). However, high solubility of NH_3 gas minimized mass-transfer limitations, which favored its removal in the biotrickling filter.

Under these conditions, over 99% removal efficiency was achieved at the loading of 44 g NH_3 m^{-3} h^{-1} and 36 g H_2S m^{-3} h^{-1}. Maximum elimination capacity of NH_3 was 67 g m^{-3} h^{-1} at 98%, while the maximum elimination capacity of H_2S was 119 g m^{-3} h^{-1} at 87%. 4 s was a very short EBRT. If a longer EBRT (e.g. >8 s) and higher concentration (e.g. >100 ppmv) was applied, maximum elimination capacity should be increased.

7.3.1.4 Interaction of NH_3 and H_2S removal at high concentrations

Inlet concentration of H_2S and NH_3 was increased to understand the situation under high loadings (phase 4). Various H_2S concentrations (0-400 ppmv) were introduced at an EBRT of 8 s, when NH_3 concentration was fixed at 400 ppmv. On the other hand, NH_3 concentrations were varied between 0 and 400 ppmv with 200 ppmv of H_2S. Removal efficiency and elimination capacity of NH_3/H_2S were determined (Figure 7.8).

It can be seen that the removal of NH_3 was not affected by H_2S concentration of up to 200 ppmv (i.e. 137 g H_2S m^{-3} h^{-1}), and 95% of NH_3 was removed at 200 ppmv of H_2S. When H_2S concentration was greater than 200 ppmv, the removal efficiency of NH_3 decreased. The percentages of NO_2/NO_3-N in liquid were 65 and 55% at 200 and 400 ppmv of H_2S, respectively (Figure 7.9a). This indicates that nitrification was inhibited at high loadings of H_2S. Thus, the removal efficiency of gaseous NH_3 decreased (Figure 7.8). The maximum elimination capacity of NH_3 at high loadings was 131 g m^{-3} h^{-1} (Figure 7.8).

As shown in Figure 7.8, the removal of H_2S was not influenced significantly when NH_3 concentration was increased up to 200 ppmv (68 g NH_3 m^{-3} h^{-1}). As the inlet NH_3 concentration was increased from 200 to 400 ppmv, the removal efficiency of H_2S decreased from 87 to 78%. Meanwhile, the ratio of SO_4-S in liquid decreased from 85 to 75% (Figure 7.9b). This indicates that H_2S was partially oxidized into other sulfur instead of sulfate at high loading of NH_3.

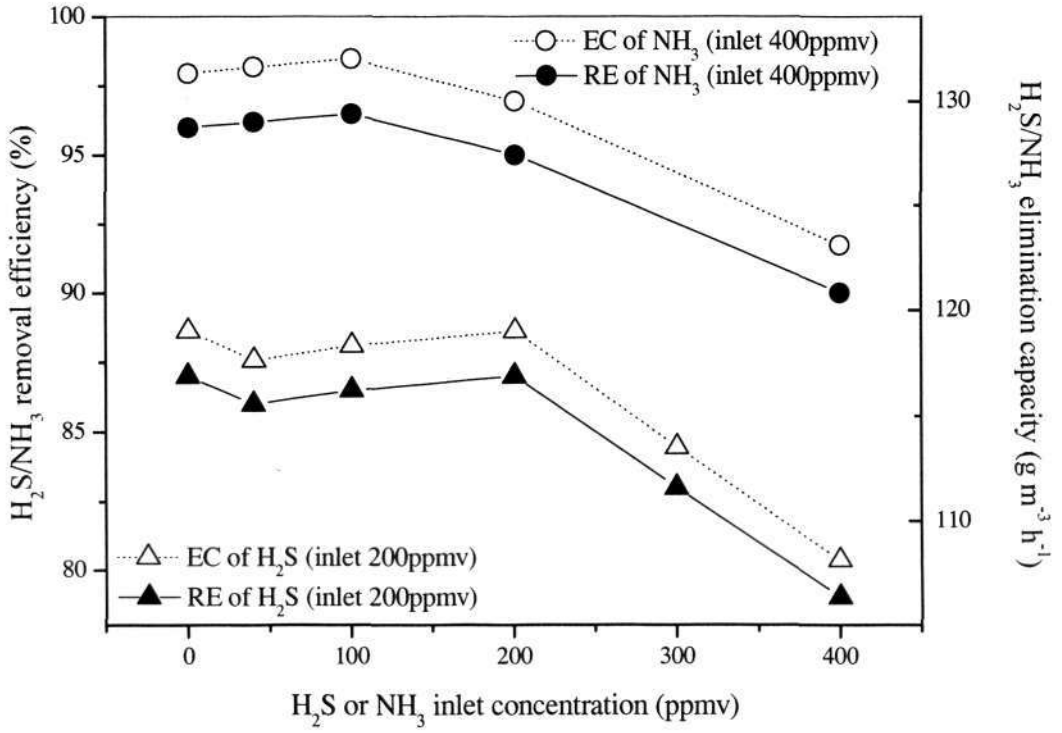

Figure 7.8 Influence of H_2S concentration on the removal of NH_3 and vice versa at 8 s of EBRT (RE: removal efficiency and EC: elimination capacity)

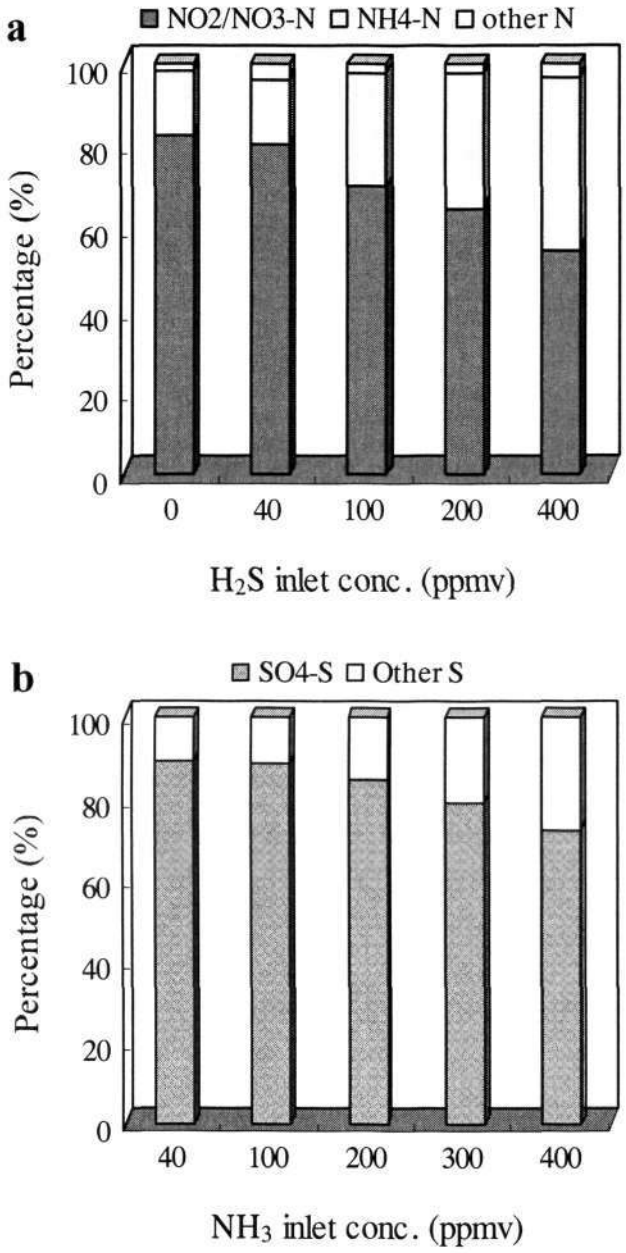

Figure 7.9 Influence of H_2S concentration on NH_3 (inlet 400 ppmv) biodegradation products (a) and influence of NH_3 concentration on H_2S (inlet 200 ppmv) biodegradation products (b) in liquid (EBRT =8 s)

7.3.1.5 Shock loading

When the inlet loading of H_2S was suddenly increased to 137 from 27 g m^{-3} h^{-1}, the removal efficiencies of H_2S dropped to 84 from 96% (Figure 7.10a). At the same time, as the inlet loading of NH_3 was suddenly increased to 68 from 14 g m^{-3} h^{-1}, the removal efficiencies of NH_3 dropped to 95 from 100% (Figure 7.10b). The removal efficiency of the HBTF recovered immediately after 6 h of the shock loading.

During the shock loading, the ratios of SO_4-S decreased to 15% of the captured H_2S from 96% before the shock loading (Figure 7.10a). This indicates the significant formation of intermediate product (e.g. elemental sulfur) during the shock loading. Meanwhile, only 18% of the captured NH_3 was biodegraded during the shock loading, which was much lower than 83% before (Figure 7.10b). The low ratio of NO_2/NO_3^- indicates the significant effect of adsorption and chemical neutralization with SO_4^{2-} for the removal of NH_3 gas during the shock loading. Nevertheless, once the shock loading stopped, the ratios of SO_4-S and NO_2/NO_3-N gradually increased to the original level.

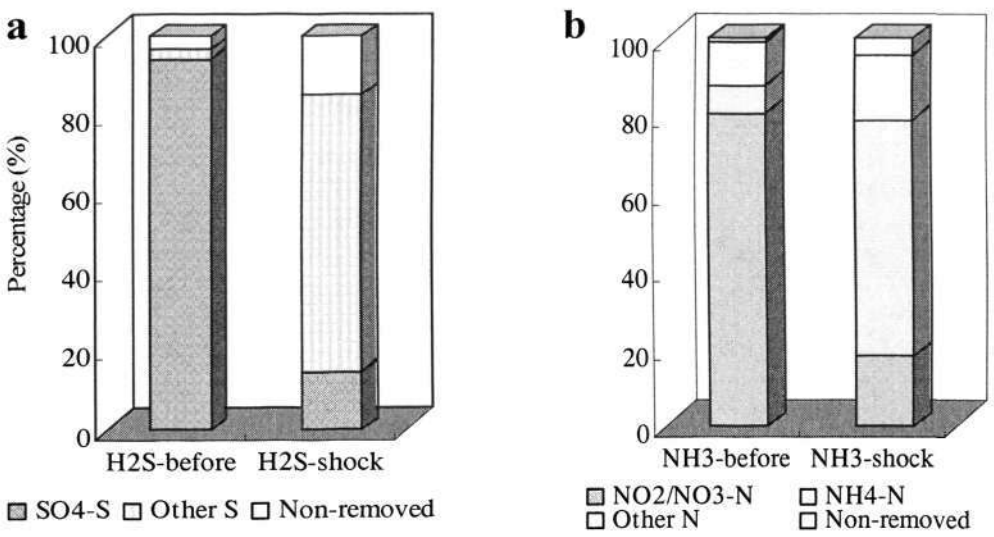

Figure 7.10 Biodegradation products of H_2S (a) and NH_3 (b) before and during shock loading

7.3.1.6 Starvation and restart

During phases 2, 3 and 5, the effect of substrates starvation was investigated when H_2S and NH_3 were not supplied for 2, 11 and 48 days, respectively. Only air and recirculation solution was provided in the HBTF. After that, the system was re-supplied with the same loading of H_2S and NH_3 before the interruption, i.e. 27 and 14 g m^{-3} h^{-1} respectively.

As shown in Figure 7.11a, 2 hours were required to recover the original removal efficiency of H_2S in the case of 2 days of starvation. After 11 days of starvation, when H_2S was re-introduced, 89% of H_2S was removed on the first 4 hours. On 6th hour, the removal efficiency decreased to 82%, and gradually increased to 96% (the original level) on 30th hour. The initial high removal of H_2S could be due to the adsorption in the system and the follow-up recovery of high removal was attributed to the biodegradation by bacteria that was adapted to the change. After 48 days of starvation, 72 hours were required to recover the removal of H_2S. In the case of NH_3 (Figure 7.11b), the removal efficiency recovered immediately after 2 days of starvation period. For 11 and 48 days of starvation, 6 and 80 hours were necessary to recover the HBTF, respectively.

Carbon samples were collected for SEM observation before and after 11 days of starvation. As shown in Figure 7.12a, a well-formed biofilm on carbon surface were observed before the starvation. Some interstices/gaps on the biofilm allow H_2S and NH_3 gas to pass through into the carbon. The physical adsorption of H_2S or NH_3 can still happen when shock loadings are encountered, even though the biodegradation might play a more important role under the steady-state. After 11 days of starvation, dead cells, extracellular polymeric substances (EPS) were found to accumulate on the carbon surface (Figure 7.12b).

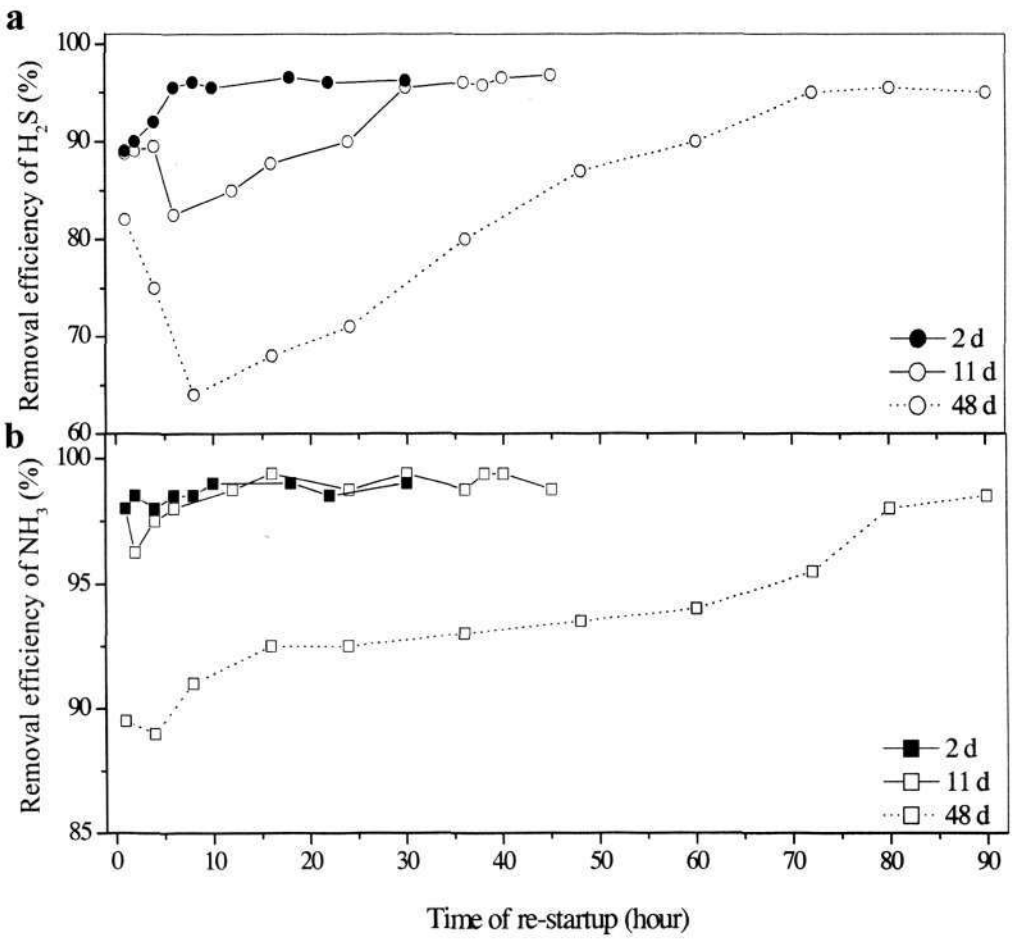

Figure 7.11 System responses of H_2S (a) and NH_3 (b) after 2, 11 and 48 days of starvation

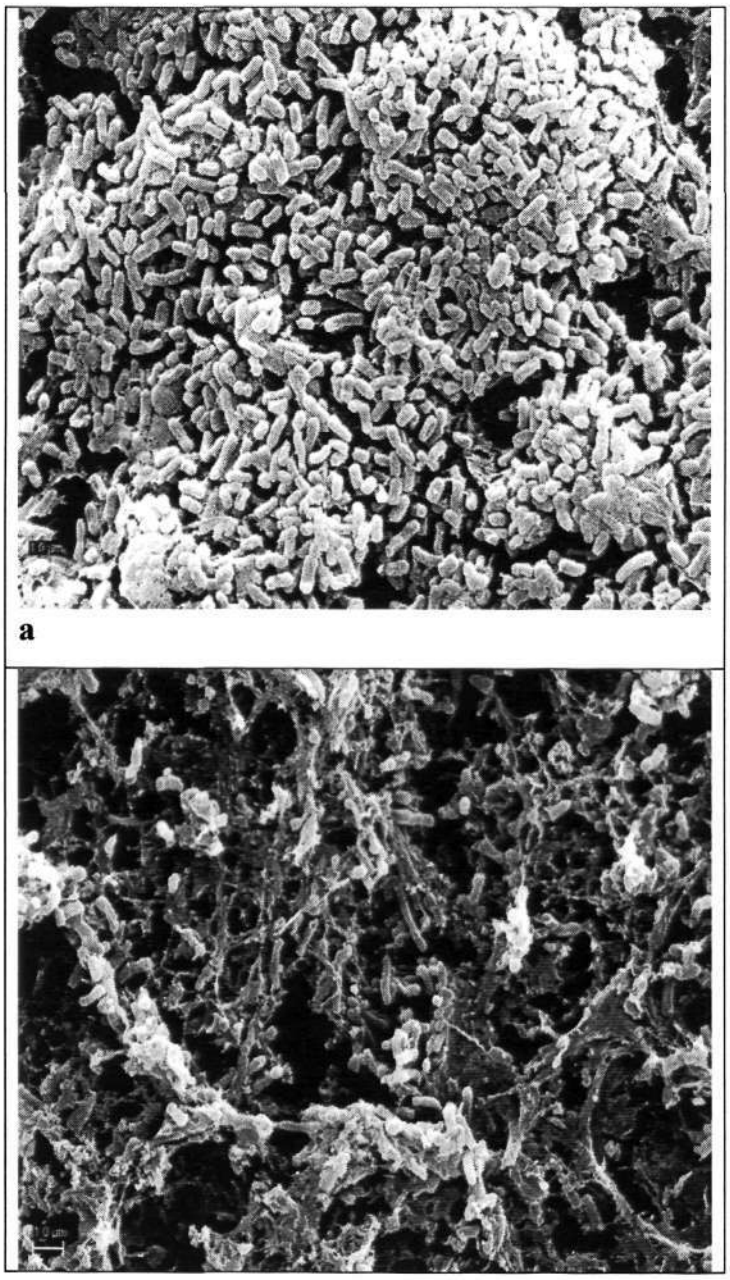

Figure 7.12 Biofilm developed on exhausted carbon before (a) and after 11 days of starvation (b) in the HBTF

7.3.2 Biomass concentration and biological activity of biofilm

Variations of biomass concentration along the HBTF bed were investigated (Figure 7.13). The biomass concentrations on carbon samples from the inlet section were ranged between 1.3 and 1.6 mg protein g^{-1} dry carbon. They were higher than those from the outlet of the HBTF, i.e. 0.4-1.0 mg protein g^{-1} dry carbon. The difference in biomass concentration along the bed decreased with operation time. This indicates that the biomass was distributed more even along the HBTF bed over extended operation.

This change in biomass distribution along the bed was probably resulted from the change of the gradient in pollutants concentration. As shown in Figure 7.14, contaminants were rapidly degraded in the inlet section of the HBTF on day 80, while the contaminants were degraded relatively even along the HBTF on day 190. The relatively even distribution of biomass along the HBTF benefited the stable operation of biofiltration. It was due to avoiding the problems of bed clogging and rapid activity loss caused by excessive biomass accumulated in the inlet section of bioreactors (Song and Kinney, 2000). The relatively even distribution of biomass along the HBTF bed could be attributed to the horizontal reactor design and continuously trickling. It was reported that the biomass concentration in the inlet section was 30 times higher than that in the outlet section in a vertical biofilter (Song and Kinney, 2000).

Moreover, the biomass concentration in the HBTF was relatively low, ranging from 0.4 to 1.6 mg protein g^{-1} carbon (Figure 7.13). This could be attributed to autotrophic NH_3 and H_2S degrading cultures (with the slow growth rate) and continuously liquid trickling. In addition, the starvation could also be beneficial to control the biomass accumulation. However, as mentioned in section 7.3.1.2, it is also required to periodically remove some biomass from the filter to maintain a good performance over long-term operation.

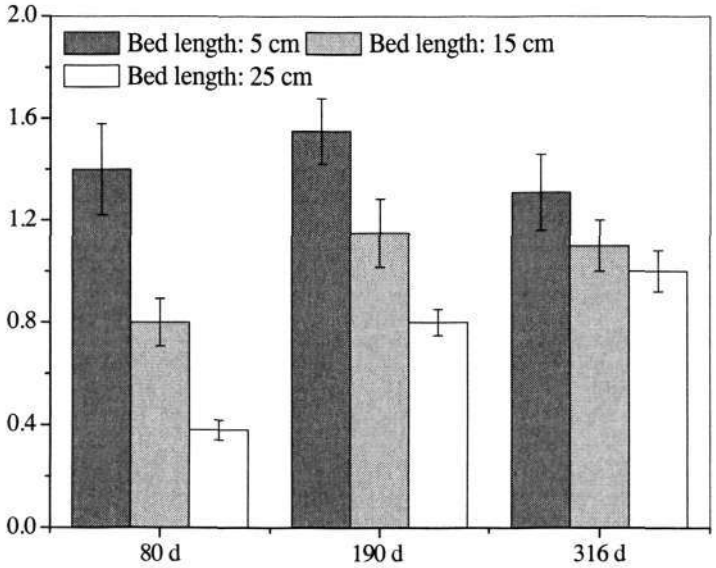

Figure 7.13 Protein concentration of biofilm on carbon samples along the HBTF on days 80, 190 and 316

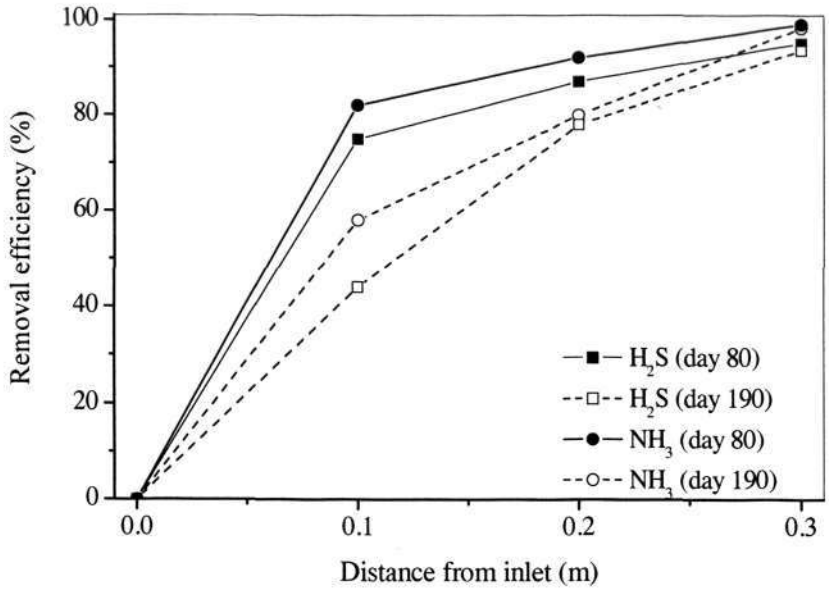

Figure 7.14 Removal efficiencies of H_2S and NH_3 along the HBTF on days 80 and 190

The biological activity of SOB and nitrifying biofilm on carbon was quantified by substrate-induced oxygen uptake rate (SOUR). Spatial variations of biological activity of biofilm samples along the HBTF were investigated (Figure 7.15). On day 80, biological activity of biofilm for sulfur ($SOUR_S$) was the highest at the inlet section and decreased along the length of the HBTF. However, the activity of nitrifying biofilm was the highest at the middle section of the HBTF. The phenomena could be explained by the inhibition of free ammonia due to high NH_3 loadings at the inlet section and by the ammonium limitation at the outlet of bioreactors (Villaverde et al., 1997). In addition, the low activity of nitrifying biofilm in the inlet of the HBTF may also be attributed to high loading of H_2S in the section.

On day 190, biological activity of biofilm along the HBTF became more even than that on day 80 (Figure 7.15). The spatial change was possibly due to high loadings of pollutants applied during this period (Figure 7.5) and the change of the gradient in pollutant concentration (Figure 7.14). In addition, the change indicates that certain nitrifying culture might be acclimatized by high concentration of NH_3 and H_2S in the inlet section.

Under steady-state conditions, the numbers of autotrophic nitrifying bacteria (AOB and NOB) and SOB on carbon were 2.3×10^{6}-6.2×10^{7} and 3.1×10^{7}-3.7×10^{8} cell g^{-1} dry carbon, respectively. The amount of nitrifying bacteria in the middle section was slightly higher than those in other sections of the HBTF, while that of SOB was higher in the inlet section. The distributions were consistent with the results of SOUR spatially (Figure 7.15). The stable settlement of the two groups of bacteria in the system was responsible for the simultaneous biodegradation of H_2S and NH_3. A specific oxidation rate can be obtained by using the maximum removal rate (Figures 7.6) and cell number in the HBTF, as described by Yani et al. (1998). The specific uptake rates were 6.2×10^{-13}-11.5×10^{-12} g S $cell^{-1}$ h^{-1} and 3.8×10^{-12}-9.9×10^{-11} g N $cell^{-1}$ h^{-1}.

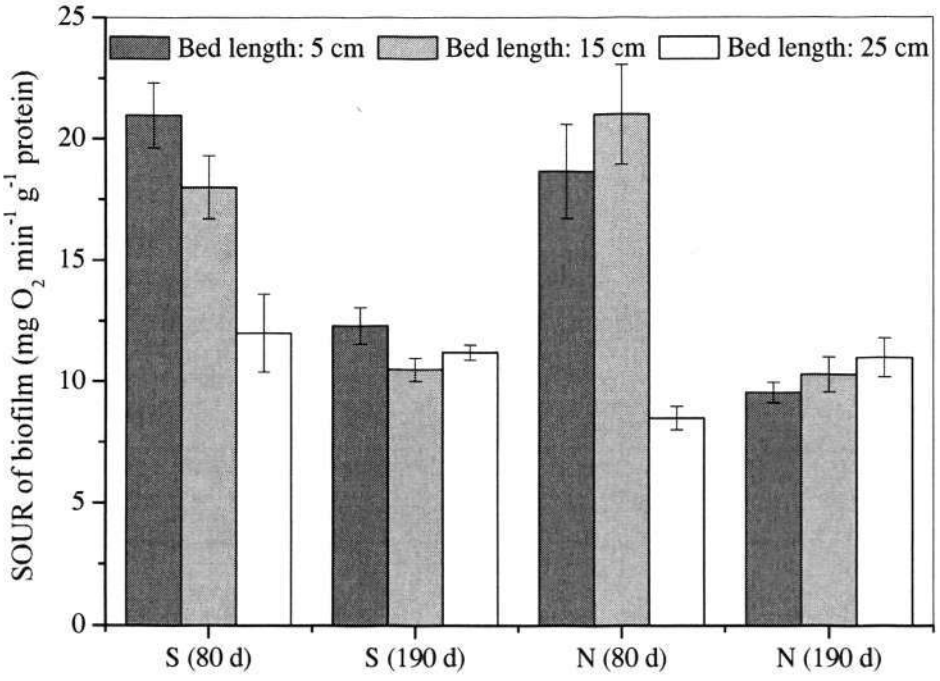

Figure 7.15 Biological activities of biofilm on carbon samples along the HBTF on days 80 and 190

7.3.3 Distribution of nitrogen and sulfur

Over 316 days of operation, the total removed S and N were 1508 g (i.e. 45.7 wt% S/dry carbon) and 899 g (i.e. 27.2 wt% N/dry carbon) in the HBTF system, respectively. The fate of the removed S and N was evaluated through the distribution of these compounds on carbon and in recirculation liquid.

The content profiles of S and N on carbon samples in the HBTF are shown in Figure 7.16. During the initial 80 days, the S content decreased gradually, from 2.8 to 1.6 wt%, and an increasing trend was observed for the N element. It indicates that S compounds on exhausted carbon were bio-regenerated, while some of NH_3 gas was adsorbed into the

carbon. The contents of S and N were relatively low after stages 3 and 5 (starvation), and the S and N was accumulated at stage 4 (high loadings) (Figure 7.16). Compared with that on exhausted carbon (7.8 wt% S in Table 7.1), the contents of S on BAC in the HBTF were much lower throughout the entire operation. It demonstrated that the service life of exhausted carbon was extended greatly.

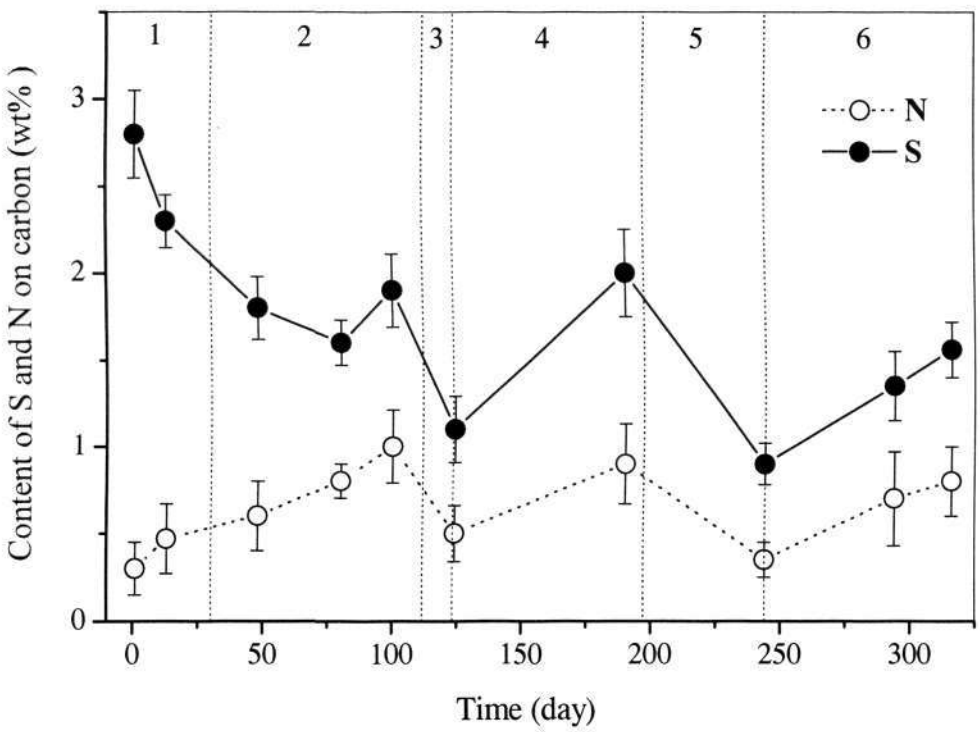

Figure 7.16 Content profiles of sulfur and nitrogen on carbon samples in the HBTF (middle section)

The contents of S and N on carbon along the HBTF were also investigated (Figure 7.17). On day 80, the content of S and N on carbon decreased significantly from the inlet to the outlet section of the HBTF. The distribution could be attributed to the high pollutants concentration in the inlet section and very low pollutants concentration in the outlet section of the HBTF (Figure 7.14). Considering exhausted carbon as packing material in the HBTF, the phenomena suggests that high H_2S concentration in the inlet section provided little concentration gradient to drive desorption of pre-adsorbed sulfur from the carbon. In contrast, low concentration in the outlet caused a large driving force for the release of sulfur compounds from the carbon. On days 190 and 316, the difference in the distribution of S and N along the HBTF decreased. It might result from the change of pollutant gas concentration along the HBTF over extended operation (Figure 7.14).

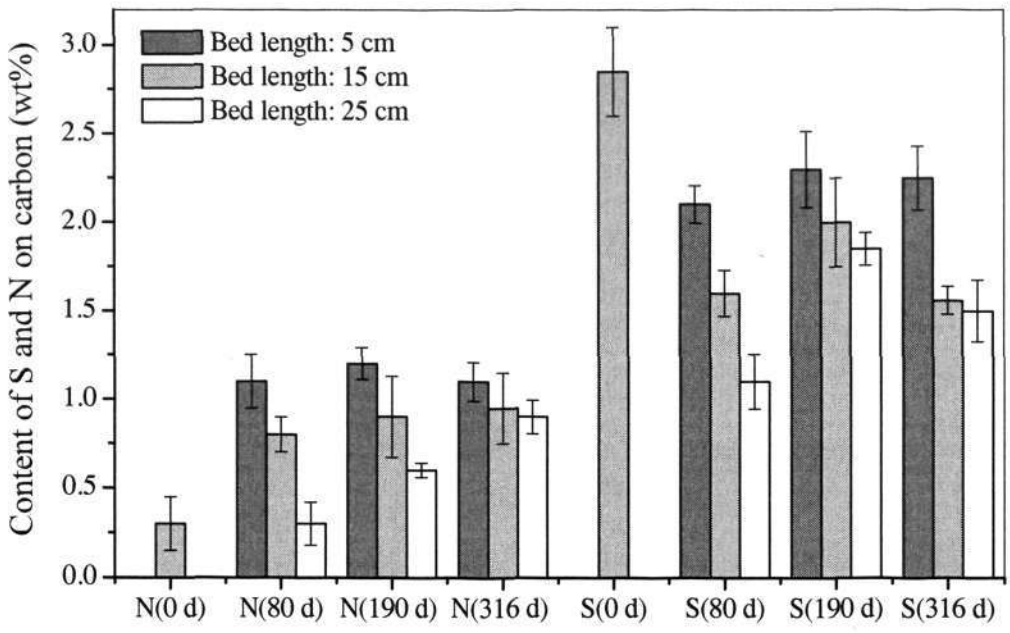

Figure 7.17 Content profiles of sulfur and nitrogen on carbon samples along the HBTF on days 80, 190 and 316

The results show the insignificant accumulation of degradation products (0.9-2.8 wt% S and 0.3-1.0 wt% N) in the HBTF over 316 days of operation (Figure 7.16). This benefits the stable operation of the HBTF, due to preventing the accumulation of metabolic products in a toxic concentration. The low accumulation was mostly attributed to complete biodegradation of H_2S, sulfate as main product (>95% in most cases), which can be washed off from the bed more easily than elemental S. In addition, frequently refreshing liquid medium was essential to discharge the biodegradation products on the packing material out of the system.

Meanwhile, NH_3 was biodegraded to NO_2^-/NO_3^- with high ratio (>85% in most cases). The results show that NH_3 were removed mainly via nitrification rather than physical/chemisorptions in the system. In addition, supplied NH_3 can also be served as the nitrogen source for cell synthesis. The overall reaction describing complete biodegradation of H_2S and NH_3 can be given (Rittmann and McCarty, 2001):

$$0.0625H_2S + 0.0625HS^- + 0.01H_2O + 0.04CO_2 + 0.01HCO_3^- + 0.01NH_4^+ + 0.2O_2 = 0.01C_5H_7O_2N + 0.125SO_4^{2-} + 1.1875H^+ \quad \text{Eq.7-2}$$

$$0.13NH_4^+ + 0.005HCO_3^- + 0.02CO_2 + 0.225O_2 = 0.005C_5H_7O_2N + 0.125NO_3^- + 0.25H^+ + 0.12\,H_2O \quad \text{Eq.7-3}$$

From Eq.7-2 and Eq.7-3, 87.3 g N was required for cell synthesis in H_2S and NH_3 biodegradation process during 316 days of operation. The amount occupied about 10% of total removed NH_3 in the HBTF. It explains that about 90% of captured NH_3 can be measured in liquid phase.

7.3.4 Change of carbon surface characteristics

The pH and surface structures of carbon samples from the HBTF were identified (Table 7.3). The results show that the pH values of carbon samples in the HBTF were near neutral over 316 days of operation. This overcomes the system acidification which happened usually in conventional biofilters (Yang and Allen, 1994; Chung et al., 2001). The neutral

pH values are better for the adsorption of H_2S gas firstly and then for further biodegradation, than under acidic conditions in conventional biofilters (Yang and Allen, 1994). Moreover, it was also the proper pH range for the growth of both SOB and nitrifying culture. In addition, the pH values of carbon from each location along the HBTF bed were almost identical (Table 7.3). This is possibly attributed to the horizontal reactor design.

Table 7.3 pH and surface structure of carbon samples in the HBTF

Sample	Distance from the inlet (cm)	pH	Surface structure			
			V_{mic} ($cm^3\ g^{-1}$)	S_{BET} ($m^2\ g^{-1}$)	S_{mic} ($m^2\ g^{-1}$)	S_{ext} ($m^2\ g^{-1}$)
Day 80	5	6.7	0.153	705	355	340
	15	7.1	0.156	717	362	355
	25	7.4	0.171	727	365	362
	Average	**7.1**	**0.160**	**716**	**361**	**352**
Day 190	5	6.5	0.154	690	346	336
	15	6.9	0.163	697	353	345
	25	6.8	0.169	692	358	349
	Average	**6.7**	**0.162**	**693**	**352**	**343**
Day 316	5	6.6	0.160	680	356	324
	15	6.7	0.176	703	360	343
	25	6.4	0.163	684	344	340
	Average	**6.5**	**0.166**	**689**	**353**	**336**
FC		9.9	0.180	910	400	510
EC		6.1	0.133	772	306	455

V_{mic}: Micropore volume; S_{BET}: BET surface area; S_{mic}: Micropore area; S_{ext}: External surface area ; FC: fresh carbon; and EC: exhausted carbon

For surface structure of carbon samples, micropore volume (V_{mic}) and surface area (S_{mic}) remained at similar level while external surface area (S_{ext}) decreased slightly over 316 days of operation (Table 7.3). With regards to surface structures of carbon samples along the HBTF bed (Table 7.3), the S_{ext}, V_{mic} and S_{mic} increased slightly from the inlet to outlet of the bed on day 80. After 316 days of operation, surface properties for carbon samples along the filter bed became even. This result was consistent with the distribution of the biomass concentration (Figure 7.13) and the content of S and N on the carbon along the HBTF (Figure 7.17).

The stable V_{mic} and S_{mic} of carbon indicate that biodegradation played a major role in the removal of pollutants while the adsorption was only an intermediate process. This let the adsorption still happening during shock loadings. Decreased S_{ext} might be attributed to the accumulation of biomass (Figure 7.13) and of degradation products on carbon surface (Figure 7.16). Stable surface characteristics of carbon significantly contributed to the high performance in the HBTF over a long-term operation. In addition, compared with those of exhausted carbon (0.133 $cm^3\ g^{-1}$ and 306 $m^2\ g^{-1}$), the V_{mic} and S_{mic} of carbon samples in the HBTF (0.153-0.176 $cm^3\ g^{-1}$ and 344-365 $m^2\ g^{-1}$) were higher and was still far from exhausted again until 316 days of operation.

7.3.5 Microbial community

The denaturing gradient gel electrophoresis (DGGE) technique has already been used successfully to explore bacterial diversity and population shift in response to environmental changes (Tresse et al., 2002; Li and Moe, 2004; Sercu et al., 2005). In this study, DGGE was employed to produce genetic fingerprints that could provide information on the composition and diversity of microbial communities in the H_2S and NH_3-degrading microbial biofilm in the HBTF. Each band on the DGGE profile corresponded to a gene fragment of unique 16S rRNA sequences and accordingly represented a specific species in the microbial community. The intensity of a band represents the relative abundance of the corresponding microbial species (Casamayor et

al., 2000). DNA was extracted from the biofilm in the HBTF. PCR amplification and DGGE analysis of community 16S rRNA genes were performed in replicate on pooled aliquots of extracted nucleic acids. Almost identical fingerprints were obtained for replicate samples. The Dice coefficient (Cs) was used to quantify the similarity of these community fingerprints. A Cs value of 0% indicates that the samples are completely different, and Cs value of 100% indicates that the samples are identical.

7.3.5.1 Temporal analysis

Figure 7.18 shows the temporal DGGE profiles of amplified 16S rRNA gene fragments of biofilm samples from the HBTF over 316 days of operation. By comparing Cs, cluster analysis was performed with the un-weighted pair group method using arithmetic averages (UPGMA) algorithm to study general patterns of community similarity among the samples (Figure 7.19).

It can be seen that a good diverse community in biofilm was developed on the carbon in the HBTF (Figure 7.18). The biofilm samples have low similarity with the inoculated nitrifying culture (IN) at the Cs of 26-50% and with the inoculated SOB (IS) at the Cs of 20-43%. This suggests that the biomass established in the HBTF was subjected to further adaptation. The pollutants-degrading culture in the batch reactor did not enrich for high numbers of bacteria with ability for simultaneous biodegradation of H_2S and NH_3 in long-term colonization in the particular HBTF. It was reported that the community structure of nitrifying culture shifted with the addition of sulfide (Erguder et al., 2008). Thus, the biodegradation of NH_3 might be attributed to the acclimation of sulfide-tolerant nitrifying bacteria in the HBTF system.

As shown in Figure 7.18, the microbial community on days 48-112 was relatively unstable, with a moderate similarity of 62-80%. This could be due to different inlet loadings applied during this period (phase 2 in Figure 7.5). The increasing loading of H_2S and NH_3 likely resulted in some growth inhibition for low loading utilizing H_2S and NH_3

degraders, thereby changing the fingerprint patterns. The changing bacterial population should be more suitable for degrading high loading of pollutants.

A change in microbial community was observed between the samples on days 112 and 123 (Figure 7.18). Some bands present in microbial community on 112 disappeared in the lane on day 123. This implies that the bacterial diversity decreased on day 123. Furthermore, common bands (i.e.,_those identified at the same relative position) were observed to have decreased relative intensities on day 123. This reflects a difference in relative abundance of certain common bacterial species. Thes changes might be attributed to11 days of substrates starvation (phase 3 in Figure 7.5).. Similarly, a change in microbial community was observed between the samples on days 190 and 245 (Figure 7.18). These changes of bacterial community on days 123 and 245 may in turn be partially responsible for decreased performance of the HBTF just after 11 days and 48 days of substrates starvation period (Figure 7.5). A highly stable microbial community was achieved on days 264-316 under the constant loading of H_2S and NH_3. As mentioned in section 7.3.1.2, on day 264 and 294, the removal efficiencies of H_2S and NH_3 decreased, and improved subsequently after water washing carbon bed (Figures 7.5). It further confirmed that decreased removal efficiency of pollutants on these days was caused by biomass accumulation but not by the microbial community.

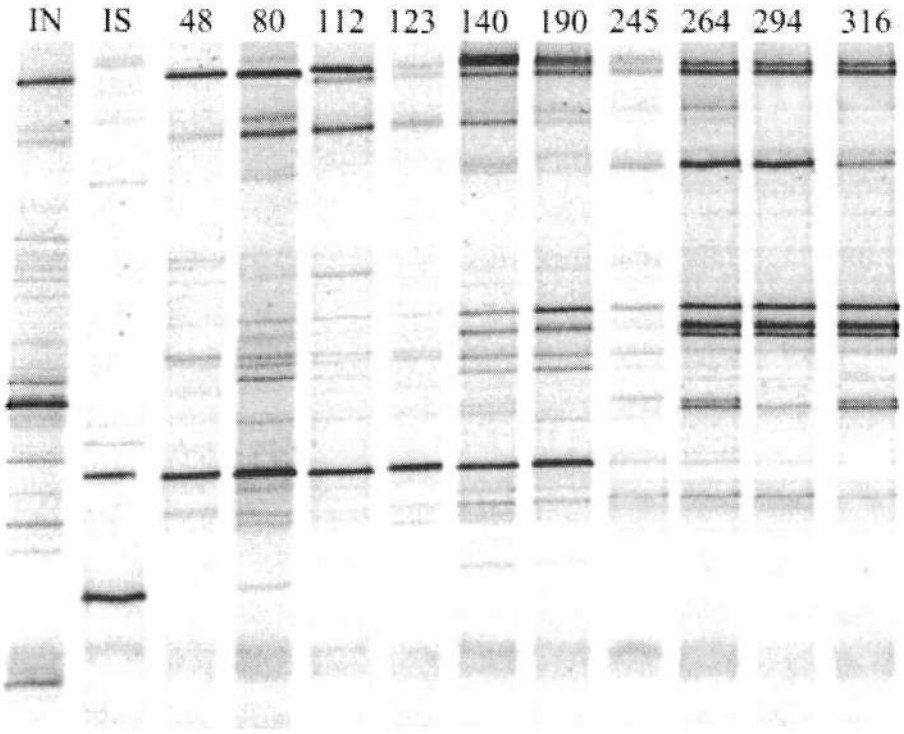

Figure 7.18 DGGE patterns of the samples from the middle section of the HBTF temporally (IN: Nitrifying inoculums; IS: SOB inoculums; and the day when the sample was taken is denoted by the corresponding number at the top of each gel column)

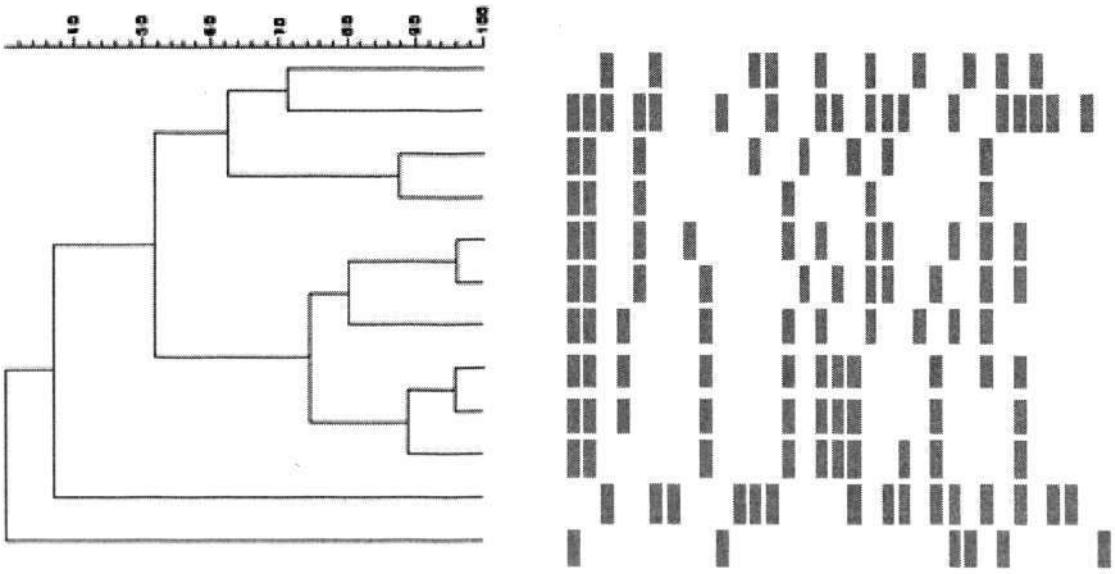

Figure 7.19 UPGMA dendrograms revealing the similarity of PCR-DGGE fingerprints of biofilm samples from the HBTF (middle section) temporally (IN: Nitrifying inoculums; IS: SOB inoculums; and the day when the sample was taken is denoted by the corresponding number at the top of each gel column)

The samples in the HBTF could be grouped into two main clusters with regard to the bacterial populations (Figure 7.19). The samples on day 48-123 formed one main cluster at the Cs of 52-88%, and those on day 140-316 formed another main cluster at the Cs of 67-96%. The two main clusters had a similarity at 51%. The community structures from day 140-316 were more similar than those from day 48-123. The bacterial population on day 48-112 showed moderate similarity at 62-80%. The Cs was 88% between the samples on days 112 and 123. The Cs of bacterial population on days 190 and 245 was obtained at 78%. The samples on days 264 and 316 have high similarity at Cs of 87-96%.

The results of DGGE of PCR-amplified 16S rRNA gene fragments revealed high population diversity in the present HBTF, which favored the performance stability for a long-term operation. In addition, the bacterial community structures in the HBTF were relatively stable under the conditions of constant loadings (days 264-316 in Figure 7.18). On the other hand, the microbial community was less stable during the abnormal operating conditions, e.g., changing inlet loadings and substrates starvation (days 48-245). The cluster analysis demonstrated that the microbial community structures from days 48-245 were less similar than those from days 264-316. This suggests that the microbial community could adapt to the changing operating conditions (days 48-245). This indicates that not only some degree of stability, but also the adequate dynamics of the bacterial community structure capable of adapting to accommodate varying reactor conditions are important for the stable performance in the HBTF.

7.3.5.2 Spatial analysis

Figure 7.20 shows the DGGE banding pattern of the samples along the section of the HBTF on days 80 and 190. By comparing Cs, cluster analysis was performed with the UPGMA algorithm to study general patterns of community similarity among the samples (Figure 7.21).

As shown in Figure 7.20, the microbial community structures differed as a function of the section of the HBTF in early period (day 80), even though the whole HBTF were inoculated with the same culture. The microbial populations in the inlet section of the HBTF were more diverse than those in the other sections. The Cs values were ranged from 45 to 96%. Furthermore, common bands (i.e., those identified at the same relative position in different lanes) were observed to have varying relative intensities. This reflects a difference in relative abundance of certain common bacterial species along the section of the HBTF. However, the microbial community structures of the samples along the HBTF became highly similar (79-100%) after a long-term operation (190 days).

The samples from the six sections of the HBTF on day 80 could be grouped into two main clusters with regard to bacterial populations (Figure 7.21). H1 and H2 (closest to the inlet) formed one main cluster (96%), and the other four sections formed another main cluster. The two main clusters had a similarity of 66%. On day 190, the microbial communities were also grouped into two main clusters (Figure 7.21). B5 and B6 (closest to the outlet) formed one main cluster at a Cs value of 96%, while the other four sections were each most closely and formed another main cluster. The two main clusters have a Cs of 84%.

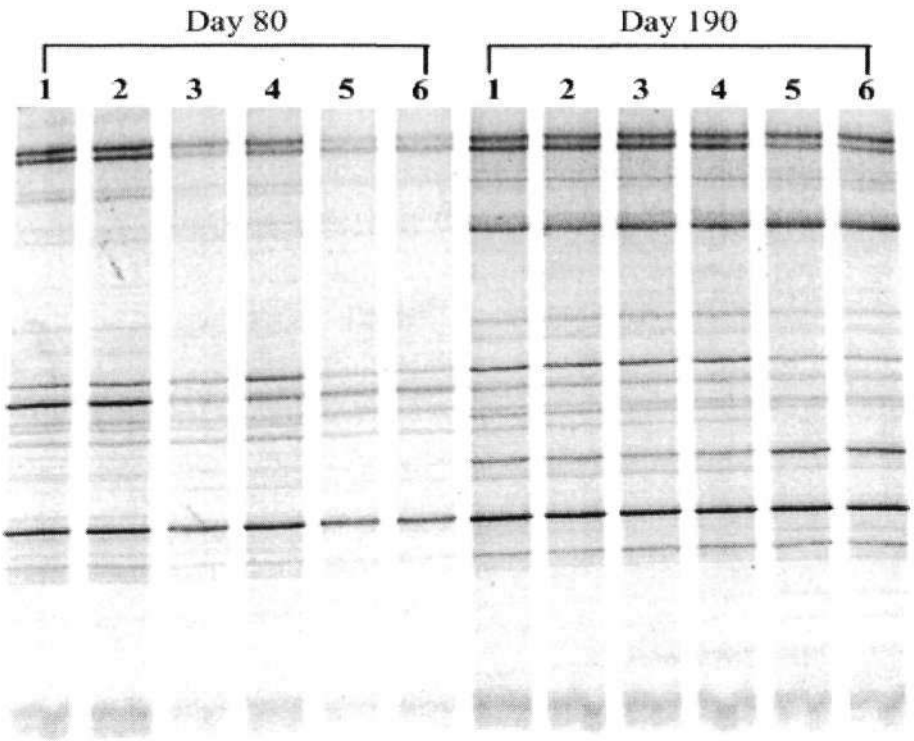

Figure 7.20 DGGE patterns of biofilm samples along the section of HBTF on days 80 and 190 (1-6 designating the distance to the inlet of the bed: 5, 10, 15, 20, 25, 30 cm)

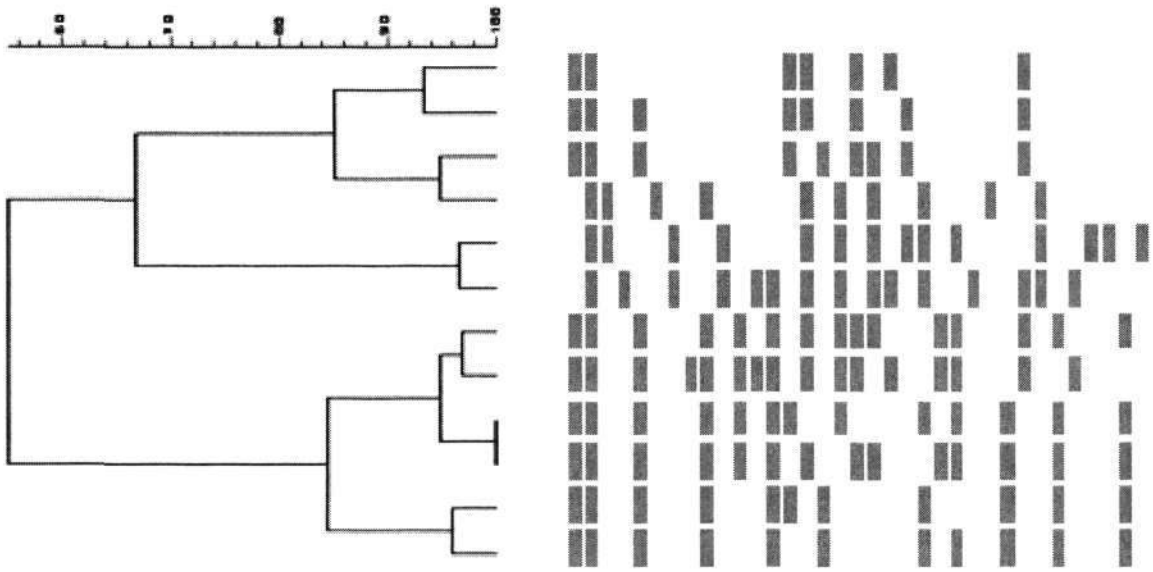

Figure 7.21 UPGMA dendrograms revealing the similarity of PCR-DGGE fingerprints of samples along the HBTF on days 80 and 190 (H denotes day 80 and B denotes day 190, with 1-6 designating the distance to the inlet of the bed: 5, 10, 15, 20, 25, 30 cm)

The results demonstrate that the microbial community structures of samples along the HBTF on day 190 were more similar than those on day 80. It indicates that the growth conditions on day 190 were probably much more similar throughout the HBTF than those on day 80. A difference in pollutant concentrations along the HBTF could apply a sufficiently large selective pressure to influence the microbial community composition. As shown in Figure 7.14, on day 80, contaminants were rapidly degraded in the inlet sections of the HBTF, and hence, microorganisms in the middle and outlet sections were exposed to markedly lower pollutants concentrations. It also suggests that differences in specific growth rates at the prevailing contaminant concentrations at each location likely served as a selective pressure to increase the relative abundance of certain microorganisms with respect to others (Figure 7.20).

On day 190, the contaminants were degraded relatively even along the HBTF (Figure 7.14). The degraded amount of contaminants in the outlet section of the HBTF were about 10 and 3 times lower than those in the inlet section on days 80 and 190, respectively. The change trends of the microbial community in the HBTF were also consistent with the change of biomass concentration (Figure 7.13) and content of S and N (Figure 7.17) on carbon along the HBTF bed on days 80 and 190.

7.3.6 Cost evaluation

In designing an air-phase bioreactor, the main goal is to meet a performance level while minimizing capital and operating costs. The capital and operating costs were needed to evaluate. A cost analysis of the activated carbon biofilter was described previously (Chung et al., 2004). The capital costs included ($/m^3): the reactor, 1700; media, 45; air compressor, 430; water pump, 200; pipes, 100; and microbial inoculation, 15; as well as other miscellaneous costs, 10. The total capital cost of the system was estimated as $2500/m^3 of filter bed, a price which would fall by about one-third if the system was scaled up for field application (vanLith et al., 1997). Operating costs include electricity consumption, water consumption and disposal, nutrient supplement, and medium replacement and disposal (Chung et al., 2004). The operating costs were $0.68/1000 m^3/yr, which is less than the $3/1000 m^3/yr and $1.9/1000 m^3/yr reported previously for the same evaluated items (Fouhy, 1992; Deshusses and Cox, 1999).

Compared with the above system, the capital and operating costs in the present system are expected to be relatively lower. Firstly, the cost of reactor will decrease if the horizontal chemical scrubbers which are currently used in wastewater treatment plants are to be converted into biotrickling filters (Gabriel and Deshusses, 2003). Secondly, the exhausted carbon from H_2S adsorption process, i.e., solid waste, requires lower cost, compared with fresh activated carbon. Thirdly, a horizontal design is also expected to work well with a relatively low pressure drop compared with a vertical design. A high pressure drop will result in higher energy consumption requirements. Under the EBRT of

180-30 s, the pressure drop ranged between 8 and 65 mm H_2O m^{-1} (Chung et al., 2004), while in the present study it ranged between 1 and 16 mm H_2O m^{-1} under the EBRT of 60-2 s.

7.4 Conclusions

It was highly efficient and effective for long-term simultaneous biodegradation of H_2S and NH_3 by the HBTF system over 316 days. Complete removal and biodegradation of H_2S and NH_3 was obtained at the beginning 30 days of operation. Over 95% and 90% of NH_3 and H_2S were removed in most cases, respectively. During the steady state, NH_3 and H_2S were almost completely removed when the EBRT were >4 and 8 s, respectively. Maximum elimination capacities of NH_3 and H_2S were 131 and 119 g m^{-3} h^{-1} respectively. The results of metabolic products of H_2S and NH_3 explore that the physical/chemical adsorption and biodegradation played different roles in the removal of H_2S and NH_3 under the steady-state and unsteady-state conditions.

The long-term high performance of the HBTF was significantly attributed to low accumulation of biomass and products, stable carbon characteristics and microbial communities. The biomass concentration on carbon was ranged between 0.4 and 1.6 mg protein g^{-1} carbon and the biomass was distributed evenly along the bed over extended operation. This avoids the problem of bed clogging. Moreover, the accumulation of biodegraded products on carbon was low. This benefits the stable operation of the HBTF, due to preventing the accumulation of metabolic products in a toxic concentration. The neutral pH values of carbon overcome the system acidification and stable micropore structure of carbon let the adsorption still happening during shock loadings. Furthermore, the PCR-DGGE results show the high population diversity of biofilm in the HBTF. The population communities have both some degree of stability and the adequate dynamics capable of adapting to accommodate varying reactor conditions. These advantages of the HBTF system significantly contributed to the high performance in the HBTF over a long-term operation.

Chapter 8
Conclusions & Recommendations

8.1 Conclusions

In this thesis, the experimental results enable the following conclusions to be made:

Biofilm could be developed on exhausted carbon successfully using part of the pre-adsorbed sulfur as the energy source for bacterial growth.

The biofilm can be formed on exhausted carbon using part of the pre-adsorbed sulfur as the sole energy source for bacterial growth in off-line trials. Around 18-47% of the pre-adsorbed sulfur on carbon was regenerated. On-line biofilter immobilization showed better biofilm development on exhausted carbon than in off-line incubation. During the biofiltration, the pre-adsorbed sulfur compounds on exhausted carbon were also biodegraded dramatically. Therefore, it is highly feasible to transfer exhausted carbon into biological activated carbon (BAC) for the removal of H_2S in biofiltration.

The biofilters using exhausted carbon demonstrated a fast start-up and worked well at a short empty bed residence time (EBRT).

The biofilters packed with exhausted carbon showed a quick start-up (about 80 hours). The quick start-up was attributed to the pre-adsorbed sulfur on exhausted carbon, which could act as an additional sulfur source for microbial growth. The biofilters achieved high removal efficiency greater than 95% at a short EBRT of 4 s. The removal efficiency of H_2S was almost identical in the biofilters packed with exhausted carbon and fresh carbon. Therefore, it is greatly effective and economical to apply

exhausted carbon in biofiltration for the removal of H_2S.

Different mechanisms of H_2S removal in biofilters employing exhausted carbon and fresh carbon were explored and explained by developing a mathematical model.

The developed model can predict very well the experimental data of removal efficiency in the columns packed with exhausted carbon (Column EC) and fresh carbon (Column FC). During the start-up stage, the removal of H_2S in Column EC was attributed to the adsorption mechanism much less than in Column FC. The removal of H_2S by the adsorption was affected greatly by the biodegradation. The ratios of H_2S removal by the biodegradation in Column EC were higher than those in Column FC during the start-up period. The steady-state biodegradation was obtained in a shorter time in Column EC (15 days) than Column FC (24 days). Under steady-state conditions, the elimination of H_2S was mainly attributed to the biodegradation mechanism. The adsorption into carbon could be ignored.

Substrates acclimation strategy is a crucial step for simultaneous biodegradation of H_2S and NH_3 in a biofiltration process

Different removal performances of H_2S and NH_3 were obtained in the three biofilters with various substrates acclimation strategies. A shorter acclimation time for the biodegradation of NH_3 was achieved in the biofilter feeding NH_3 followed by H_2S. This strategy also exhibited higher removal efficiency of NH_3 (> 95%) under high loadings of H_2S and NH_3. Moreover, the removal of NH_3 gas under this strategy was significantly attributed to nitrification, rather than the adsorption and chemical reaction in other two biofilters. A microbial population capable of degrading NH_3 which was acclimatized firstly in the biofilter benefited the fast acclimation and high removal of NH_3 in the co-removal system.

Simultaneous biodegradation of H_2S and NH_3 was highly efficient and effective by a horizontal biotrickling filter (HBTF) system over 316 days of operation

Long-term simultaneous biodegradation of H_2S and NH_3 was achieved in the HBTF packed with exhausted carbon and inoculated by mixed autotrophic culture. Over 95%

and 90% of NH_3 and H_2S were removed in most cases, respectively. Maximum elimination capacities of NH_3 and H_2S were 131 and 119 g m^{-3} h^{-1} respectively. The results of metabolic products of NH_3 and H_2S explore that the physical/chemical adsorption and biodegradation played different roles in the removal of H_2S and NH_3 under the steady and unsteady-state conditions. NH_3 was biodegraded into NO_2/NO_3^- with high ratio (> 85%) and H_2S was biodegraded into sulfate as main product (> 95%) in most cases.

The long-term high performance of the HBTF was significantly attributed to low accumulation of biomass and products, stable carbon characteristics and microbial communities.

The low biomass concentration on carbon bed (0.4-1.6 mg protein g^{-1} carbon) avoided the problem of bed clogging. The low accumulation of biodegraded products on carbon bed (0.9-2.8 wt% S and 0.3-1.0 wt% N) benefited the stable operation of the HBTF, due to preventing the accumulation of metabolic products in a toxic concentration. The near neutral pH values of carbon overcome the system acidification and stable micropore structure of carbon let the adsorption still happening during shock loadings. Furthermore, the results of polymerase chain reaction (PCR) and denaturing gradient gel electrophoresis (DGGE) show the high population diversity in the HBTF. The population communities have both some degree of stability and the adequate dynamics capable of adapting to accommodate varying reactor conditions. These advantages of the HBTF system significantly contributed to the high performance in the HBTF over a long-term operation.

8.2 Recommendations

There are several areas where extensions to this work can be considered for further study.

The optimum conditions for better re-use of exhausted carbon

Future research is still required to determine the optimum conditions for better re-use of exhausted carbon in biofiltration for the removal of H_2S. Particularly, some factors,

such as the types of activated carbon, porous structure of activated carbon, microorganism types and optimum process configuration need further investigation. In addition, co-removal of other pollutants, such as ammonia, probably influence desorption of the pre-adsorbed sulfur compounds on exhausted carbon. Exploring this effect is significantly important for the broad application of exhausted carbon for the removal of other gaseous pollutants.

Study of the functional bacteria in the bioreactor

Although the DGGE technology provided detailed information on the bacterial community structures of biofilm in bioreactors (Chapters 6 and 7), they may not adequately reflect the entire pool of bacteria in the bioreactor for simultaneous biodegradation of H_2S and NH_3. Hence, other microbiological techniques, such as FISH, CLMS, Gene cloning and real time PCR may be conductive to give a deep insight into the functional bacteria in the reactors. The determination and isolation of these persistent species in the bioreactor are the focus of a separate investigation.

REFERENCES

Abumaizar, R.J., Kocher, W., Smith, E.H., 1998. Biofiltration of BETX contaminated air streams using compost-activated carbon filter media. J. Hazard. Mater. 60, 111-126.

Abumaizar, R.J., Smith, E.H., Kocher, W., 1997. Analytical model of dual-media biofilter for removal of organic air pollutants. J. Environ. Eng.-ASCE 123, 606-614.

Adib, F., Bagreev, A., Bandosz, T.J., 1999. Effect of pH and surface chemistry on the mechanism of H_2S removal by activated carbons. J. Colloid Interf. Sci. 216, 360-369.

Aesoy, A., Odegaard, H., Bentzen, G., 1998. The effect of sulphide and organic matter on the nitrification activity in a biofilm process. Water Sci. Technol. 37, 115-122.

Aktas, O., Cecen, F., 2006. Effect of activation type on bioregeneration of various activated carbons loaded with phenol. J. Chem. Technol. Biotechnol. 81, 1081-1092.

Alonso, C., Suidan, M.T., Kim, B.R., Kim, B.J., 1998. Dynamic mathematical model for the biodegradation of VOCs in a biofilter: Biomass accumulation study. Environ. Sci. Technol. 32, 3118-3123.

Alonso, C., Suidan, M.T., Sorial, G.A., Smith, F.L., Biswas, P., Smith, P.J., Brenner,

R.C., 1997. Gas treatment in trickle-bed biofilters: Biomass, how much is enough? Biotechnol. Bioeng. 54, 583-594.

Amanullah, M., Farooq, S., Viswanathan, S., 1999. Modeling and simulation of a biofilter. Ind. Eng. Chem. Res. 38, 2765-2774.

APHA, 1999. Standard Methods for the Examination of Water and Wastewater. American Public Health Association, Washington DC, USA.

Armeen, A., 2006. Biofiltration for Odour Control in Livestock Facilities. PhD thesis. University of Alberta, Edmonton, Alberta.

Atlas, J.E., Bartha, R., 1981. Microbial Ecology: Fundamentals and Applications. Addison-Wesly Pulb Company, MA.

Bagreev, A., Adib, F., Bandosz, T.J., 2001. pH of activated carbon surface as an indication of its suitability for H_2S removal from moist air streams. Carbon 39, 1897-1905.

Bagreev, A., Rahman, H., Bandosz, T.J., 2002. Study of regeneration of activated carbons used as H_2S adsorbents in water treatment plants. Adv. Environ. Res. 6, 303-311.

Bandosz, T.J., 2002. On the adsorption/oxidation of hydrogen sulfide on activated carbons at ambient temperatures. J. Colloid Interface Sci. 246, 1-20.

Bansal, R.C., Goyal, M., 2005. Activated Carbon Adsorption. Taylor & Francis Group, Boca Raton, FL.

Baquerizo, G., Maestre, J.P., Sakuma, T., Deshusses, M.A., Gamisans, X., Gabriel, D., Lafuente, J., 2005. A detailed-model of a biofilter for ammonia removal: Model parameters analysis and model validation. Chem. Eng. J. 113, 205-214.

Black, J.G., 2005. Microbiology: Principles and Explorations. Chichester Wiley, New York.

Bowker, R.P.G., 1999. Overview of odor control strategies for wastewater treatment plants. Proceedings - Virginia Water Environment Association.

Brennan, B.M., Donlon, M., Bolton, E., 1996. Peat biofiltration as an odour control technology for sulphur-based odours. J. Chart. Inst. Water E. 10, 190-198.

Brock, T.D., Madigan, M.T., 1991. Biology of Microorganisms. Prentice Hall, Imprint Englewood Cliffs, N.J.

Burrowes, P.A., Witherspoon, J.P., Quigley, C.J., Easter, C.C., 2001. Biofilters - wastewater collection and treatment odour experiences of a sustainable technology in North America. Proceedings of the 1st IWA International Conference on Odour and VOCs, Sydney, Australia.

Busca, G., Pistarino, C., 2003. Abatement of ammonia and amines from waste gases: a summary. J. Loss Prevent. Proc. 16, 157-163.

Casamayor, E.O., Schafer, H., Baneras, L., Pedros-Alio, C., Muyzer, G., 2000. Identification of and spatio-temporal differences between microbial assemblages from two neighboring sulfurous lakes: Comparison by microscopy and denaturing gradient gel electrophoresis. Appl. Environ. Microb. 66, 499-508.

Chang, H.T., Rittmann, B.E., 1987. Mathematical modeling of biofilm on activated carbon. Environ. Sci. Technol. 21, 273-280.

Chen, Y.X., Yin, J., Wang, K.X., 2005. Long-term operation of biofilters for biological removal of ammonia. Chemosphere 58, 1023-1030.

Chen, Y.X., Yin, J., Wang, K.X., Fang, S., 2004. Effects of periods of nonuse and fluctuating ammonia concentration on biofilter performance. J. Environ. Sci. Heal. A 39, 2447-2463.

Cho, K.S., Hirai, M., Shoda, M., 1992. Enhanced removal efficiency of malodorous gases in a pilot-scale peat biofilter inoculated with *Thiobacillus thioparus*

DW44. J. Ferment. Bioeng. 73, 46-50.

Cho, K.S., Ryu, H.W., Lee, N.Y., 2000. Biological deodorization of hydrogen sulfide using porous lava as a carrier of *thiobacillus thiooxidans*. J. Biosci. Bioeng. 90, 25-31.

Cho, K.S., Zhang, L., Hirai, M., Shoda, M., 1991. Removal characteristics of hydrogen sulfide and methanethiol by *thiobacillus sp.* isolated from peat in biological deodorization. J. Ferment. Bioeng. 71, 44-49.

Choi, J.H., Kim, Y.H., Joo, D.J., Choi, S.J., Ha, T.W., Lee, D.H., Park, I.H., Jeong, Y.S., 2003. Removal of ammonia by biofilters: A study with flow-modified system and kinetics. J. Air Waste Manage. 53, 92-101.

Chung, Y.-C., Ho, K.-L., Tseng, C.-P., 2007. Two-stage biofilter for effective NH_3 removal from waste gases containing high concentrations of H_2S. J. Air Waste Manage. 57, 337-347.

Chung, Y.C., Huang, C., Tseng, C.P., 1996a. Biodegradation of hydrogen sulfide by a laboratory-scale immobilized *Pseudomonas putida CH11* biofilter. Biotechnol. Progr. 12, 773-778.

Chung, Y.C., Huang, C., Tseng, C.P., 1996b. Operation optimization of *Thiobacillus thioparus CH11* biofilter for hydrogen sulfide removal. J. Biotechnol. 52, 31-38.

Chung, Y.C., Huang, C., Tseng, C.P., 1997. Biotreatment of ammonia from air by an immobilized *Arthrobacter oxydans CH8* biofilter. Biotechnol. Progr. 13, 794-798.

Chung, Y.C., Huang, C., Tseng, C.P., 2001. Biological elimination of H_2S and NH_3 from waste gases by biofilter packed with immobilized heterotrophic bacteria. Chemosphere 43, 1043-1050.

Chung, Y.C., Huang, C., Tseng, C.P., Pan, J.R., 2000. Biotreatment of H_2S- and

NH_3-containing waste gases by co-immobilized cells biofilter. Chemosphere 41, 329-336.

Chung, Y.C., Huang, C.P., Pan, J.R., Tseng, C.P., 1998. Comparison of autotrophic and mixotrophic biofilters for H_2S removal. J. Environ. Eng. ASCE 124, 362-367.

Chung, Y.C., Lin, Y.Y., Tseng, C.P., 2004a. Control of H_2S waste gas emissions with a biological activated carbon filter. J. Chem. Technol. Biotechnol. 79, 570-577.

Chung, Y.C., Lin, Y.Y., Tseng, C.P., 2004b. Operational characteristics of effective removal of H_2S and NH_3 waste gases by activated carbon biofilter. J. Air Waste Manage. 54, 450-458.

Chung, Y.C., Lin, Y.Y., Tseng, C.P., 2005. Removal of high concentration of NH_3 and coexistent H_2S by biological activated carbon (BAC) biotrickling filter. Bioresource Technol. 96, 1812-1820.

Clemens, J., Cuhls, C., 2003. Greenhouse gas emissions from mechanical and biological waste treatment of municipal waste. Environ. Technol. 24, 745-754.

Cox, H.H.J., Deshusses, M.A., 2002a. Co-treatment of H_2S and toluene in a biotrickling filter. Chem. Eng. J. 87, 101-110.

Cox, H.H.J., Deshusses, M.A., 2002b. Effect of starvation on the performance and re-acclimation of biotrickling filters for air pollution control. Environ. Sci. Technol. 36, 3069-3073.

Cox, H.H.J., Houtman, J.H.M., Doddema, H.J., Harder, W., 1993. Enrichment of fungi and degradation of styrene in biofilters. Biotechnol. Lett. 15, 737-742.

Cox, H.H.J., Nguyen, T.T., Deshusses, M.A., 2000. Toluene degradation in the recycle liquid of biotrickling filters for air pollution control. Appl. Microbiol. Biotechnol. 54, 133-137.

Coyne, M.S., 1999. Soil Microbiology: An Exploratory Approach. Delmar Publishers, Albany, NY.

Demeestere, K., Van Langenhove, H., Smet, E., 2002. Regeneration of a compost biofilter degrading high loads of ammonia by addition of gaseous methanol. J. Air Waste Manage. 52, 796-804.

Den, W., Pirbazari, M., 2002. Modeling and design of vapor-phase biofiltration for chlorinated volatile organic compounds. AICHE J. 48, 2084-2103.

Deshusses, M.A., Hamer, G., Dunn, I.J., 1995a. Behavior of biofilters for waste air biotreatment.1. Dynamic-model development. Environ. Sci. Technol. 29, 1048-1058.

Deshusses, M.A., Hamer, G., Dunn, I.J., 1995b. Behavior of biofilters for waste air biotreatment.2. Experimental evaluation of a dynamic-model. Environ. Sci. Technol. 29, 1059-1068.

Devinny, J.S., Deshusses, M.A., Webster, T.S., 1999. Biofiltration for Air Pollution Control. Lewis Publishers, Boca Rotan, FL.

Devinny, J.S., Ramesh, J., 2005. A phenomenological review of biofilter models. Chem. Eng. J. 113, 187-196.

Diks, R.M.M., Ottengraf, S.P.P., Vrijland, S., 1994. The existence of a biological equilibrium in a trickling filter for waste-gas purification. Biotechnol. Bioeng. 44, 1279-1287.

Duan, H.Q., Koe, L.C.C., Yan, R., 2005a. Treatment of H_2S using a horizontal biotrickling filter based on biological activated carbon: reactor setup and performance evaluation. Appl. Microbiol. Biotechnol. 67, 143-149.

Duan, H.Q., Koe, L.C.C., Yan, R., Chen, X.G., 2006. Biological treatment of H_2S using pellet activated carbon as a carrier of microorganisms in a biofilter. Water

Res. 40, 2629-2636.

Duan, H.Q., Yan, R., Koe, L.C.C., 2005b. Investigation on the mechanism of H_2S removal by biological activated carbon in a horizontal biotrickling filter. Appl. Microbiol. Biotechnol. 69, 350-357.

Dumont, E., Andres, Y., Le Cloirec, P., Gaudin, F., 2008. Evaluation of a new packing material for H_2S removed by biofiltration. Biochem. Eng. J. 42, 120-127.

Elias, A., Barona, A., Arreguy, A., Rios, J., Aranguiz, I., Penas, J., 2002. Evaluation of a packing material for the biodegradation of H_2S and product analysis. Process Biochem. 37, 813-820.

Ergas, S.J., Shroeder, E.D., Chang, D.P.Y., Morton, R.L., 1995. Control of volatile organic compound emissions using a compost biofilter. Water Environ. Res. 67, 816-821.

Fernandez, A.S., Hashsham, S.A., Dollhopf, S.L., Raskin, L., Glagoleva, O., Dazzo, F.B., Hickey, R.F., Criddle, C.S., Tiedje, J.M., 2000. Flexible community structure correlates with stable community function in methanogenic bioreactor communities perturbed by glucose. Appl. Environ. Microb. 66, 4058-4067.

Ford, D.L., Churchwell, R.L., Kachtick, J.W., 1980. Comprehensive analysis of nitrification of chemical processing wastewaters. J. Water Pollut. Con. F. 52, 2726-2746.

Fortin, N.Y., Deshusses, M.A., 1999. Treatment of methyl tert-butyl ether vapors in biotrickling filters. 1. Reactor startup, steady state performance, and culture characteristics. Environ. Sci. Technol. 33, 2980-2986.

Fuller, E.N., Schettle.Pd, Giddings, J.C., 1966. A new method for prediction of binary gas-phase diffusion coeffecients. Ind. Eng. Chem. 58, 18-27.

Gabriel, D., Deshusses, M.A., 2003. Retrofitting existing chemical scrubbers to

biotrickling filters for H_2S emission control. Proc. Natl. Acad. Sci. 100, 6308-6312.

Gabriel, D., Maestre, J.P., Martin, L., Gamisans, X., Lafuente, J., 2007. Characterisation and performance of coconut fibre as packing material in the removal of ammonia in gas-phase biofilters. Biosyst. Eng. 97, 481-490.

Galera, M.M., Cho, E., Tuuguu, E., Park, S.J., Lee, C., Chung, W.J., 2008. Effects of pollutant concentration ratio on the simultaneous removal of NH_3, H_2S and toluene gases using rock wool-compost biofilter. J. Hazard. Mater. 152, 624-631.

Goncalves, J.J., Govind, R., 2008. H_2S abatement in a biotrickling filter using iron(III) foam media. Chemosphere 73, 1478-1483.

Gracian, C., Malhautier, L., Fanlo, J.L., Le Cloirec, P., 2002. Biofiltration of air loaded with ammonia by granulated sludge. Environ. Prog. 21, 237-245.

Graham, J.R., 1996. GAC based gas phase biofiltration. Proceedings of the 1996 USC-TRG Conference on Biofiltration, Los Angeles, CA.

Grant, W.D., Long, P.E., 1981. Environmental microbiology. Halsted Press, New York.

Guo, J., Xu, W.S., Chen, Y.L., Lua, A.C., 2005. Adsorption of NH_3 onto activated carbon prepared from palm shells impregnated with H_2SO_4. J. Colloid Interf. Sci. 281, 285-290.

Hartikainen, T., Ruuskanen, J., Vanhatalo, M., Martikainen, P.J., 1996. Removal of ammonia from air by a peat biofilter. Environ. Technol. 17, 45-53.

Haug, R.T., 1993. The Practical Handbook of Compost Engineering. Lewis Publishers, Boca Raton, FL.

Hautakangas, H., Mihelcic, J.R., 1999. Optimization and modeling of biofiltration for

odour control. WEF's 72nd Annual Conference and Exposition, New Oelean, LA.

Herzberg, M., Dosoretz, C.G., Tarre, S., Green, M., 2003. Patchy biofilm coverage can explain the potential advantage of BGAC reactors. Environ. Sci. Technol. 37, 4274-4280.

Hirai, M., Kamamoto, M., Yani, M., Shoda, M., 2001. Comparison of the biological H_2S removal characteristics among four inorganic packing materials. J. Biosci. Bioeng. 91, 396-402.

Hirai, M., Ohtake, M., Shoda, M., 1990. Removal kinetics of hydrogen sulfide, methanethiol and dimethyl sulfide by peat biofilters. J. Ferment. Bioeng. 70, 334-339.

Ho, K.-L., Chung, Y.-C., Tseng, C.-P., 2008. Continuous deodorization and bacterial community analysis of a biofilter treating nitrogen-containing gases from swine waste storage pits. Bioresource Technol. 99, 2757-2765.

Hodge, D.S., Devinny, J.S., 1995. Modeling removal of air contaminants by biofiltration. J. Environ. Eng. ASCE 121, 21-32.

Hong, J.H., Park, K.J., 2005. Compost biofiltration of ammonia gas from bin composting. Bioresource Technol. 96, 741-745.

Hutchinson, D.H., Robinson, C.W., 1990. A microbial regeneration process for granular activated carbon II. regeneration studies. Water Res. 24, 1217-1223.

Jensen, A.B., Webb, C., 1995. Treatment of H_2S-containing gases: a review of microbiological alternatives. Enzyme Microb. Tech. 17, 2-10.

Jin, Y., Veiga, M.C., Kennes, C., 2005a. Autotrophic deodorization of hydrogen sulfide in a biotrickling filter. J. Chem. Technol. Biot. 80, 998-1004.

Jin, Y., Veiga, M.C., Kennes, C., 2005b. Effects of pH, CO_2, and flow pattern on the

autotrophic degradation of hydrogen sulfide in a biotrickling filter. Biotechnol. Bioeng. 92, 462-471.

Jones, K.D., Martinez, A., Maroo, K., Deshpande, S., Boswell, J., 2004. Kinetic evaluation of H_2S and NH_3 biofiltration for two media used for wastewater lift station emissions. J. Air Waste Manage. 54, 24-35.

Joshi, J.A., 2000. Transformation of gaseous ammonia in biofilters. PhD thesis, The State University of New Jersey, New Jersey.

Jubinville, R.A., Stallings, R.B., Bowen, W., 1997. Implementation of a comprehensive odor control program at the New London, CT WPCF. J. New England Water Environ. Association 31, 40-48.

Kanagawa, T., Qi, H.W., Okubo, T., Tokura, N., 2004. Biological treatment of ammonia gas at high loading. Water Sci. Technol. 50, 283-290.

Kapahi, R., Gross, M., 1995. Biofiltration for VOC and ammonia emissions control. BioCycle 36, 87-90.

Kar, S., Swaminathan, T., Baradarajan, A., 1996. Studies on biodegradation of a mixture of toxic and nontoxic pollutant using *Arthrobacter* species. Bioprocess Eng. 15, 195-199.

Kennes, C., Veiga, M.C., 2001. Bioreactors for Waste Gas Treatment. Kluwer Academic Publishers, Dordrecht.

Kim, D.J., Miyahara, T., Noike, T., 1997. Effect of C/N ratio on the bioregeneration of biological activated carbon. Water Sci. Technol. 36, 239-249.

Kim, H.S., Kim, Y.J., Chung, J.S., Xie, Q., 2002. Long-term operation of a biofilter for simultaneous removal of H_2S and NH_3. J. Air Waste Manage. 52, 1389-1398.

Kim, J.H., Rene, E.R., Park, H.S., 2007. Performance of an immobilized cell biofilter for ammonia removal from contaminated air stream. Chemosphere 68, 274-280.

Kim, J.H., Rene, E.R., Park, H.S., 2008. Biological oxidation of hydrogen sulfide under steady and transient state conditions in an immobilized cell biofilter. Bioresource Technol. 99, 583-588.

Kim, N.J., Hirai, M., Shoda, M., 2000a. Comparison of organic and inorganic packing materials in the removal of ammonia gas in biofilters. J. Hazard. Mater. 72, 77-90.

Kim, N.J., Sugano, Y., Hirai, M., Shoda, M., 2000b. Removal of a high load of ammonia gas by a marine bacterium, *Vibrio alginolyticus*. J. Biosci. Bioeng. 90, 410-415.

Kim, S.-H., Pirbazari, M., 1989. Bioactive adsorber model for industrial wastewater treatment. J. Environ. Eng. ASCE 115, 1235-1256.

Kim, S., Deshusses, M.A., 2003. Development and experimental validation of a conceptual model for biotrcikling filtration of H_2S. Environ. Prog. 22, 119-128.

Kim, S., Deshusses, M.A., 2005. Understanding the limits of H_2S degrading biotrickling filters using a differential biotrickling filter. Chem. Eng. J. 113, 119-126.

Klimenko, N., Smolin, S., Grechanyk, S., Kofanov, V., Nevynna, L., Samoylenko, L., 2004. Bioregeneration of activated carbons by bacterial degraders after adsorption of surfactants from aqueous solutions. Colloid. Surface. A 230, 141-158.

Koe, L.C.C., Wu, L., Loo, Y.Y., Wu, Y., Chai, J.W., Koh, Y.M., 2002. A successful conversion of a chemical scrubber to a biotrickling filter - some experiences. Proc. ENVIRO 2002 Conv. Exhibition. IWA, Melbourne, Australia.

Koe, L.C.C., Yang, F., 1999. The effectiveness of the cover and treatment scheme for controlling odourous emissions at a municipal wastewater treatment facility. Proceedings - The CIWEM and IAWQ Joint International Conference on

Control and Prevention of Odours in the Water Industry, London, England.

Koe, L.C.C., Yang, F., 2000. A bioscrubber for hydrogen sulphide removal. Water Sci. Technol. 41, 141-145.

Kowalchuk, G.A., Stephen, J.R., DeBoer, W., Prosser, J.I., Embley, T.M., Woldendorp, J.W., 1997. Analysis of ammonia-oxidizing bacteria of the beta subdivision of the class Proteobacteria in coastal sand dunes by denaturing gradient gel electrophoresis and sequencing of PCR-amplified 16S ribosomal DNA fragments. Appl. Environ. Microbiol. 63, 1489-1497.

Krupa, S.V., 2003. Effects of atmospheric ammonia (NH_3) on terrestrial vegetation: a review. Environ. Pollut. 124, 179-221.

Laanbroek, H.J., Bodelier, P.L.E., Gerards, S., 1994. Oxygen-consumption kinetics of *Nitrosomonas-europaea* and *Nitrobacter-hamburgensis* grown in mixed continuous cultures at different oxygen concentrations. Arch. Microbiol. 161, 156-162.

Laustsen, T.A., Marran, K.S., Little, H.L., Coladonato, S., 1999. Design parameters for a biofilter that successfully treats volatile organic compounds from a combined sewer. WEFTEC'99, New Orlean, LA.

Lee, E.Y., Cho, K.S., Ryu, H.W., 2005. Simultaneous removal of H_2S and NH_3 in biofilter inoculated with *Acidithiobacillus Thiooxidans TAS*. J. Biosci. Bioeng. 99, 611-615.

Leson, G., Winer, A.M., 1991. Biofiltration: an innovative air pollution control technology for VOC emission. J. Air Waste Manage. 41, 1045-1054.

Li, C., Moe, W.M., 2004. Assessment of microbial populations in methyl ethyl ketone degrading biofilters by denaturing gradient gel electrophoresis. Appl. Microbiol. Biotechnol. 64, 568-575.

Li, X.Z., Wu, J.S., Sun, D.L., 1998. Hydrogen sulphide and volatile fatty acid removal from foul air in a fibrous bed bioreactor. Water Sci. Technol. 38, 323-329.

Liang, C.-H., Chiang, P.-C., 2007. Mathematical model of the non-steady-state adsorption and biodegradation capacities of BAC filters. J. Hazard. Mater. 139, 316-322.

Liang, C.H., Chiang, P.C., Chang, E.E., 2003. Systematic approach to quantify adsorption and biodegradation capacities on biological activated carbon following ozonation. Ozone-Sci. Eng. 25, 351-361.

Liang, Y., Quan, X., Chen, J., Chung, J.S., Sung, J.Y., Chen, S., Xue, D., Zhao, Y., 2000. Long-term results of ammonia removal and transformation by biofiltration. J. Hazard. Mater. 80, 259-269.

Lim, K.H., 2001a. Waste air treatment with a biofilter: For the case of adsorption capacity limited. J. Chem. Eng. Japan 34, 776-789.

Lim, K.H., 2001b. Waste air treatment with a biofilter: For the case of excess adsorption capacity. J. Chem. Eng. Japan 34, 766-775.

Lin, Y.H., Leu, J.Y., 2008. Kinetics of reactive azo-dye decolorization by *Pseudomonas luteola* in a biological activated carbon process. Biochem. Eng. J. 39, 457-467.

Madigan, M.T., Martinko, J.M., Parker, J., 2002. Biology of Microorganisms (tenth edition). Pearson Education, Inc., Upper Saddle River.

Malhautier, L., Gracian, C., Roux, J.C., Fanlo, J.L., Le Cloirec, P., 2003. Biological treatment process of air loaded with an ammonia and hydrogen sulfide mixture. Chemosphere 50, 145-153.

Marek, J., Paca, J., Gerrard, A.M., 2000. Dynamic responses of biofilters to changes in the operating conditions in the process of removing toluene and xylene from

air. Acta Biotechnol. 20, 17-29.

Martin, R.W., Mihelcic, J.R., Crittenden, J.C., 2004. Design and performance characterization strategy using modeling for biofiltration control of odorous hydrogen sulfide. J. Air Waste Manage. 54, 834-844.

Mason, C.A., Ward, G., Abu-Salah, K., Keren, O., Dosoretz, C.G., 2000. Biodegradation of BTEX by bacteria on powdered activated carbon. Bioproc. Biosyst. Eng. 23, 331-336.

McNevin, D., Barford, J., 2000. Biofiltration as an odour abatement strategy. Biochem. Eng. J. 5, 231-242.

McNevin, D., Barford, J., Hage, J., 1999. Adsorption and biological degradation of ammonium and sulfide on peat. Water Res. 33, 1449-1459.

Medina, V.F., Webster, T.S., Devinny, J.S., 1995. Treatment of gasoline residuals by granular activated carbon based biological filtration. J. Environ. Sci. Heal. A 30, 407-412.

Montgomery, J.M., 1985. Water Treatment Principles and Design. Wiley, New York.

Morgan, S.F., Sleep, B.E., Allen, D.G., 2001. Effects of biomass growth on gas pressure drop in biofilters. J. Environ. Eng. ASCE 127, 388-396.

Morton, R., Caballero, R., 1996. The biotrickling story. Wat. Environ. Technol. 8, 39-45.

Ng, Y.L., Yan, R., Chen, X.G., Geng, A.L., Gould, W.D., Liang, D.T., Koe, L.C.C., 2004. Use of activated carbon as a support medium for H_2S biofiltration and effect of baceteria immobilization on available pore surface. Appl. Microbiol. Biotechnol. 66, 259-265.

Nicolai, R.E., 2002. Biofiltration of Livestock Facility Exhaust air. PhD thesis. University of Minnesota, Minnesota.

Nicolai, R.E., Janni, K.A., 2001. Biofilter media mixture ratio of wood chips and compost treating swine odors. Water Sci. Technol. 44, 261-267.

Oh, Y.S., Bartha, R., 1994. Design and performance of a trickling air biofilter for chlorobenzene and o-dichlorobenzene vapors. Appl. Environ. Microbiol. 60, 2717-2722.

Orshansky, F., Narkis, N., 1997. Characteristics of organics removal by PACT simultaneous adsorption and biodegradation. Water Res. 31, 391-398.

Ottengraf, S.P.P., Meesters, J.J.P., Vandenoever, A.H.C., Rozema, H.R., 1986. Biological elimination of volatile xenobiotic compounds in biofilters. Bioprocess Eng. 1, 61-69.

Pagans, E.L., Font, X., Sanchez, A., 2005. Biofiltration for ammonia removal from composting exhaust gases. Chem. Eng. J. 113, 105-110.

Page, A.L., 1982. Methods of Soil Analysis, part 2 - Chemical and Microbiological Properties (2nd Edition). American Society Agronomy, Madison, Wisconsin, USA.

Park, J.S., 2004. Biodegradation of Paint VOC Mixtures in Biofilters. PhD thesis, The University of Texas at Austin.

Perry, R.H., Green, D.W., 1999. Perry's Chemical Enigineers' Handbook. McGraw-Hill, New York.

Pinnette, J.R., Giggey, M.D., Marcy, G.J., 1994. Performance of biofilters at two agitated bin composting facilities. A&WMA's 87th Annual Conference & Exhibition., Ohio.

Prosser, J.I., 1989. Autotrophic nitrification in bacteria. Adv. Microb. Physiol. 30, 125-181.

Rattanapan, C., Boonsawang, P., Kantachote, D., 2009. Removal of H_2S in down-flow

GAC biofiltration using sulfide oxidizing bacteria from concentrated latex wastewater. Bioresource Technol. 100, 125-130.

Rittmann, B.E., McCarty, P.L., 2001. Environmental Biotechnology: Principles and Applications. McGraw-Hill, Boston.

Rowe, R., Todd, R., Waide, J., 1977. Microtechnique for most probable number analysis. Appl. Environ. Microbiol. 33, 675-680.

Rozich, A.F., Colvin, R.J., 1986. Effects of glucose of phenol biodegradation by heterogeneous populations. Biotechnol. Bioeng. 28, 965-971.

Schedel, M., Trtiper, H.G., 1980. Anaerobic oxidation of thiosulfate and elemental sulfur in thiobacillus denitrificans. Arch. Microbiol. 124, 205-210.

Scholz, M., Martin, R.J., 1997. Ecological equilibrium on biological activated carbon. Water Res. 31, 2959-2968.

Schroeder, E.D., 2002. Trends in application of gas-phase bioreactor. Reviews in Environ. Sci. Biotechnol. 1, 65-74.

Sercu, B., Boon, N., Beken, S.V., Verstraete, W., Van Langenhove, H., 2007. Performance and microbial analysis of defined and non-defined inocula for the removal of dimethyl sulfide in a biotrickling filter. Biotechnol. Bioeng. 96, 661-672.

Sercu, B., Nunez, D., Van Langenhove, H., Aroca, G., Verstraete, W., 2005. Operational and microbiological aspects of a bioaugmented two-stage biotrickling filter removing hydrogen sulfide and dimethyl sulfide. Biotechnol. Bioeng. 90, 259-269.

Shanchayan, B., Parker, W., Pride, C., 2006. Dynamic analysis of a biofilter treating autothermal thermophilic aerobic digestion offgas. J. Environ. Eng. Sci. 5, 263-272.

Shareefdeen, Z., Baltzis, B.C., 1994. Biofiltration of toluene vapor under steady-state and transient conditions: theory and experimental results. Chem. Eng. Sci. 49, 4347-4360.

Shareefdeen, Z., Baltzis, B.C., Oh, Y.S., Bartha, R., 1993. Biofiltration of methanol vapor. Biotechnol. Bioeng. 41, 512-524.

Shareefdeen, Z., Singh, A., 2005. Biotechnology for Odor and Air Pollution Control. Springer-Verlag Berlin Heidelberg, Berlin, Germany.

Shinabe, K., Oketani, S., Ochi, T., Matsumura, M., 1995. Characteristics of hydrogen sulfide removal by *Thiobacillus Thiooxidans KS1* isolated from a carrier-packed biological deodorization system. J. Ferment. Bioeng. 80, 592-598.

Shuler, M.L., Kargi, F., 1992. Bioprocess engineering. Prentice Hall, New Jersey.

Silva, M., Fernandes, A., Mendes, A., Manaia, C.M., Nunes, O.C., 2004. Preliminary feasibility study for the use of an adsorption/bio-regeneration system for molinate removal from effluents. Water Res. 38, 2677-2684.

Smet, E., Chasaya, G., Van Langenhove, H., Verstraete, W., 1996. The effect of inoculation and the type of carrier material used on the biofiltration of methyl sulfides. Appl. Microbiol. Biotechnol. 45, 293-298.

Smet, E., Van Langenhove, H., Maes, K., 2000. Abatement of high concentrated ammonia loaded waste gases in compost biofilters. Water Air Soil Poll. 119, 177-190.

Song, J., Kinney, K.A., 2000. Effect of vapor-phase bioreactor operation on biomass accumulation, distribution, and activity: Linking biofilm properties to bioreactor performance. Biotechnol. Bioeng. 68, 508-516.

Song, J., Kinney, K.A., 2002. A model to predict long-term performance of vapor-phase bioreactors: A cellular automaton approach. Environ. Sci. Technol.

36, 2498-2507.

Song, J., Kinney, K.A., 2005. Microbial response and elimination capacity in biofilters subjected to high toluene loadings. Appl. Microbiol. Biotechnol. 68, 554-559.

Sorial, G.A., Smith, F.L., Suidan, M.T., Brenner, R.C., 2001. Removal of ammonia from contaminated air by trickle bed air biofilters. J. Air Waste Manage. 51, 756-765.

Speitel, G.E., Dovantzis, K., Digiano, F.A., 1987. Mathematical modeling of bioregeneration in GAC columns. J. Environ. Eng. ASCE 113, 32-48.

Speitel, G.E., Zhu, X.J., 1990. Sensitivity analyses of biodegradation adsorption models. J. Environ. Eng. ASCE 116, 32-48.

Speitel, G.E.J., Lu, C.J., Turakhia, M., Zhu, X.J., 1989. Biodegradation of trace concentrations of substituted phenols in granular activated carbon columns. Environ. Sci. Technol. 23, 68-74.

Srna, R.F., Baggaley, A., 1975. Kinetic response of perturbed marine nitrification systems. J. Water Pollut. Con. F. 47, 472-486.

Stoeckli, F., Guillot, A., Slasli, A.M., 2004. Specific and non-specific interactions between ammonia and activated carbons. Carbon 42, 1619-1624.

Sublette, K.L., Sylvester, N.D., 1987. Oxidation of hydrogen sulfide by *Thiobacillus Denitrificans*: desulfurization of natural gas. Biotechnol. Bioeng. 29, 249-257.

Sun, Y., Clanton, C.J., Janni, K.A., Malzer, G.L., 2000. Sulfur and nitrogen balances in biofilters for odorous gas emission control. T. ASAE 43, 1861-1875.

Suzuki, I., 1999. Oxidation of inorganic sulfur compounds: chemical and enzymatic reactions. Can. J. Microbiol. 45, 97-105.

Swaminathan, K., Chakrabarti, T., Subrahmanyam, P.V.R., 1999. Substrate-substrate

interaction of resorcinol and catechol in upflow anaerobic fixed film - Fixed bed reactors in mono and multisubstrate matrices. Bioproc. Biosyst. Eng. 20, 349-353.

Swanson, W.J., Loehr, R.C., 1997. Biofiltration: Fundamentals, design and operations principles, and applications. J. Envion. Eng. 123, 538-546.

Taghipour, H., Shahmansoury, M.R., Bina, B., Movahdian, H., 2008. Operational parameters in biofiltration of ammonia-contaminated air streams using compost-pieces of hard plastics filter media. Chem. Eng. J. 137, 198-204.

Tanji, Y., Kanagawa, T., Mikami, E., 1989. Removal of dimethyl sulfide, methyl mercaptan, and hydrogen sulfide by immobilized *Thiobacillus thioparus* TK-m. J. Ferment. Bioeng. 67, 280-285.

Traegner, U.K., Suidan, M.T., 1989. Evaluation of surface and film diffusion coefficients for carbon adsorption. Water Res. 23, 267-273.

Tresse, O., Lorrain, M.J., Rho, D., 2002. Population dynamics of free-floating and attached bacteria in a styrene-degrading biotrickling filter analyzed by denaturing gradient gel electrophoresis. Appl. Microbiol. Biotechnol. 59, 585-590.

Turk, A., Sakalis, E., Lessuck, J., Karamitsos, H., Rago, O., 1989. Ammonia injection enhances capacity of activated carbon for hydrogen sulfide and methyl mercaptan. Environ. Sci. Technol. 23, 1242-1245.

Vaith, K., Cannon, M., Milligan, D., Heydorn, J., 1996. Comparing scrubbing technologies. Water Environ. Technol. 8, 35-38.

Villaverde, S., GarciaEncina, P.A., FdzPolanco, F., 1997. Influence of pH over nitrifying biofilm activity in submerged biofilters. Water Res. 31, 1180-1186.

Voice, T.C., Pak, D., Zhao, X., Shi, J., Hickey, R.F., 1992. Biological activated carbon

in fluidized bed reactors for the treatment of groundwater contaminated with volatile aromatic hydrocarbons. Water Res. 26, 1389-1401.

Walker, G.M., Weatherley, L.R., 1998. Bacterial regeneration in biological activated carbon systems. Process Saf. Environ. 76, 177-182.

Wani, A.H., Branion, R.M.R., Lau, A.K., 1998. Effects of periods of starvation and fluctuating hydrogen sulfide concentration on biofilter dynamics and performance. J. Hazard. Mater. 60, 287-303.

Wani, A.H., Lau, A.K., Branion, R.M.R., 1999. Biofiltration control of pulping odors - hydrogen sulfide: performance, macrokinetics and coexistence effects of organo-sulfur species. J. Chem. Technol. Biot. 74, 9-16.

Weber, F.J., Hartmans, S., 1995. Use of activated carbon as a buffer in biofiltration of waste gases with fluctuating concentration of toluene. Appl. Microbiol. Biotechnol. 43, 365-369.

Webster, T.S., Devinny, J.S., Torres, E.M., Basrai, S.S., 1997. Microbial ecosystems in compost and granular activated carbon biofilters. Biotechnol. Bioeng. 53, 296-303.

Weckhuysen, B., Vriens, L., Verachtert, H., 1994. Biotreatment of ammonia- and butanal-containing waste gases. Appl. Microbiol. Biotechnol. 42, 147-152.

Williamson, K., McCarty, P.L., 1976. Model of substrate utilization by bacterial films. J. Water Pollut. Con. F. 48, 9-24.

Witherspoon, J.R., SIdhu, A., Castleberry, J., Coleman, L., reynolds, K., Card, T., 1999. Case study - Odor emission estimates and control strategies using models and sampling for East Bay Municipal Utility District's sewer collection system and wastewater treatment plant. Proceedings - The CIWEM and IAWQ Joint International Conference on Control and Prevention of Odours in the Water Industry, London, England.

Wright, W.F., Schroeder, E.D., Chang, D.P.Y., 2005. Regular transient loading response in a vapor-phase flow-direction-switching biofilter. J. Environ. Eng. ASCE 131, 1649-1658.

Wu, L., Loo, Y.Y., Koe, L.C.C., 2001. A pilot study of a biotrickling filter for the treatment of odorous sewage air. Wat. Sci. Technol. 44, 295-299.

Xie, Y.F., Zhou, H.J., 2002. Use of BAC for HAA removal Part 2, Column study. J. Am. Water Works Ass. 94, 126-134.

Yan, R., Chin, T., Ng, Y.L., Duan, H.Q., Liang, D.T., Tay, J.H., 2004a. Influence of surface properties on the mechanisms of H_2S removal by alkaline activated carbons. Environ. Sci. Technol. 38, 316-323.

Yan, R., Liang, D.T., Tsen, L., Tay, J.H., 2002. Kinetics and mechanisms of H_2S adsorption by alkaline activated carbon. Environ. Sci. Technol. 36, 4460-4466.

Yan, R., Ng, Y.L., Chen, X.G., Geng, A.L., Gould, W.D., Duan, H.Q., Liang, D.T., Koe, L.C.C., 2004b. Batch experiment on H_2S degradation by bacteria immobilized on activated carbons. Water Sci. Technol. 50, 299-308.

Yang, Y.H., Allen, E.R., 1994. Biofiltration control of hydrogen sulfide 1. Design and operational parameters. J. Air Waste Manage. 44, 863-868.

Yani, M., Hirai, M., Shoda, M., 1998. Removal kinetics of ammonia by peat biofilter seeded with night soil sludge. J. Ferment. Bioeng. 85, 502-506.

Yoon, I.K., Park, C.H., 2002. Effects of gas flow rate, inlet concentration and temperature on biofiltration of volatile organic compounds in a peat-packed biofilter. J. Biosci. Bioeng. 93, 165-169.

Zhao, X., Hickey, R.F., C. Voice, T., 1999. Long-term evaluation of adsorption capacity in a biological activated carbon fluidized bed reactor system. Water Res. 33, 2983-2991.

Zhou, D.Z., 2000. Biological treatment of sewage air using a horizontal biotrickling filter. National University of Singapore, Singapore.

Zhou, H.J., Xie, Y.F., 2002. Using BAC for HAA removal part 1: Batch study. J. Am. Water Works Ass. 94, 194-200.

Zhu, L., Abumaizar, R.J., Kocher, W.M., 1998a. Biofiltration of benzene contaminated air streams using compost-activated carbon filter media. Environ. Prog. 17, 168-172.

Zhu, X., Cao, H., Suidan, M.T., 1998b. The effect of moisture content on VOC removal in trickle-bed biofilters. Proceedings of the 91st Annual Meeting & Exhibition of the Air & Waste Management Association, Pittsburgh, PA.